VOLUME 8 NUMBER 1 2015 ISSN 2218-7979

International Journal of Biology and Chemistry

Al-Farabi Kazakh National University

International Journal of Biology and Chemistry is published twice a year by al-Farabi Kazakh National University, al-Farabi ave., 71, 050040, Almaty, the Republic of Kazakhstan
website: http://ijbch.kaznu.kz/

Any inquiry for subscriptions should be sent to:
Prof. Mukhambetkali Burkitbayev, al-Farabi Kazakh National University
al-Farabi ave., 71, 050040, Almaty, the Republic of Kazakhstan
e-mail: Mukhambetkali Burkitbayev@kaznu.kz

Editorial

The most significant achievements in the field of natural sciences are reached in joint collaboration, where important roles are taken by biology and chemistry. Therefore publication of a Journal, displaying results of current studies in the field of biology and chemistry, facilitates highlighting of theoretical and practical issues and distribution of scientific discoveries.

One of the basic goals of the Journal is to promote the extensive exchange of information between the scientists from all over the world. We welcome publishing original papers and materials of Biological and Chemical Conferences, held in different countries (after the process of their subsequent selection).

Creation of special International Journal of Biology and Chemistry is of great importance, because a great amount of scientists might publish their articles and it will help to widen the geography of future collaboration. We will be glad to publish also the papers of the scientists from the other continents.

The Journal aims to publish the results of the experimental and theoretical studies in the field of biology, biotechnology, chemistry and chemical technology. Among the emphasized subjects are: modern issues of technologies for organic synthesis; scientific basis of the production of physiologically active preparations; modern issues of technologies for processing of raw materials, production of new materials and technologies; study on chemical and physical properties and structure of oil and coal; theoretical and practical issues in processing of hydrocarbons; modern achievements in the field of nanotechnology; results of studies in the fields of biology, biotechnology, genetics, nanotechnology, etc.

We hope to receive papers from a number of Scientific Centers, which are involved in the application of the scientific principles of biology, biotechnology, chemistry and chemical technology on practice and carrying out research on the subject, whether it relates to the production of new materials, technology and ecological issues.

UDC 504.5:574

[1*]Nurseitova M., [2]Muratova B., [2]Toregozhina Zh.,
[3]Jurjanz S., [2,4]Konuspayeva G.1., [4,5]Faye B.

[1]Research and Production Enterprise LPP «Antigen», Co Ltd, 4,
Azerbayeva str., Abay, 040905 Almaty oblast, Kazakhstan
[2]Al-Farabi Kazakh National University, 71 av. Al Farabi, 050073 Almaty, Kazakhstan
[3]UR AFPA-INRA, Universite de Lorraine, TSA 40602, 54518 Vandoeuvre cedex, France
[4]Al-Kharj Camel project, P.O. Box 761. Al-Kharj, 11941. Saudi Arabia
[5]CIRAD - Departement Environnements et Societes, Campus International de Baillarguet,
TA C-DIR / B 34398 Montpellier Cedex 5, France
*E-mail: mnurseitova2@gmail.com

Bioaccumulation and decontamination mechanisms of persistent organic pollutants (PCB, DDT) in bodies of Bactrian camels

The present study aimed to determine the mechanisms of bioaccumulation and decontamination of Polychlorinated biphenyls (PCBs) and Dichlorodiphenyltrichloroethane (DDT) in the body of two-humped camels *Camelus bactrianus*. The experiment has been carried out in Suzak region of South Kazakhstan. Four lactating two humped camels received 0.8 mg of indicator PCBs (1.3 μg/kg body weight) and DDT 0.12 (DDT 0.2 μg/Kg body weight) mg per camel/day during two months and followed by a 4-month decontamination period. Milk and hump fat of experimental camels have been sampled. Milk samples were analyzed using a liquid-liquid and hump fat using solid extraction by gas chromatography and mass spectrometry method. Concentrations of PCBs and DDT in milk and hump reached a plateau at the end of the 2 months exposure period. Transfer rates into milk ranged between 2% for PCB 101 and 71 % for PCB 180 of the daily dose, which was generally lower than rates observed in ruminants. In the same time, the most important part of the contaminants has been stored in the humps. At the end of experimentation, the total quantity of PCBs excreted in milk was estimated to 28.6 μg and the total quantity accumulated during the contamination period in humps was 5530 μg. Despite a huge variability between the different congeners of iPCBs, the intermediate storage of lipophilic compounds in the humps reduced the concentrations excreted in milk but on the other hand would extent the duration of the decontamination period in comparison with ruminants.
Key words: bioaccumulation, decontamination, camels.

Introduction

Persistent organic pollutants (POPs) are organic compounds that are resistant to environmental degradation and capable of causing negative effects on human health and the environment [1]. Due to these properties, in 18 May of 2001, 110 countries signed the Stockholm Convention on Conference of United Nation Organization, where the countries agree: to prohibit and put out of production, use, and release of POPs. Initially, twelve POPs have been recognized as causing adverse effects on humans and the ecosystem and within are PCBs as industrial chemicals and DDT among pesticides [2]. There are 209 congeners of PCBs with different physical, chemical and biological properties. PCBs have been used in power and chemical plants; they have been included in transformer and capacitor oils as additives to paints, plastics, rubber, as well as in lubricants and insulating materials. DDT is one of the pesticides, which included to the list of POPs. It is an effective insecticide widely used in agriculture over years during the last century to control the insect vectors of typhus, malaria and dengue fever. Also, it was made available to farmers as an agricultural insecticide [3]. The lactating ruminant may be exposed to DDT and PCB when they are eating contaminated feed or soil during grazing as these compounds are accumulated in the body [4]. According to the previous published data regarding impact of PCBs congeners 54, 80, 155 and one derivative of DDT 4.4 DDE in ruminant (sheep) previously contaminated by intramuscular injection under experimental conditions, the toxic equivalent of pollutants (on a fat basis) was approximately 2.5

 Printed in Kazakhstan

times higher in milk than in blood [5]. Moreover, studies of the transfer of PCB to milk in goats exposed to a long-term intake of contaminated hay under experimental conditions also shown that the contaminants had rapidly high concentrations of PCBs in milk after one-week exposure [6]. These studies of kinetics of contamination and decontamination of the animals in order to precise the transfer of pollutants in lactation goats and sheep were carried out in European countries. But researches on the transfer of pollutants and the mechanism of distribution of contaminants in camel organs (hump-fat, milk) have never been carried out and the concentration of this pollutant has not been studied in comestible parts of animals. Camels have a special characteristic as a biological model among all farm animals, and in general all mammals. Camels have the ability to survive and adapt to hard environmental conditions. Metabolic studies of PCBs and DDT in the body of *Camelus bactrianus* allow to understand the adaptive ability to survive in polluted environments. In the comparative studies of the effect of organic and inorganic selenium supplementation on selenium status in camel, metabolism of selenium in camel organism is observed to be less than in cattle [7]. Physiological characteristics of laboratory animals are considered from the standpoint of comparison with human physiology. Impact of these pollutants helped get a general idea, how they can affect the humans. Studies on the sheep and goats were conducted to control the meat of these animals as the object of the food chain. On the one hand, these studies supplement scientific data as a potential contamination object in the food chain. On the other hand, studies on such special biological models as *Camelus bactrianus* allow to better understand the biological intake of pollutants such as PCBs and DDT. In addition, it is necessary to take into account the fact that in the desert regions camels are sometimes the only type of livestock; as a result they are the only source of milk, meat and wool for humans. That's why this work devoted to study the entry and distribution of DDT and PCBs in the body of camels, as well as ways of removing these contaminants.

Materials and methods

The main three steps of this experiment were: (1) contamination of the animals to reach a steady state situation, (2) determination of the POPs concentration in the different compartments (blood. fat and milk), and (3) monitoring of the decontamination process**.** Regarding the first step, it was necessary to assess the importance of the different compartments: (1.1) weight of the animal, (1.2) weight of the hump as main site of fat storage, (1.3) milk production (especially its fat content). Regarding the second and the third steps, the changes of the POPs concentrations during contamination and decontamination stage are assessed in the different compartments.

For experiment four lactating *Camelus Bactrianus,* 7-16 years old were used. The weight of animals ranged from 400 to 520 kg. Before experiment, data about age, calving date, and parity were reported as well as sex of calves. All camels have been identified with ear tags. The animals were in healthy conditions all along the study.

Experimental camels were exposed to DDT (Pestanal, analytical standard – 31041, Fluka) and PCBs mixture (Aroclor 1254 – analytical standard- 48586, Sigma-Aldrich), which were introduced in gelatin capsules (length – 2 cm. diameter – 9 mm) by hexane solvent. The capsules were filled with icing sugar fixing the introduced chemicals and allowing the evaporation of the solvent.. The contaminants for one camel were quantified for PCBs 1.3 µg/kg and DDT 0.2 µg/kg body weight by day. In one capsule the concentration of PCBs was 0.8 mg and DDT 0.12 mg per camel/day. As each camel received one capsule during 56 days, the total exposure doses of one camel was 44 mg of PCBs and 6.7 mg of DDT. The daily supply of capsules was realized inside of bread. In order to reach the concentration plateau (steady state) more rapidly, a primary dose of 9.13 mg for PCBs and 1.41 mg DDT was given by intravenous injection on the first day of exposure. This dose with PCBs and DDT solution was prepared in oil solvent (Cremophor EL - reference 95921 SUPELCO). The primary dose was 12 times higher than dose in capsules. During the experiment the milk, serum of blood and hump fat were sampled. Also, the body, hump measurements were made and milk yield was estimated, the milk composition (fat content. dry matter and density) was determined at each sampling date.

Analytical works have been done in CPHMA (The Center of Physico-Chemical methods of Analysis), Laboratory of Ecology of the Biosphere, in GH-Agilent, with mass spectrometric and flame ionization detection Agilent 6890N / 5973N, equipped with a system of pre-concentration of liquid and solid samples Agilent-Velocity XPT.

Milk and blood serum were analyzed using a liquid-liquid and fat using solid extraction followed by cleanup on a multi-layer silica gel column, evaporative concentration to 20 µL and analysis on 7890A/5975C TAD TVL GC-MS (Agilent, USA)

equipped with Combi-PAL autosampler (CTC Analytics AG, Switzerland). Two µL of sample was injected to split/splitless inlet heated to 250^{0}C in splitless mode. Separation was done on a DB-5MS 60 m x 0.25 mm. 0.25 µm film column (Agilent, USA) at a constant flow of helium (purity 99.995%, Orenburg-Tehgas, Russia) equal to 1 mL/min. Detection was done in selected ion monitoring mode (SIM) using 6-group program for detection of target ions. PCB209 was used as internal standard spiked to samples in amount of 300 pg.

The results have been expressed by the mean of four camels within three periods ± standard error of the mean (SEM): period 1 – contamination period; period 2 – first two months of decontamination period with fat mobilization; period-3 – second two months of decontamination period with fat storage. The statistical differences between the 3 periods were assessed by variance analysis (ANOVA) using XL-stat software (Addinsoft©). Only the difference between periods was tested.

Results and their discussion

The metabolism of POPs includes the intake, the transport of biological fluid in blood and lymph, their storage in adipose tissue and the excretion through feaces, urine and milk. In the frame of our experiment the concentration in hump fat and excretion in milk has been assessed in order to determine the bioaccumulation and decontamination mechanisms of pollutants in these different compartments. In the gastrointestinal tract, after ingestion of the capsule with contaminants, pollutants enter into forestomach of the camel, and then entered in the bloodstream. The blood transferred the pollutants to other compartments, especially in adipose tissue, the hump representing the main part. A part of the contaminants is excreted with milk in lactating ruminants and probably also through the feaces. For a better understanding, the results were expressed according to the 3 main periods of the experiment: (1) the mean values during the two months of contamination (contamination period), (2) the mean values during the first 2 months of decontamination, and (3), the mean values during the last two months of decontamination. However, the kinetics was presented by taking into account the mean of the 4 camels and the sum of PCBs on the one hand and of DDT/DDE on the other hand.

At the beginning of the contamination period, the lipophilic properties of pollutants lead to a rapid increasing of their concentrations in hump, and because the animals are in phase of fat storage, in total quantity. At the same time, the concentrations in milk did not increase in a notable manner. When the plateau was reached after two months of contamination, the concentrations in blood and milk increased, showing the elimination of pollutants (Fig. 1, 2).

It seems that the main storage of organic pollutants in the hump would first slow the transfer into milk but also extend the time necessary for decontamination in comparison to other ruminants.

By considering the cumulative excretion in milk all along the experiment and the quantity of pollutants in hump at the beginning of the experiment, the global kinetics of bioaccumulation and excretion process could be summarized for both PCB and DDT (Fig. 1, 2).

This phenomenon is accentuated because of the hump weight decreased after starting decontamination (during summer time) due to the fat mobilization. The concentration and the quantity of pollutants stored in hump decreased regularly all along the decontamination period. The elimination in milk appeared low in quantity because the transfer to milk is in low percentage (between 2 and 9% depending to congeners) contrary to other species as cow and goat. A similar trend occurred for PCBs and DDT.

At the end of experimentation, the total quantity of PCB and DDT excreted in milk were estimated to 28.6 and 0.95 µg respectively and the total quantity accumulated during the contamination period in hump was 5530.4 and 54.3 µg respectively. In consequence, the percentage of excreted pollutants in milk was low: only 0.52% for PCB and 1.74% for DDT on average. The percentage of pollutants accumulated in hump was less than 15% of the total intake with a higher proportion for PCB than for DDT. After 4 months of decontamination, the total quantity of PCB and DDT was disappearing respectively 47.4% and 35.5% of the maximum concentration at the contamination period.

Conclusion

Besides the assessment of the live weight, hump volume and milk yield in field conditions, the main conclusions of our work regarding the transfer of POPs in Bactrian camel model are as follows:

The role of the camel hump (from 5.3 to 21.5 kg) as a pivotal organ (due to its importance in the cycle lipid storage/lipid mobilization) in the metabolism of pollutants having lipophilic properties is verified.

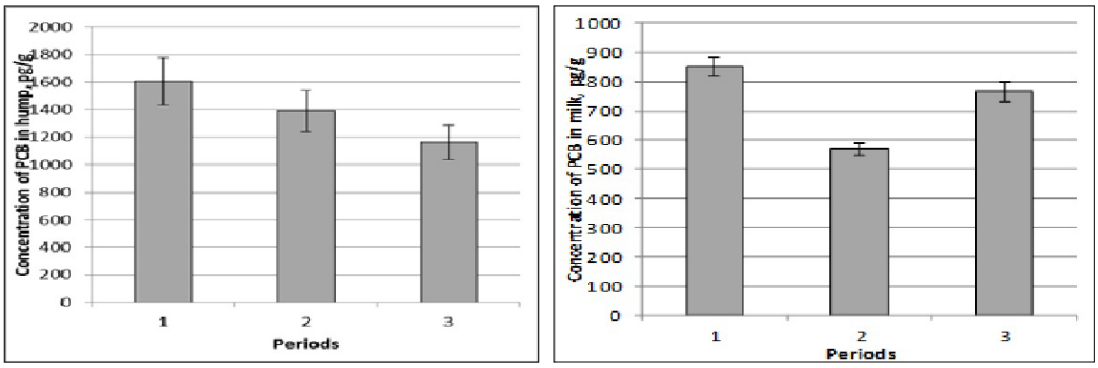

Figure 1 – Mean concentration of PCBs and SEM in hump tissue (left side) and in milk (right side) during the 3 periods of experimentation: 1 – contamination; 2 – first two months of decontamination; 3 – last two months of decontamination

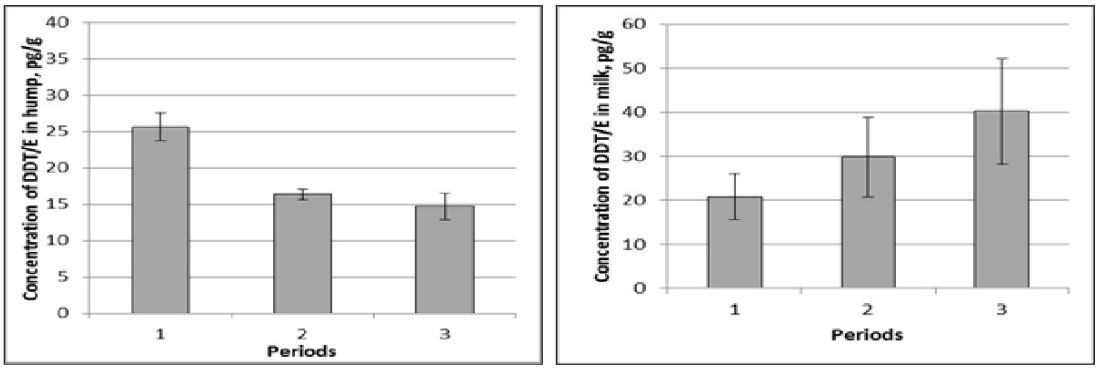

Figure 2 – Mean concentration of DDT/E and SEM in hump tissue (left side) and in milk (right side) during the 3 periods of experimentation: 1 – contamination; 2 – first two months of decontamination; 3 – last two months of decontamination

At reverse, in spite of the importance of this route of excretion and thanks to its fat content, only small concentrations of pollutants are observed in milk. On average, after 6 months of experiment, the percentage excreted in milk was 0.52% (PCBs) and 1.74% (DDT) of the cumulative POPs in the hump, but there is a high variability between congeners.

Based on the maximum quantity of pollutants in hump during the contamination period and the quantity available at the end of experiment, the percentage of loss of PCB was 47.4% and for DDT, it was 35.5% that means the camel could be completely decontaminated within less than one year.

Moreover, based on literature data, the concentrations of pollutants in milk were low compared to milk from other contaminated dairy animals as goats and cows. The carry-over rate (COR) was 8.9% for PCB52 in our study vs according to the literature 25% in goats, and 7.7% for PCB180 in our study vs 55% in goats and 65% in cows. As the carry over rate for camels seems to be very low, in comparison to other ruminants. we could conclude that:

a. The camels would transfer pollutants in milk slowlier than other ruminants;

b. The application of transfer rates stated in other ruminants may overestimate the exposure of dairy camels.

c. Complete decontamination of camels would certainly take more time than in other ruminants

The present work has been achieved in a private farm. The lack of experimental camel farms in research structures of Kazakhstan is an important constraint for the future research activities regarding this specie. Regarding the important place of camel products in food habits in Kazakhstan, this lack should be considered in future development of research facilities. In the international scientific community interested by the camel (International Society for Camelid Research and Development – ISOCARD), the studies regarding the behavior of camel faced to pollution are very few. The present study appears original and innovative for camel scientists over the world and confirms the interest of this species as a biological model in such research regarding the im-

pact of environmental pollution on animal products. The special focus on Bactrian Camels poorly studied in the scientific literature allowed to enlarge existing knowledge about this specie emblematic of Central Asia.

References

1 Aarhus Protocol on Long-range Transboundary Air Pollution. Persistent Organic Pollutants. – 1998 //www.unece.org. 30.04.2015.

2 The Stockholm Convention on Persistent Organic Pollutants. – 2009. //www.chm.pops.int.10.05.2015.

3 Ritter L., Solomon K.R., Forget J. Persistent organic pollutants/ Report of International Programme on Chemical Safety (IPCS) within the framework of the Inter-Organization Programme for the Sound Management of Chemicals (IOMC). – 2004. – P. 34

4 Jurjanz S., Feidt C., Pe´ rez-Prieto L., Ribeiro A., Filho H.M.N., Rychen G.and Delagarde R. Soil intake of lactating dairy cows in intensive strip grazing systems//Animal. – 2012. – No. 6:8. – P. 1350–1359.

5 Berg V., Lyche J.L., Gutle A.C., Lie E., Utne Skaare J., Aleksandersen M., Ropsta E. Distribution of PCB 118 and PCB 153 and hydroxylated PCB metabolites (OH-CBs) in maternal, fetal and lamb tissues of sheep exposed during gestation and lactation // Chemosphere. – 2010. – Vol. 80. – P. 1144–1150.

6 Rychen G., Jurjanz S., Toussaint H., Feidt C. Dairy ruminant exposure to persistent organic pollutants and excretion to milk //Animal. – 2008. – No. 2:2. – P. 312–323.

7 Faye B., Saleh S.K., Konuspayeva G., Musaad A., Bengoumi M., Seboussi R.Comparative effect of organic and inorganic selenium supplementation on selenium status in camel // Journal of King Saud University – Science. – 2014. – No. 26. – P. 149–158.

UDC 577.27; 612.017.1:616-006

*Abramova V.A., Kali A., Abdolla N., Yurikova O.Yu., Perfilyeva Yu.V., Ostapchuk Ye.O., Tleulieva R.T., Madenova S.K., Belyaev N.N.

M.A.Aitkhozhin Institute of Molecular Biology and Biochemistry, Almaty, Kazakhstan
*E-mail: mglory91@mail.ru

Influence of tumor cells on natural killer cell phenotype and cytotoxicity

Natural Killer (NK) cells are known to lyse tumor cells lacking MHC-I and expressing ligands for activating receptors, thereby participating in cancer immune surveillance. However, their function and phenotype change significantly in cancer patients. The precise molecular mechanism(s) involved in this phenomenon remain unknown. The aim of the present study was to investigate changes of both receptor phenotype and cytotoxic activity of NK cells co-cultured with K562 and HepG2 cells in dual-chamber Transwell® plates. A decrease of NK cell cytotoxicity against K562 cells was demonstrated. This effect was not a result of changes in perforin, granzyme or CD107a expression by NK cells or by production of cytokines (IFNγ, TNFα, IL-10, and TGFβ). No changes in the expression of a majority of NK cell receptors (CD16, CD69, 2B4, NKG2A, NKG2D, NKp30, NKp44, NKp46, and DNAM1) were observed. Only an increase in the percentage of NK cells bearing inhibitory receptor TIGIT was found as a result of co-culture with tumor cells. Possible molecular mechanisms of altered NK cell cytotoxicity involving TIGIT are discussed.
Key words: NK cells, cytotoxicity, cancer immune surveillance.

Introduction

Natural Killer (NK) cells play a key role in immune surveillance in cancer. They dispatch susceptible cells by various mechanisms, including antibody-dependent cellular cytotoxicity, receptor-mediated induction of apoptosis, and triggered release of cytotoxic granules containing perforin and granzyme [1]. Initiation of killer NK cells begins with recognition of specific ligands expressed on target cells by a panel of receptors functionally categorized as activating or inhibitory. The NK cell response represents a net result of the interplay of signals from these activating and inhibitory receptors [2].

NK cell function and phenotype are severely altered in various types of malignant tumors, such as colorectal, breast, lung, hepatic, and others [3-6]. Various soluble factors secreted by tumor cells and their immunosuppressive microenvironment, including Treg cells, myeloid-derived suppressor cells, tolerogenic dendritic cells, and others, contribute to these changes [3]. However, NK cell function and phenotype change significantly in cancer patients, and the molecular mechanism(s) involved remain unknown.

The aim of the present study was to study changes of both receptor phenotype and cytotoxic activity of human NK cells co-cultured with K562 and HepG2 cells in dual-chamber Transwell® plates. Results revealed a decrease of NK cell cytotoxicity under the influence of soluble tumor factors, accompanied by an increase in the percentage of NK cells expressing inhibitory receptor TIGIT.

Materials and methods

Blood samples and cell lines

This study was approved by relevant institutional review boards and all volunteers gave written informed consent according to the Helsinki Declaration. Peripheral blood samples were obtained from healthy volunteers. Human erythroleukemia K562 and hepatocarcinoma HepG2 cell lines were purchased from ATCC (USA). Cells were cultured in complete culture medium consisting of RPMI-1640 supplemented with 10% fetal calf serum, 2 mM glutamine, 100 U/ml penicillin, and 100 mg/ml

 Printed in Kazakhstan

streptomycin (Sigma-Aldrich, USA) at 37°C and 5% CO_2. Before use, adherent HepG2 cells were detached from Petri dishes with a 0.05% trypsin solution and washed in RPMI-1640 medium.

Antibodies

The following labeled anti-human monoclonal antibodies (mAbs) were used for flow cytometry: anti-CD3-FITC, anti-CD56-PE, anti-CD56-PerCP, anti-CD107a-PerCP-Cy5.5, and anti-CD16-PE (Biolegend, USA); anti-NKp44-APC, anti-TIGIT-biotin, anti-DNAM-1-APC, anti-NKp46-APC, anti-CD69-FITC, anti-Perforin-APC, anti-NKp30-APC, anti-2B4-FITC, and anti-NKG2D-APC (Miltenyi Biotec, Germany); anti-NKG2D-PE and anti-Granzyme-PE (BD Biosciences, USA); anti-NKG2A-PerCP (R&D Systems, USA). Streptavidin-PE (R&D Systems, USA) was used for detection of cells linked to anti-TIGIT-biotin.

Cell separation

Peripheral blood mononuclear cells were isolated from venous peripheral blood by Hystopaque-1077 (Sigma-Aldrich) density gradient centrifugation. NK cells were purified by immunomagnetic separation using an NK Isolation Kit and VarioMACS cell separator (Miltenyi Biotech) according to the manufacturer's instruction. The purity of $CD3^-CD56^+$ cell populations exceeded 90% as estimated by flow cytometry.

Design of experiment in Transwell plates

NK cells ($5x10^5$) were placed in the bottom chamber of dual-chamber Transwell® plates (Sigma-Aldrich) in 1750 µl of complete culture media. Upper wells were filled with 250 µl of culture media containing $5x10^5$ HepG2 or K562 cells. Only NK cells were incubated in control wells. Co-culture lasted for 48 h at 37°C and 5% CO_2, then NK cells were collected, labeled with mAbs, and subjected to flow cytometry. The following receptors were analyzed on gated $CD3^-CD56^+$ cells: CD16, NKG2A, NKG2D, NKp30, NKp44, NKp46, CD69, DNAM1, TIGIT, and 2B4.

Flow cytometry

For surface and intracellular staining, cells were first incubated with mAbs specific for surface markers according to the manufacturer's protocols, then fixed and permeabilized with Fixation/Permeabilization solution (BD Pharmingen, USA), mixed well, and incubated for 20 min in the dark at room temperature. Cells were then washed with Perm/Wash Buffer (BD Biosciences) and stained with mAbs specific for intracellular molecules. Afterwards, cells were washed with phosphate-buffered saline, resuspended in flow solution, and immediately analyzed by flow cytometry with FACSCalibur (BD Biosciences) and CellQuest software (BD Biosciences).

NK cell cytotoxicity assay

A 3-(4,5-dimethylthiazol-2-il)-2,5-diphenyltetrazolium bromide (MTT) assay was used to assess NK cell cytotoxicity. After incubation with K562 cells, HepG2 cells, or alone in Transwell® plates, NK cells were collected, counted, and a part of them were subjected to cytotoxicity assay. K562 cells were used as a target. Effector and target cells in a 2:1 ratio were co-cultured in round bottom 96-well plates (Sigma-Aldrich) in 200 µl of complete culture medium for 72 h. Both NK and K562 cells alone were used as controls. Until the last 4 h of cultivation, 50 µl of MTT stock solution (500 µg/ml; Sigma-Aldrich) was added. After cultivation, supernatants were removed and formazan crystals were dissolved in 150 µl DMSO (Sigma-Aldrich) and absorbance determined at an optical density (OD) of 492/630 nm. The index of cytotoxicity (IC) was calculated as follows:

$$IC(\%) = 100\left(\frac{[C_{NK} + C_{K562} - E]}{[C_{NK} + C_{K562}]}\right),$$

where C_{NK} and C_{K562} are the OD of control wells and E is the OD of the experimental well.

NK cell cytotoxicity against K562 cells was also assessed by surface staining for CD107a and intracellular staining for perforin and granzyme B. For this, NK cells were co-cultured together with K562 cells as described above and then stained with anti-CD107a antibodies and incubated for 1 h, after which Brefeldin A (Biolegend, USA) was added according to manufacturer's instruction. After 3 hours, cells were collected, washed with phosphate-buffered saline, and subjected to intracellular staining for perforin and granzyme B according to manufacturer's instruction.

Cytokine secretion

Supernatants from co-cultures in Transwell® plates were collected and frozen at -20°C. Sandwich ELISA was performed using human IL-10, IFNγ (BD Biosciences), and TGFβ1 (R&D Systems) ELISA sets according the manufacturer's instructions.

Statistical analysis

Data are represented as mean values ± quadratic error. The Student's t-test was used to analyze data. P-values of 0.05 were chosen as the limit of statistical significance.

Results and their discussion

Analysis of NK cell cytotoxicity after co-culture with tumor cells

The cytotoxicity of NK cells against K562 cells is considered a gold standard for assessment of NK cell activity. In our study, the IC of NK cells after co-culture with HepG2 and K562 cells approached 52.2±9.3% and 53.4±10.3%, respectively, contrary to 65.5±10.8% in the absence of co-cultured tumor cell lines. Since donor NK cells naturally differ by their primary cytolytic activity, we normalized IC values to controls (NK cells incubated alone in Transwell® plates), which were considered as 100%. Thereafter, NK cell cytotoxicity after incubation with both tumor cell lines reached 20% (Fig. 1).

Perforin and granzyme, along with death receptor family ligands, are executioners of NK cell mediated cytotoxicity. CD107a is a marker of degranulation highly correlated with emptying or NK cell cytotoxic granules [7]. Unexpectedly, we did not find statistically significant differences in CD107a, perforin, or granzyme expression in NK cells co-cultured with tumor cell lines (Table 1).

Phenotyping of NK cells

Transwell® plates allow free exchange of soluble factors and secreted exosomes between co-cultured cells. We examined alterations of NK cell activating (DNAM-1, NKG2D, NKp30, NKp44, NKp46) and inhibitory receptors (TIGIT, NKG2A), as well as CD16 (FcRγIII), involved in antibody-dependent cellular cytotoxicity. However, changes in the expression of a majority of receptors/markers did not reach statistical significance (Table 2).

Taking into account the complex interplay between TIGIT and its activating counterpart, DNAM-1 [8], and their role in tumor surveillance, we analyzed independent and co-expression of DNAM-1 and TIGIT. A significant increase of NK cells expressing TIGIT alone after co-culture with both HepG2 and K562 cells was observed (Table 3). Levels of DNAM-1^{+}TIGIT^{-} and DNAM-1^{+}TIGIT^{+} NK cells did not change significantly (Table 3, Fig. 2).

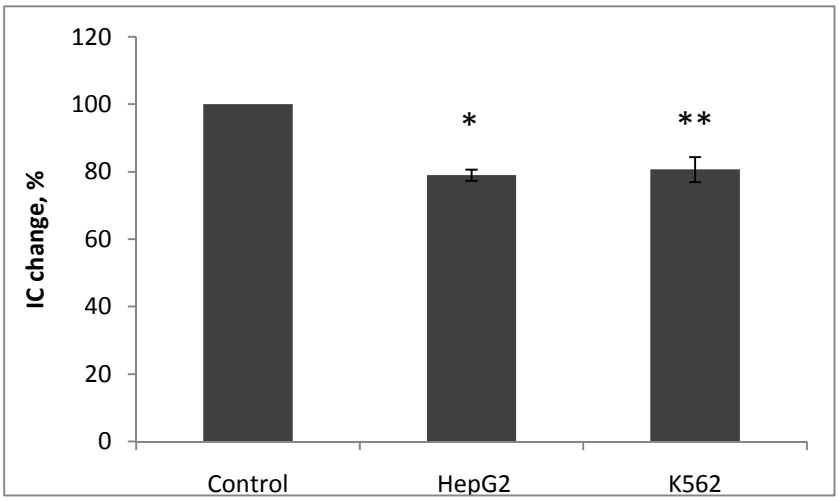

Figure 1 – Cytotoxicity of NK cells against K562 target after co-culture with HepG2 or K562 tumor cell line, assessed by MTT test. Data are normalized as percent of cytotoxicity index (IC) of NK cells, cultured in Transwell® plates alone, and are represented as M±m, n=3.
*P=0.007, **P=0.038

Table 1 – Percent of NK cells expressing molecules, associated with cytotoxicity

Items	Variants of test	Granzyme	Perforin	CD107a
1	NK alone	85.9±2.7	93.4±1.0	99.2±0.4
2	NK + HepG2	80.0±7.2	89.2±2.8	94.4±5.3
3	NK + K562	80.5±3.3	89.6±1.8	96.1±3.0
4	n	3	4	5
5	P_{1-2}	P>0.05		
6	P_{1-3}	P>0.05		

Table 2 – Percent of NK cells expressing particular receptors

Items	Variants of test	CD16	CD69	2B4	NKG2A	NKG2D	NKp30	NKp44	NKp46
1	NK alone	69.9±11.5	2.5±0.4	86.5±21.7	4.1±2.3	76.3±5.6	5.7±2.4	1.8±0.8	89.5±3.2
2	NK+HepG2	79.8±1.3	5.3±2.4	81.2±10.2	3.5±1.8	76.6±8.7	7.4±3.4	2.9±1.3	91.0±3.6
3	NK+K562	73.4±6.0	8.5±5.4	82.8±10.5	7.1±3.0	69.9±11.6	3.5±0.9	2.7±0.6	89.1±4.4
4	n	5	7	7	5	6	7	6	5
5	P_{1-2}	P>0.05							
6	P_{1-3}	P>0.05							

Table 3 – Percent of NK cells, expressing DNAM-1, TIGIT or their combinations, by NK cells

Items	Variants of test	DNAM-1	TIGIT	DNAM-1^{+}TIGIT $^{+}$
1	NK alone	94.8±2.0	4.7±1.4	6.1±2.4
2	NK+HepG2	94.2±1.2	10.4±2.5	16.9±5.1
3	NK+K562	95.6±1.1	12.0±2.5	18.8±6.7
4	n	3	5	3
5	P_{1-2}	0.811	0.042	0.204
6	P_{1-3}	0.767	0.015	0.273

Analysis of cytokine production

Cytokines are known to modulate NK cell activity. We analyzed participation of proinflammatory (IFNγ, TNFα) and anti-inflammatory (IL-10, TGFβ) cytokines in modulation of NK cytotoxicity by determining their concentrations in no-culture supernatants. No changes in the concentration of any of these cytokines were found in the culture media after NK cell co-culture with tumor cells (Table 4).

The functional incapacitation of NK cells infiltrating tumors is well established [5]. Much research has been performed to analyze NK cell peculiarities in the presence of tumor cells *in vitro* and in cancer patients, but precise molecular mechanism(s) of this phenomenon remain unknown. Theoretically, two influences could alter NK cell cytolytic activity: cell-to-cell contact and/or the impact of soluble factors. In this study, we analyzed the influence of possible soluble factors secreted by two different tumor cell lines during co-culture with NK cells in dual-chamber Transwells® on NK cytolytic activity, as well as NK cell receptor/marker expression and cytokine production.

Table 4 – Cytokine levels in conditioned media, pg/ml, M±m.

Items	Variants of test	IFNγ	TNFα	IL-10
1	NK alone	1579±43	170±3	257±8
2	NK+HepG2	1630±11	170±2	266±4
3	NK+K562	1707±40	182±6	268±14
4	n	3	3	3
5	P_{1-2}	P>0.05		
6	P_{1-3}			

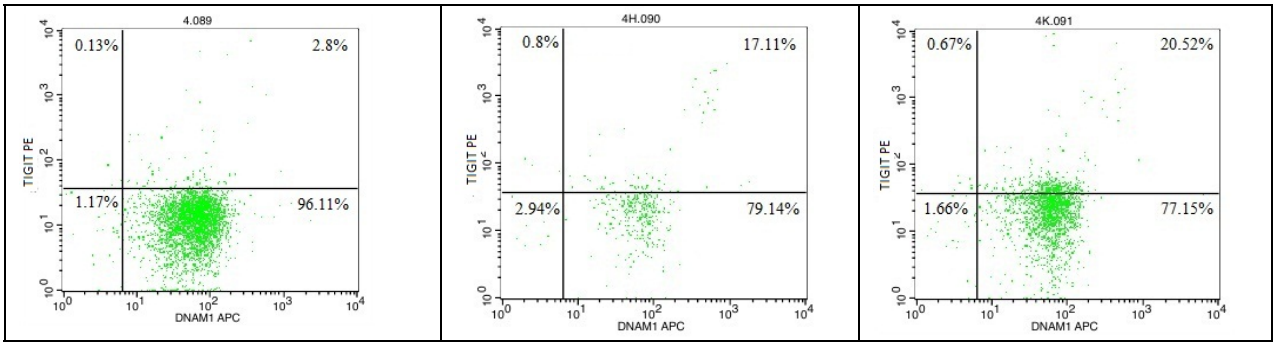

A B C

Figure 2 – Representative data of flow cytometry showing co-expression of DNAM-1 and TIGIT on NK cells after Transwell® co-culture experiments. A – NK cells cultured alone; B – NK cells after co-culture together with HepG2 cells; NK cells after co-culture together with K562 cells

A decrease in NK cell cytotoxicity to K562 cells after co-culture with either HepG2 or K562 cells probably involved certain soluble tumor factors. We showed that the decrease of NK cell activity was not associated with an alteration in perforin and granzyme expression, two proteins known to mediate the cytolytic impact of NK cells. Moreover, we did not observe changes in CD107a presentation on the NK cell surface. These results indicate the fundamental readiness of NK cells to cytolytic activity.

Taken together, decreased NK cell function possibly results from deterioration of target ligand recognition by NK cell receptors due to inhibition of receptor expression. Our analysis of a panel of NK cell receptors (CD16, CD69, 2B4, NKG2D, NKp30, NKp44, NKp46) did not elucidate any changes in their expression after co-culture with tumor cell lines. In addition, there was no change in the expression of inhibitory receptor NKG2A. However, we did detect an increase in the expression of another inhibitory receptor, TIGIT, on NK cells after co-culture with HepG2 and K562 cells. This finding is of particular interest because the NK cell response is determined by the net outcome of signals from activating and inhibitory receptors [2]. Many NK cell activating or inhibitory receptors share a common ligand [8, 9]. Distinctive examples are DNAM-1, TIGIT, and CD96, all critical regulators of NK cell function which share CD155 and CD112 ligands (members of nectin and nectin-like protein families) [10]. CD155 is a dominant ligand over CD112 for DNAM-1 and TIGIT [11]. CD155 (Necl5, PVR, Tage4) is an immunoglobulin-like receptor found on certain tumors [10, 12, 13].

Although functional involvement of TIGIT in altered NK cytotoxicity was not examined, our findings could theoretically be explained as follows. HepG2 and K562 cells express CD112 and CD155 [13] and secrete exosomes [14]. If CD112 or CD155 are enriched on exosomes or secreted as free soluble forms and bind TIGIT, thereby activating this inhibitory receptor, its engagement could depress NK cell cytotoxicity. However, this hypothesis does not explain the observed increase in the percentage of $TIGIT^+$ NK cells.

Recently it has been shown that K562 cells can secrete exosomes rich in microRNAs, many of which are involved in modulation of Wnt signaling pathways [14], which could change transcription of the gene encoding TIGIT. The role of Wnt signaling has been investigated previously in differentiation of NK cell lineages [15]. It is of interest to study other facets of this pathway in NK cell biology.

In conclusion, our study demonstrates an increase of NK cells expressing inhibitory receptor TIGIT that may decrease the natural cytotoxicity of these cells. It is of interest to determine whether this phenomenon is recapitulated in cancer patients and could represent a novel parameter in assessment of NK cell function.

References

1 Farag S.S., Caligiuri M.A. Human natural killer cell development and biology // Blood Rev. – 2006. – No20. – P. 123–137.

2 Lanier L.L. NK cell receptors // Annu. Rev. Immunol. – 1998. – No16. – P. 359-93.

3 Vitale M., Cantoni C., Pietra G., Mingari M.C., Moretta L. Effect of tumor cells and tumor microenvironment on NK-cell function // Eur. J. Immunol. – 2014. – No44. – V.6. – P.1582-92.

4 Taketomi A., Shimada M., Shirabe K., Kajiyama K., Gion T., Sugimachi K.Natural killer cell activity in patients with hepatocellular carcinoma A new prognostic indicator after hepatectomy // Cancer. – 1998. – V. 83. – Issue 1. – P. 58–63.

5 Mamessier E., Pradel L.C., Thibult M.-L., Drevet C., Zouine A., Jacquemier J., Houvenaeghel G., Bertucci F., Birnbaum D., Olive D. Peripheral blood NK cells from breast cancer patients are tumor-induced composite subsets // J. Immunol. – 2013. – No190. – V.5. – P. 2424-2436.

6 Jin S., Deng Y., Hao J.-W., Li Y., Liu B., Yu Y., Shi F.D., Zhou Q.H. NK cell phenotypic modulation in lung cancer environment // PLoS ONE. – 2014. – No9. – V.10. – e109976.

7 Alter G., Malenfant J.M., Altfeld M. CD107a as a functional marker for the identification of natural killer cell activity // J. Immunol. Methods. – 2004. – No294. – V.1-2. – P.15-22.

8 Stanietsky N., Mandelboim O. Paired NK cell receptors controlling NK cytotoxicity // FEBS Letters. – 2010. – No584. – P. 4895–4900.

9 Pauken K.E., Wherry E.J. TIGIT and CD226: tipping the balance between costimulatory and coinhibitory molecules to augment the cancer immunotherapy toolkit // Cancer Cell. – 2014. – No26. – P. 785-787.

10 Ogita H., Takai Y. Nectins and nectin-like molecules: roles in cell adhesion, polarization, movement, and proliferation // Life. – 2006. – No58. – V.5-6. – P. 334 – 343.

11 Nagumo Y., Iguchi-Manaka A., Yamashita-Kanemaru Y., Abe F., Bernhardt G., Shibuya A., Shibuya K. Increased CD112 expression in methylcholanthrene-induced tumors in CD155-deficient mice // PLoS. – 2014. – V. 9. – Issue 11. – e112415.

12 Atsumi S., Matsumine A., Toyoda H., Niimi R., Iino T., Sudo A. Prognostic significance of CD155 mRNA expression in soft tissue sarcomas // Oncol. Lett. – 2013. – No5. – V.6. – P.1771–1776.

13 Carlsten M., Norell H., Bryceson Y.T., Poschke I., Schedvins K., Ljunggren H.-G., Kiessling R., and Malmberg K.-J. Primary human tumor cells expressing CD155 impair tumor targeting by down-regulating DNAM-1 on NK cells // J. Immunol. – 2009. – No183. – P. 4921–4930.

14 Feng D.Q., Huang B., Li J., Liu J., Chen X.M., Xu Y.M., Chen X., Zhang H.B., Hu L.H., Wang X.Z. Selective miRNA expression profile in chronic myeloid leukemia K562 cell-derived exosomes // Asian Pac. J. Cancer. Prev. – 2013. – No14.– V.12. – P.7501-7508.

15 Aoyama K., Delaney C., Varnum-Finney B., Kohn A.D., Moon R.T., Bernstein I.D. The interaction of the Wnt and Notch pathways modulates natural killer versus T cell differentiation // Stem Cells. – 2007. – No25. – V.10. – P. 2488-2497.

UDC 575.17:58.088 (574.51)

*Pozharskiy A.S., Chekalin S.V.

Institute of Botany and Phytointroduction, Almaty, Kazakhstan
*E-mail: aspozharsky@gmail.com

Molecular study of *Berberis iliensis* M. Pop. and *Berberis sphaerocarpa* Kar. et Kir. wild populations in South-East Kazakhstan using ISSR markers

Berberis iliensis is a rare endangered plant species with decreasing natural area. Interspecific hybrids *Berberis iliensis* × *Berberis sphaerocarpa* are even more rare phenomenon. In this work 6 populations of *Berberis iliensis,* 4 populations of *Berberis sphaerocarpa* and a single *Berberis oblonga* population are analysed. DNA from barberry leaves was extracted using SDS method. ISSR analysis was conducted with 5 primers. UPGMA tree and STRUCTURE diagram of 11 populations were constructed. Obtained results show relations between *Berberis iliensis* and *Berberis sphaerocarpa* in pure and hybrid populations and lay a first basis for further investigation of Kazakhstan barberry species.
Key words: *Berberis iliensis, Berberis sphaerocarpa, Berberis oblonga,* ISSR.

Introduction

Berberis L. is the largest genus of *Berberidaceae* family including approximately 500 species, growing in Eurasia, North-East Africa, North and South America [1]. Most of them are widely used as food, medical and decorative plants. Some species are cultivated worldwide. The number of wild species of *Berberis* growing in Kazakhstan varies from 6 to 9 accordingly to different authors [2, 3]. *B. iliensis* M. Pop is a rare endemic species with decreasing natural area under protected stutus [4]. As a part of protecting measures a study of wild populations is conducted by laboratory of dendrology of Institute of Botany and Phytointroduction (Almaty, Kazakhstan) since 2009. During field studies a population containing plants with uncommon traits was discovered in Temirlik gorge (Ketmen mountains). These individuals were identified as inter-specific hybrids between *B. iliensis* and *B. sphaerocarpa* [5]. Such hybrids were not described previously. They are of particular interest, because *B. iliensis* and *B. sphaerocarpa* belong to different genus sections, *Integerrimae* and *Heteropodae*, respectively, and examples of hybridization between species from these sections are unknown. Hybrids of *B.iliensis* and *B. sphaerocarpa* are more rare than *B.iliensis* itself. So, it is important to conduct comprehensive research of barberries diversity in Kazakhstan on a level of populations as well as species in order to evaluate inter-specific genetic variation and clarify taxonomic status of local species. It is particularly important in order to protect such endangered species as *B. iliensis* and its rare hybrid forms from extinction. In this work, we performed analysis of six *B. iliensis* and four *B. sphaerocarpa* populations. Three populations of *B. iliensis* from Temirlik gorge and right banks of the Big Usek and Usek rivers were assumed to be hybrid populations with *B. sphaerocarpa.* Also, one population of *B. oblonga* Schneid. was analyzed in order to compare its kinship to *B. iliensis* and *B. sphaerocarpa.*

Materials and methods

Leaves of 134 plant samples in total were collected from wild populations in Almaty region (Table 1, Fig. 1). Harvested plant materials were stored at -80°C. DNA was isolated from frozen leaves by SDS method as described in [6]. Quantity and quality of extracted DNA were evaluated by electrophoresis in 1% agarose gel and measured by spectrophotometer NanoDrop2000 (Thermo Scientific, EU) at wavelengths 260, 280, 230 nm. 65 samples with optimal quantity and quality of DNA were selected for further analysis.

PCR was performed in 25 μl of reaction mix containing 2.5 mM of magnesium chloride (3.0 for

 Printed in Kazakhstan

ISSR), 10 mM of deoxyribonucleozide triphosphates, 10 mM of each ISSR primer, 0.5 unit of *Taq* DNA polymerase in standard 1x Taq buffer by Fermentas (Thermo Scientific, EU). 5 ISSR primers from [7] were used (Table 2). Amplification of ISSR markers was ran with following program: 1.5 min initial denaturation at 94°C, then 45 cycles of denaturation at 94°C for 40 s, annealing at specific temperature for each primer for 45 s, elongation at 72°C for 1.5 min, and final extension at 72°C for 15 min. PCR products were resolved by electrophoresis in 1,8% agarose gel in SB buffer with voltage 80 V for 3,5 h, stained by ethidium bromide and visualized in ultraviolet rays.

The ISSR band patterns were scored as «1» for presence and «0» for absense. Distance matrix based on Jaccard coefficients was calculated and visualized using FAMD 1.2 and MEGA 4 software [8, 9]. Bayesian MCMC analysis was performed on STRUCTURE software using admixture model with no prior location information; 100,000 cycles were done for both burn-in period and MCMC algorithm; 20 iterations for each *K* from 2 to 15 were run [10]. Results for each *K* over 20 runs were aligned by CLUMPP [11] and visualized by DISTRUCT [12]. The true *K* value was obtained by Evanno method as implemented in STRUCTURE HARVESTER website [13].

Table 1 – Analyzed populations of *B.iliensis, B. sphaerocarpa* and *B. oblonga.*

Species	Place	North longitude	East latitude	Altitude, m
Berberis iliensis	Akzhar	44° 56,320’	75° 48,628’	370
	Bakanas	44° 46,350’	76° 19,200’	395
	Darbazakum	43° 58,820’	79° 36,918’	505
	Right bank of Usek river	44° 27,461’	79° 49,326’	1170
	Right bank of the Big Usek river	44° 27,800’	79° 49,340’	1250
	Temirlik	43° 17,050’	79° 12,252’	1080
Berberis sphaerocarpa	Altyn Emel	44° 11,429’	78° 33,711’	1300
	Big Kirgyzsay	43° 19,174’	79° 31,220’	1470
	Turgen	43° 21,420’	77° 37,865’	1220
	Talgar	43° 13,762’	77° 16,848’	1570
Berberis oblonga	Aksu Dzhabagly	42° 19,727’	70° 19,727’	1460

Table 2 – ISSR primers used for analysis [7]

Primer ID	Length	Sequence	Annealing temperature
201274	14	5’ – CACACACACACARY – 3’	40°C
201275	14	5’ – CACACACACACARG – 3’	42°C
201276	16	5’ – AGAGAGAGAGAGAGYC – 3’	48,2°C
201277	14	5’ – GTGTGTGTGTGTYR – 3’	40°C
201278	14	5’ – GTGTGTGTGTGTAY – 3’	40°C

Results and their discussion

101 bands in total were obtained, 20.4 per primer in average, 99 of them are polymorphic. 32.0±7.0 band presences per individual were observed. Data were analyzed and dendrogram was constructed with unweighted pair group method with arithmetic mean (UPGMA) (Fig. 2). Three distinct clusters are observed. The first cluster corresponds to three *B. iliensis* populations from valley of Ili river. Populations from delta of Ili river (Akzhar and Bakanas sites) form one mixed subcluster, and a population from Darbazakum forms distinct subcluster. The second cluster corresponds to *B. sphaerocarpa* populations with one *B. oblonga* population. The third cluster combine three *B. iliensis* populations which are

considered as hybrid (from Temirlik gorge and the right bank of Big Usek river) and a population from the right bank of Usek river. STRUCTURE analysis was performed, and the true number of clusters was estimated as K=2 by highest ΔK parameter (Evanno method). The second high value of ΔK was at K=6. The STRUCTURE diagram for two clusters demonstrate clearly distinct groups of pure *B. iliensis* and *B. sphaerocarpa* individuals (Fig. 3). Putative hybrid populations demonstrate mixed origin from two species with prevalence of *B. iliensis*, and this supports an assumption about interspecific hybridization. *B. oblonga* demonstrate predominant relation with *B.sphaerocarpa* cluster. With increase of K complexity of population structure also increases. The diagram for six clusters shows hybrid populations having specific cluster membership. The Altyn Emel population of *B.sphaerocarpa* and Darbazakum population of *B. iliensis* are clearly distinct from other populations of their species, respectively.

Figure 1 – Location of 11 barberry populations used for analysis. 1 – Bakanas, 2 – Akzhar, 3 – Altyn Emel, 4 – right bank of Usek river, 5 –right bank of the Big Usek river, 6 – Darbazakum, 7 – Big Kirgyzsay, 8 – Temirlik, 9 – Turgen, 10 – Talgar, 11 – Aksu Dzhabagly.

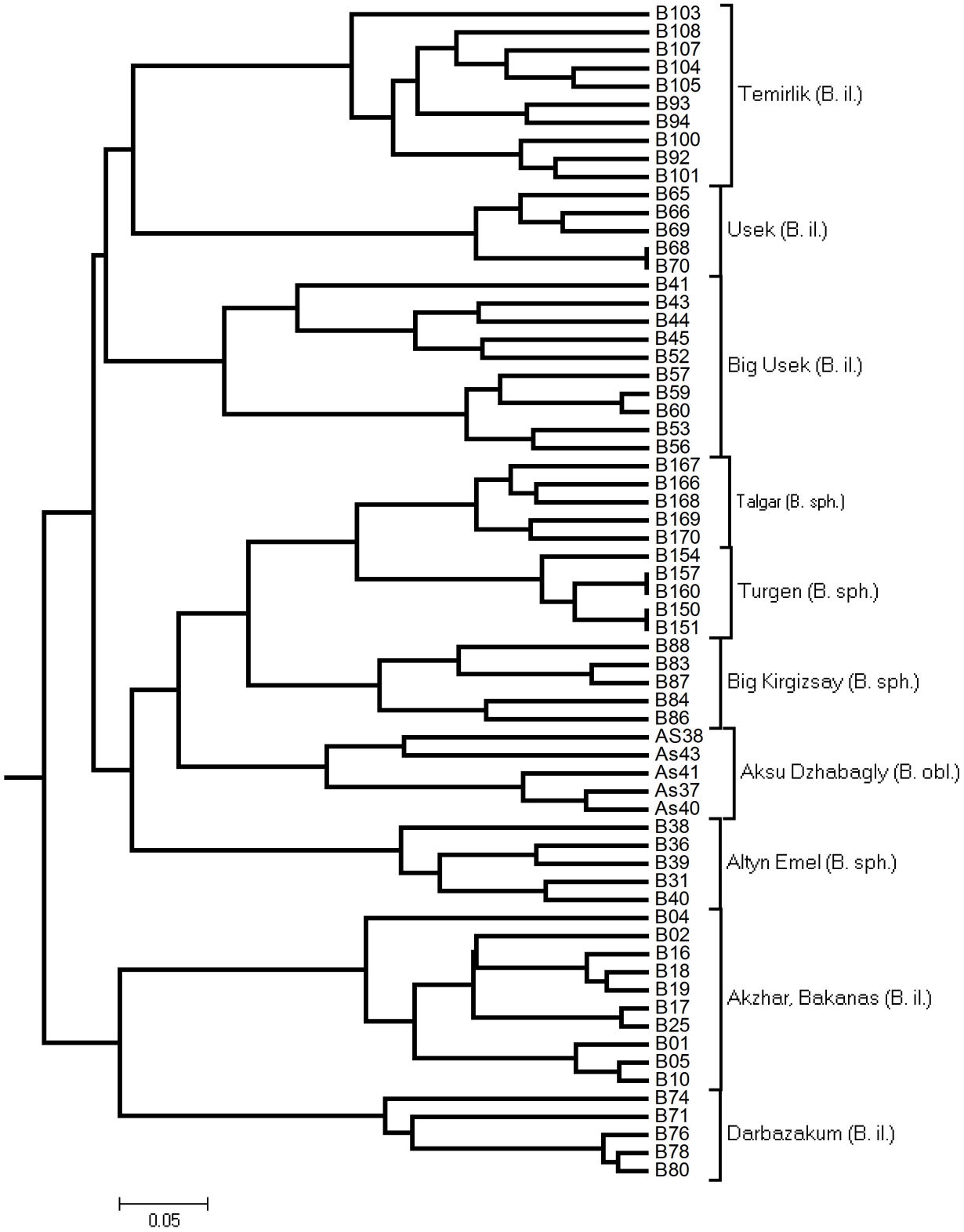

Figure 2 – UPGMA dendrogram of 65 individuals from 11 barberry populations.

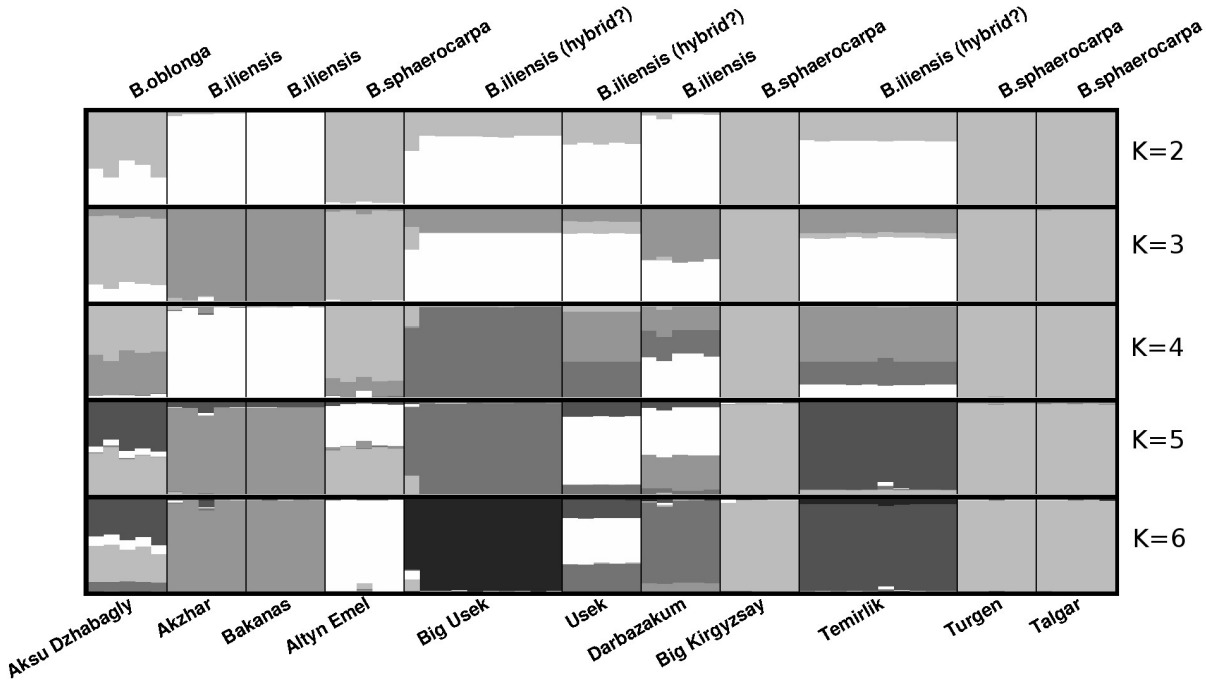

Figure 3 – STRUCTURE diagram of 11 barberry populations for *K* from 2 to 6.

Previously we obtained a proof of a hybridization between *B. iliensis* and *B. sphaerocarpa* in Temirlik population using ISSR markers (unpublished data). Results of this work support assumption about interspecific hybridization in three *B. iliensis* populations. However, there is a contradiction between results obtained using different approaches. Accordingly to UPGMA dendrogram of Jaccard distance coefficient, hybrid populations are more closely related with *B. sphaerocarpa,* but bayesian approach implemented in STRUCTURE shows predominant *B. iliensis* origin of hybrid populations. Both methods shows high similarity of *B. oblonga* population with *B. sphaerocarpa,* however data from one population are not sufficient for firm conclusion about relationship between these species. Ambiguity of data about population structure of *B. iliensis* and *B. sphaerocarpa* and their hybrid populations is probably due to low reliability of such multilocus dominant markers as ISSR and restricted sample of individuals. So, it is important to conduct further research with more reliable methods, and the present study is initial step of investigation of *Berberis* diversity in Kazakhstan on individual, population and specific levels.

Acknowledgment

We thank the head of laboratory of molecular biology of Institute of Plant Biology and biotechnology Galiakparov N.N. for kindly provided materials and equipment.

References

1 Ahrendt L. *Berberis* and *Mahonia*, a taxonomic revision// Bot. J . Linn. Soc.. – 1961. – Vol. 57. – 1–410.

2 Sokolov S. J. (ed.) Trees and shrubs of USSR part VII. - Leningrad: Academia of Science of USSR press., 1954. – 872 p.

3 Dzhangaliev A. D., Salova T. N. & Turekhanova P. M. The wild fruit and nut plants of Kazakhstan// Horticultural Reviews. – 2003. – No23. – 305-371.

4 Resolution of the Government of Republic of Kazakhstan №1034. About approval of the list of rare and endangered animal and plant species. – October 31, 2006.

5 Chekalin S. V., Muhitdinov A. S., Zaychenko O. P., Nabieva S. V., Masalova V. A., Pozharskiy A.S. Natural hybridization of *Berberis iliensis* M. Pop. and *Berberis sphaerocarpa* Kar. et Kir.// Preservation and rational use of genetic fund of wild fruit forests of Kazakhstan: Proceedings of the Interanational academic conference. – Almaty, 2013. – P. 140-145.

6 Dellaporta S.L., Wood J., Hicks J. B. A plant DNA minipreparation: version II// Plant molecular biology reporter. – 1983. – Vol.1 – No4. – 19-21.

7 Wolfe A. D., Xiang Q.-Y., Kephart S. R. Assessing hybridization in natural populations of Penstemon (Scrophulariaceae) using hypervariable intersimple sequence repeat (ISSR) bands //Molecular Ecology . – 1998. – No7. – 1107-1125.

8 Schlüter P. M., Harris S. A. Analysis of multilocus fingerprinting data sets containing missing data// Molecular Ecology Notes . – 2006. – No6. – 569-572.

9 Tamura K., Dudley J., Nei M., Kumar S. MEGA4: Molecular Evolutionary Genetics Analysis (MEGA) software version 4.0// Molecular Biology and Evolution. – 2007. – No24. – 1596-1599.

10 Pritchard J. K., Stephens M., Donnelly P. Inference of population structure using multilocus genotype data// Genetics. – 2000. – No155. – 945-959.

11 Jakobsson M. & Rosenberg N. A. CLUMPP : a cluster matching and permutation program for dealing with label switching and multimodality in analysis of population structure// Bioinformatics. – 2007. – Vol. 23. – 1801-1806.

12 Rosenberg N. A. Distruct: a program for the graphical display of population structure// Mol.Ecol. Notes. – 2004. – Vol. 4. –137–138.

13 Earl, Dent A. and vonHoldt, Bridgett M. STRUCTURE HARVESTER: a website and program for visualizing STRUCTURE output and implementing the Evanno method // Conservation Genetics Resources. – 2012. – Vol. 4 (2). – P. 359-361.

UDC 576.3/7.086:581.143:633.11

Turasheva S.K.

Al-Farabi Kazakh National University, Almaty, Kazakhstan
E-mail: svetlana.turasheva@kaznu.kz

Production of wheat doubled haploids by *in vitro* anther culture

The *in vitro* culture response of anthers, originating from high yielding and resistance to lodging F_1 soft wheat hybrid plants selected under drought conditions, was investigated. The spikes were collected when the microspores were at the mid-uninucleate stage and after 3 days at 4^0 C for cold pre-treatment, the anthers were cultured in N6 and Gamborg-Eveleg B5 (B5) solid medium. Progeny from 17 different F1 families were used and 9 of them responded to *in vitro* anther culture and 7 of them produced fertile green plants. Doubled haploid green plants were fertile and produced seeds. Induction of haploid development depends on genotype, stage of male gametophyte development, composition of nutrient media and conditions of cultivation. The effect of the composition of media and different genotypes on wheat anther culture was investigated. From the genotypes produced regenerants, the high yielding genotypes from local breeding collection of wheat produced more albino plants (35.2%) compared to high yielding genotypes from CYMMIT collection (24.92%) ones. Independent of culture medium composition a ratio of doubled haploid/haploid was 4.57:1 and a ratio of haploid/aneuploid was 18.5:1, in particular 81.28 % of green plants were doubled haploid, 17.76% were haploid and the rest (0.96%) were aneuploid

Key words: Anther culture, wheat, morphogenesis, doubled haploids, drought resistance

Introduction

The production of homozygous plants is a difficult and long procedure. Conventional methods of plant breeding need many cycles of selection to isolate promising genotype and genetically constant lines. When the conventional method is used, this procedure takes approximately twelve to fifteen years. Anther culture technique accelerates the breeding cycle by shortening the time required to attain homozygosity [1]. Double haploid techniques provide plant breeders with pure lines in a single generation. The use of elite lines as crossing parents combines the opportunity to select more efficient agronomic traits in homozygous plants. Therefore, double haploid breeding strategies have competitive advantages compared with conventional methods [2]. When the F_1 is used, this technique has the advantage that genetic uniformity is achieved only in a short time after the initial hybridization. Anther culture allows a rapid production of appropriate genotypes for breeding purposes in an effort to identify promising pure lines [3]. The production of double haploids through androgenesis represents a modern tool for the improvement of cultivated species. Developmental stage of harvested spikes, culture medium, duration of cold pretreatment and genotype may affect haploid induction in anther culture whereas among them genotype play a major role in embryo and green plant production in cereals [4]. The problem affecting the efficiency of androgenesis is the production of albino plantlets in various proportions according to the cultivars and the low numbers of plants that are regenerated. Therefore, further improvement in anther culture efficiency in wheat is needed. The target of this study was to determine optimal composition of culture medium for haploid production in different wheat genotypes.

This paper presents evidence of a beneficial effect of N6 culture media for wheat anther, resulting in significant increases in green plant regeneration and impact of genotypes on induction embryogenesis and regeneration in wheat anther culture.

Materials and methods

Donor plant materials

17 groups of spring wheat (*Triticum aestivum L.*) plants were selected and finally we had 8 different families. Progeny of 8 different F_1 soft wheat plants (families) were used for *in vitro*

 Printed in Kazakhstan

anther culture. The hybrids of soft wheat were produced from the following crosses: Lutescens293H436 xGostianum 88 (BG 1-4/98), (Gostianum88 x Lutescens 410H48) x Lutescens 410H48 (BG 1-3/98), wheat hybrids from CYMMIT SN64//SKE12* ANE/3/SX /4/BEZ/5/JUN ARAPAHOE (BG 367), DAGDAS/6/ SN64// SKE12* ANE/3/SX/4/BEZ / 5/JUN (BG 357), hybrids obtained with izogenic line Lr24 – Kazakhstanskaya 17 x Lr 24 (BG-L3), K49397 x Lr 24 (BG-L9), (Spartanka x Erytrospermum 14) x Erytrospermum 14 (BG 7-2/97, Line 86 x Celinnaya 24 (BG 6-7/97), (Mironovskya 808 x Skala) x Skala (BG 6-8/97. The donor plants were resistant to drought, leaf yellow rust and lodging.

Growth conditions of donor plants

Seeds of each family were sown in rows 3 m long within the last week of April in an experimental field at the Institute of Plant Biology and Biotechnology in south-east Kazakhstan. The experiment was established in a chestnut soil and organic matter content 1.2% (10 to 30 cm depth). All the common cultivation practices were used. Spikes of the plants were harvested for anther culture when the sheath of the flag leaf had emerged about 0.5 cm (it is equivalent to one-nuclear stage of microspores), and remained at 4^0 C for 3 days for cold pretreatment.

Anther culture conditions

The anthers whose the microspores were at the mid uninucleate stage, were excised aseptically from the spikes. The spikes were previously sterilized with 70% ethanol. The anthers were excised and inoculated into petri-dishes (60x15 mm) containing 3 ml N6 and Gamborg-Eveleg B5 (B5) medium solidified by agar, supplemented with 1 mg/l 2.4-D. The culture medium including 100 mg/l myo-inositol, 9% (w/v) sucrose.

Each petri-dish contained approximately 90 anthers. The anthers were incubated in the dark at 25^0 C during 2-4 weeks (the anthers were cultured for a further 2 weeks before first observations were made). The embyoids produced were transferred to a regeneration medium and incubated in the light (at 40-80 μmol/m^2/sec) under a 16h photoperiod at 25 ± 2^0C for 4 weeks. The regeneration medium used was N_6 solid medium, supplemented with 2% sucrose, 1.5 mg/l IAA and 1 mg/l kinetin. The root meristems of plantlets were used to determine the ploidy level (to determine the number of chromosomes of the obtained green plants). The roots were pretreated with 8-Hydroxyquinoline for three hours and fixed in 3:1 acetic alcohol. After a few days the chromosomes were stained by the Feulgen technique and slides were prepared in acetocarmine.

Green plantlets were transplanted in small pots covered by plastic bags to maintain the high humidity (60-70% humidity). After 2-3 weeks the plants were transferred to larger pots and kept at $25^0/16^0$ C day/night temperature regime with 16h photoperiod to reach the maturity and produce seeds. Seeds from the families produced green plants were treated properly to stain and count the chromosome number.

Data were recorded on the basis of morphogenesis and embryogenesis (morphogenetic structures or embryoid per 100 anther), regeneration (albino and green regenerated plants per 100 anthers) and diploidization (total double haploids). The statistical analysis was computed following the working schedule of Lakin (1990) [5]. Differences were considered significant at P=0.05.

Results and their discussion

From 17 families used in anther culture only 9 of them (52.94%) responded and produced morphogenic callus and embryoids (Table 1) (Fig. 1A, 1B). From those 9 families, 4 originated from high yielding genotypes from CYMMIT (BG 357, BG 367) and wheat hybrids obtaining by breeders from Institute of Plant Biology and Biotechnology. Five wheat hybrids originated from middle yielding genotypes. Furthermore, significant differences were found among genotypes originated from high yielding (3,53-10,18% embryoids per 100 anthers) and middle yielding plants 1,11-6,48% embryoids per 100 anther). Concerning the regeneration, 7 of the responded genotypes produced plants (Table 2) (Fig. 1C, 1D). On the other hand, 3 genotypes produced both green and albino plant-regenerants. The ratio between green and albino plants were 5,99:1 for hybrid BG 1-3/98, 1.25:1 for BG 1-4/98 on the N6 culture medium and 1:1 for genotype BG 367 on the B5 culture medium. The anther cultivation on N6 medium induced more androgenic structures (morphogenic callus+embryoids) compared to B5 culture medium for all responded wheat genotypes.

Furthermore, from the genotypes produced regenerants, the high yielding genotypes from local breeding collection of wheat produced more albino plants (35.2%) compared to high yielding genotypes from CYMMIT collection (24.92%) ones. All of green plants grown on the N6 culture medium

were fertile and produced seed. The cyto-genetical analysis showed that the 81.28% of green plants were doubled haploid, 17.76% were haploid and the rest (0.96%) were aneuploid.

Most of the families produced embryoids, morphogenetic callus and regenerants originated from high yielding genotypes. The differences between high yielding and middle yielding genotypes in embryoid production and green plant grown on the same medium may be due to genotypes because both androgenic response and regeneration capacity were greatly genotype dependent. A major problem with anther culture in cereals is the low numbers of plants that are regenerated. Often this problem is compounded by a high frequency of albinos. Mean differences among different genotypes presented $P \leq 0.05$.

Table 1 – Influence of medium composition on the morphogenesis in anther culture of wheat

Hybrid	Culture Medium	Number of anther	Morphogenic callus, %	Embryoids, %	Total number of androgenic structure, %
BG 1-3/98	N6	522	1,34±0,05	3,06±0,07	4,40
	B5	594	0,67±0,03	3,53±0,08	4,20
BG 1-4/98	N6	306	1,30±0,06	2,94±0,09	4,24
	B5	252	0,39±0,03	1,58±0,07	1,97
BG 357	N6	108	0	10,18±0,29	10,18
	B5	72	4,16±0,23	4,17±0,24	8,33
BG 367	N6	126	1,59±0,01	1,59±0,11	3,97
	B5	126	0,79±0,07	2,38±0,13	3,17
BG-L 9	N6	108	1,85±0,09	5,55±0,22	10,17
	B5	126	0,79±0,07	0,79±0,07	1,58
BG-L 3	N6	108	0	6,48±0,24	6,48
	B5	126	0	3,97±0,17	3,97
BG 7-2/97	N6	144	7,64±0,02	4,86±0,02	13,88
	B5	180	1,11±0,01	1,11±0,01	2,22
BG 6-7/97	N6	126	1,59±0,01	2,38±0,01	7,14
	B5	90	5,55±0,02	3,33±0,02	8,88
BG 6-8/97	N6	216	4,63±0,01	4,16±0,01	11,57
	B5	234	0,85±0,06	0,85±0,06	2,14

Table 2 – Number of embryoids, androgenic structures, albino and green plants production after *in vitro* anther culture of spring wheat

Genotype	Culture Medium	Number of anther	Number of androgenic structure,%	Number of regenerants, %		Total number of plantlets, %
				green	albinos	
BG 1-3/98	N6	522	4,40±0,12	26,09±0,93	4,35±0,43	30,43±0,98
	B5	594	4,20±0,11	20,00±0,82	0	20,00±0,82
BG 1-4/98	N6	306	4,24±0,15	38,8± 1,40	30,95±1,4	69,75±2,80
	B5	252	1,97±0,10	60,1±2,40	0	60,1±2,40
BG 357	N6	108	10,18±0,29	36,36±1,52	0	36,36±1,52
	B5	72	8,33±0,47	33,33±2,11	0	33,33±2,11
BG 367	N6	126	3,97±0,19	50,0±2,80	0	50,0±2,80
	B5	126	3,17±0,20	24,92±4,30	24,92±4,3	49,84±8,60
BG -L 9	N6	108	10,17±0,46	37,3±1,70	0	37,3±1,70
	B5	126	1,58±0,14	100,0±0	0	100,0±0
BG -L 3	N6	108	6,48±0,24	42,70±2,00	0	42,70±2,00
	B5	126	3,97±0,17	20,00±2,00	0	20,00±2,00
BG 7-2/97	N6	144	13,88±0,03	15,0±0,08	0	15,0±0,08
	B5	180	2,22±0,01	50,0±0,28	0	50,0±0,28

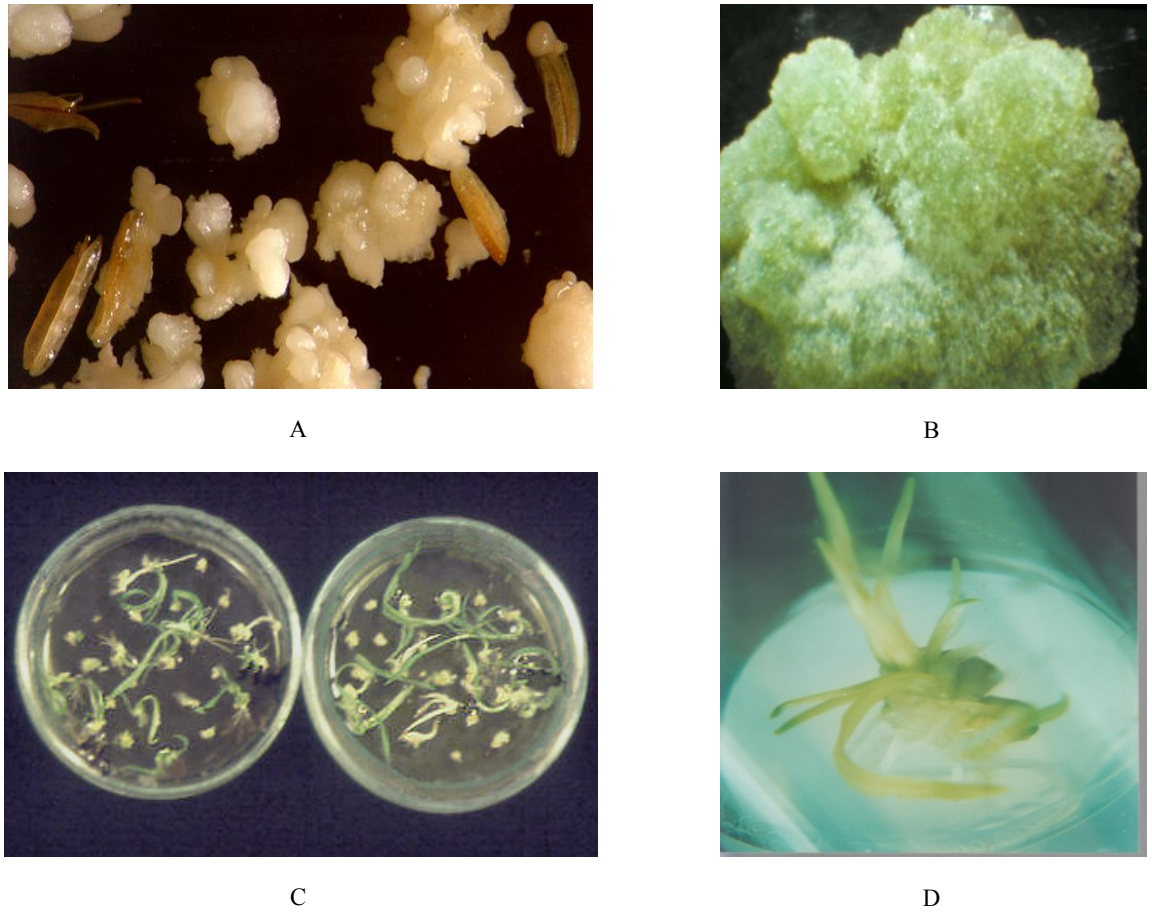

A B C D

Figure 1 – The different steps from androgenic structure, embryoid induction to maturity. Embryoid (A) and morphogenic callus induction, x40 (B), green plant regeneration in N6 medium (C), haploid plant-regenerant (D)

In these experiments, the ratio of albino/green plants produced was very high (in particular, for hybrid BG 1-4/98 - 79.76%, for genotype BG 367 - 100%). Wietholter et al (2008) whereas other researchers (Cistue et al, 2004) also reported 100% ratio of albino/green plants in some barley cultivars [6, 7]. On the other hand, in embryogenesis and regeneration frequency there were significant differences between embryoids plated on N6 culture medium and embryoids cultivated on B5 medium. A decrease of ammonium nitrate with an increase in nitrate as in B5 medium composition have been identified as important factors in improving response. The embryogenesis frequency and respectively regeneration capacity in B5 culture medium were high for wheat hybrids BG 1-3/98 (3.53±0.08%), BG 367 (2.38±0.13%), BG 6-7/97 (3.33±0.02%). However, some wheat genotypes, which anthers were cultivated in N6 medium, produced more (at 2-2.5 times more) embryoids, androgenic structure and green plantlets compared to culture medium B5 ones (Table 1, 2). The composition N6 medium including 100 mg/l myo-inositol, 9% (w/v) sucrose, 1 mg/l 2.4-D is optimal for production haploid plants in anther culture. 2.4-D is a synthetically occurring plant hormone that has auxin activity and support the growth of wheat callus culture in the presence of kinetin. S.Turasheva et al (2006) found that the presence of 2.4-D in culture media led to callus initiation and supported suspension culture growth in wheat [8]. Furthermore, auxin 2.4-D induce embryogenesis in anther and microspore culture of wheat. With 2.4-D the induction response was not usually significantly different from controls but a significantly higher number of green plants were produced in wheat anther culture.

The dispersion analysis showed that influence of genotype on induction of morphogenesis and regeneration in spring wheat anther culture more (43.75%) than impact of culture medium factor (20.24%). On the other hand, influence of culture medium on development embryos and plants in

anther culture of spring soft wheat with Lr-gene (in particular, genotypes BG -L 9, BG -L 3) more than impact of genotype factor – 0.34% and 83.65% respectively (Table 3).

Table 3 – The dispersion analysis influence of genotype (A) and culture medium (B) induction of morphogenesis and regeneration in wheat anther culture (two-factor experiment)

Factor	Degree of freedom	The amount of standard deviation	Dispersion	The contri-bution of impact ,%	P fact.	P table. (0,99)
Spring soft wheat						
A-genotype	3	380,41	126,8	43,75	1196,19	29,46
B-culture medium	3	175,93	58,64	20,24	553,22	29,46
AB	9	300,11	33,35	34,52	314,56	
Spring soft wheat with Lr-gene						
A-genotype	1	0,81	0,81	0,34	11,75	
B-culture medium	3	201,43	67,14	83,65	978,46	
AB	3	34,6	11,53	14,37	168,06	

Probably, the response of parental lines in anther culture influenced the response of progeny combination. In the first case, there is a positive correlation between the anther response of the parents and the response of F_1 hybrid. However independent of culture medium composition a ratio of doubled haploid/haploid was 4.57: 1 and a ratio of haploid/aneuploid was 18.5:1.

Conclusion

In anther culture of wheat the high yielding donor plants produced more embryoids and green fertile plants than the middle yielding plants. Furthermore, for most donor hybrid plants influence of genotype on induction of morphogenesis and regeneration in anther culture more (43.75%) than impact of culture medium factor (20.24%). There is a positive correlation between the yielding capacity of the lines and the anther response. The optimal culture medium for production of wheat doubled haploids by anther culture is N6 culture medium including 100 mg/l myo-inositol, 9% (w/v) sucrose and 1 mg/l 2.4-D.

References

1 Pickering RA, Devaux P. Haploid production: approaches and use in plant breeding. In: Genetics, Molecular Biology and Biotechnology, Barley. Ed. by PR Shewry, – Wallingford; CAB Internat., 1992. – P. 511-539.

2 Kao KN. Future prospects for crop improvement through anther and microspore culture. In: *In vitro* haploid production in higher plants (Jain S.M., Sopory S.K., Veilleux R.E., eds), 1996. – P. 367-373

3 Islam SM. The effect of colchicine pretreatment on isolated microspore culture of wheat (*Triticum aestivum L.*) // Aust J Crop Sci. – 2010. – V.4 (9). – P.660-665

4 Lazaridou TB, Lithourgidis AS, Kotzamanidis ST, Roupakias DG. Anther culture response of barley genotypes to cold pretreatments and culture media //Rus J Plant Physiol. – 2005. – No 52. – P. 696-699.

5 Lakin N.L. Introduction in biometry. – M.: Nauka, 1978. – 84 p.

6 Wietholter P., Fernandes MI, Brammer SP. Genotyping differences in proembyoid development and green plantlets regeneration through androgenesis in barley varieties // Ciencia Rural. – 2008. – Vol. 38. – P. 240-242

7 Cistue L, Valles MP, Echavarii B, Sanz JM, Castillo AM. Production of barley doubled haploids by anther and microspore culture. In: Mujib A., Cho MJ, Predieri S, Banerjee S *In vitro* application in crop improvement. – Science Publishers Inc, Plymouth, 2004. – P. 1-17.

8 Turasheva SK, Zhumabaeva BA, Zhambakin KZh, Rakhimbaev IR. The influence of auxin 2.4-D on growth of wheat suspension culture //Abstract of the second Central Asian Cereals Conference. CYMMIT. – Almaty, 2006. – P. 452-455.

UDC 615.322+633.88+547.98+661.123

*Zhussupova A.I., Gadetskaya A.V., Shalakhmetova T.M.,
Murzakhmetova M.K., Zhussupova G.E.

Al-Farabi Kazakh National University, Almaty, Kazakhstan
*E-mail: aizhan.zhusupova@gmail.com

Natural antioxidants of plant origin

In pharmacotherapy and prevention of "free radical diseases", including diseases of the cardiovascular system, gastrointestinal tract, malignancies, herbal medicinal products become important, the effect of which is based on synergistic action of the major groups of natural compounds, such as polyphenols (mainly condensed tannins and flavonoids), amino, phenolic, polyene carboxylic acids, vitamins and minerals. Herbal substances of antioxidant action obtained on the basis of Kazakhstani plants are presented and described. The allocated herbal substances are notable by their bioavailability, low toxicity, absence of allergic reactions and cumulative effects, possibility of their long-term use for treatment and prevention of diseases.

Key words: antioxidant action, Limonium Mill, polyphenols.

Introduction

According to the World Health Organization the Republic of Kazakhstan takes the leading position among the countries of Central Asia on the prevalence of "free radical diseases". The pathogenesis of these diseases reclines on common fundamental mechanisms of damage to biological membranes of body tissues associated with the increased formation of free radicals and peroxide compounds of organic and inorganic nature [1-2]. Main substrates of free radical oxidation are unsaturated lipids. A necessary condition for cells functioning is to maintain normal levels of free radical oxidation. Marked and prolonged exposure to lipid peroxidation leads to decrease in the content of biological membranes of more easily oxidized polyunsaturated fatty acids with a simultaneous increase of the fatty acid radicals and secondary products of lipid peroxidation. The damaging effect of lipid peroxidation products on cell is caused by forming hydrophilic channels in a lipid layer of membranes dramatically violating their permeability, inactivation of energy generating thiol enzymes, uncoupling of oxidative phosphorylation, which, in turn, results in the cleavage of membrane lipids, alteration of lipid-protein interactions and other irreversible consequences.

Speed and regulation of lipid peroxidation is performed by multicomponent antioxidant system [3], which provides binding and modification of free radicals, preventing the formation and destruction of peroxides, shielding the functional groups of proteins and other biomolecules. The ratio of the intensity of free radical oxidation and antioxidant activity defines the so-called status of cells, tissues and body as a whole. Aging, cardiovascular diseases, cancer, disorders of the central and peripheral nervous systems, acquired immune deficiency syndrome, diabetes, arthritis, cataracts, asthma, diseases of the gastrointestinal tract as well as other inflammatory diseases are caused or accompanied by oxidative stress, failure or defect in the physiological antioxidant defense system in a state of indivisible unity with other human defence systems – hemoprotective and immune [4-6].

To correct the imbalances of the body caused by hyperoxidation and leading to such pathological conditions, use of drugs with antioxidant action is recommended. In this regard, search of compounds with high antioxidant activity or estimation of the biological activity of this type for traditionally used drugs has great medical and general biological significance. Antioxidants, which are substances present in the systems at significantly lower concentrations compared to the oxidized substrate and inhibiting its oxidation, are used for prevention and complex therapy of peroxide pathologies [7-9].

Among the substances with antioxidant, immunostimulating and other adaptogenic properties are substances with high biological activity, derived from herbal raw materials occupy an important place.

 Printed in Kazakhstan

Compatibility of herbal medicines with physiological antioxidant system by virtue of their similarity capable of specifically inducing protective and mobilizing resources that practice the principle of "treat the body, not a disease". The advantage of herbal medicines lays in their gentle effect on the body and complexity of their therapeutic action with low toxicity, absence of cumulative effects, addiction, inducing rare allergic reactions, which is especially important in case of diseases requiring long-term treatment.

Among natural antioxidants best known are the plant polyphenols because of their potential to reduce the risk of disease and in the treatment of many diseases such as cancer, diabetes, disorders of the cardiovascular system, atherosclerosis, neurodegenerative diseases and other inflammatory processes [10-13]. First of all, it is condensed tannins and flavonoids. Condensed tannins include dimeric, oligomeric and polymeric forms of flavan-3-ols, the latter are among the most reduced form of flavonoids.

Highly efficient substance "Limonidin" is produced on the basis of commercially important plant *Limonium gmelinii* by a simple, economically and environmentally feasible technological scheme with a high yield, using aqueous solution of ethyl alcohol generated in the process as a suitable extracting agent or excipient. It is rich in polyphenolic compounds and their variety, with dominance of condensed tannins [14]. Proanthocyanidins are usually represented by linear molecules separate monomers of which are capable of limited rotation around correspondent connecting bonds, whereby the molecule may acquire a relatively stable helical conformation with phenolic groups located at the periphery.

Location of phenolic groups on "surface" of proanthocyanidins is important from the point of view of possibility of the formation of multiple hydrogen bonds with the natural substrates, such as proteins, which underlies their pharmacological action. Blocking specific regions of the surface of enzymes might lead to modification of their activity. Screening of activity of many flavans in relation to enzymes suggests that one possible mechanism of action is chelating of metal ions in the active site of enzymes, as well as the formation of insoluble complexes [15]. Many microbial enzymes (cellulase, glycosyltransferase, pectinase, etc.) inhibit their activity in presence of tannins. The authors suggest that proanthocyanidins act on the outer shell of bacteria consisting of polysaccharides and proteins, fixing it at very low concentrations. Furthermore, due to the presence of ordinary phenolic hydroxyl groups they can chelate metal ions, thereby blocking access of metal ions to microbes. It was shown that an increase in activity of hydrolyzable tannins depends on the amount of galloyl hexahydroxydiphenyl groups, condensed tannins, degree of their polymerization and the amount of phenolic groups [16]. It was found that interaction of proanthocyanidins with phospholipids of cell membranes and lysosomes restricts oxidants access to the membranes, preventing their destruction, at that more active are hexamers [17].

It has been experimentally shown that substance "Limonidin" enhances the flow of anabolic processes in the body, directly reducing accumulation of lactic acid (LA) in tumor and tissues of the body, displacing the redox process towards formation of pyruvic acid (PA). Use of substance "Limonidin" caused a sharp decline of lactate in almost all of the analyzed organs. The greatest decrease (from 17.04 to 0.3 mmol/g) was detected in kidneys; almost on 1.5 orders lower was its content in liver, on order – in tumor and spleen, three and two fold decrease was observed in lungs, heart and skeletal muscles. When analyzing marked deviations it should be noted that substance "Limonidin" facilitated restoring the normal LA content in most part of the internal organs; the greatest effect was detected in parenchymal organs – kidneys, liver and spleen. On the other hand, substance "Limonidin" facilitates increase of PA content in liver, spleen and muscles by 30-40%, in tumor – 70% in lungs, heart and kidneys – by 2-4.2 times.

The results of a comparative study of antiviral activity of substance "Limonidin" with commercial agents – amphotericin B, Oxolinic ointment and Ribavirin on models of myxovirus A/FPV/Rostock/34 and NDV (of La Sota) have shown that substance "Limonidin" has high level of suppression of reproduction of influenza and parainfluenza viruses more than commercial formulations. It is assumed that the antiviral activity is provided by attaching of tannin molecules to the viral protein envelope or to the host cell membrane and thus the virus penetration stops. This marked the activity pattern between tannins and their structure; condensed tannin activity increases with the degree of condensation [14, 18].

Substance at different doses was tested on sufficient number of laboratory animals (white mongrel rats) in different models of acute and chronic liver damage (poisoning by carbon tetrachloride, heavy metals, propellants and other xenobiotics) [19]. Silibor – an effective herbal hepatoprotective agent, widely used in medicinal practice, was used as reference drug in the experiments. It has been found that hepatoprotective activities of substance "Limonidin" and Silibor are comparable; however, single thera-

peutic dose of "Limonidin" is 2 times less than that of Silibor. Substance "Limonidin" is registered by the Ministry of Health Care and Social Development of the Republic of Kazakhstan (PhA RK 42-1259-08, RK-MP-5No.008963 from 22.09.2008) and is approved for use in medicine.

During the chemical study of *L. gmelinii* roots and substance "Limonidin" flavonols (myricetin, quercetin, isorhamnetin, myricetin monomethyl ether and new flavonol previously undescribed in literature 3,5,7,3',4',6' hexahydroxyflavon (1)), their glycosides (miritsitrin, rutin, 3-β-galactosylquercetin and 3-β-galactomyricetin, other mono- and biozides, as well as described for the first time in literature 3-α-galactopyranoside myricetin and 3-O-α-L-(2"-galloyl)-arabinopyranoside myricetin), pyrogallol, gallic and ellagic acids were identified. Main monomeric flavan is (-)-epigallocatechin gallate; various forms of flavan-3-ols: 3,5,7,3',4',6'-hexahydroxyflavan (2) (-)-epigallocatechin-(4β→8)-(-)-3,5,7,3',4',6' – hexahydroxyflavan (3) (+)-gallocatechin-(4α→8)-[(-)-epigallocatechin]5-(4β→8)-(-) – epigallocatechin gallate (4) are identified as new, previously undescribed in literature [20; 21]:

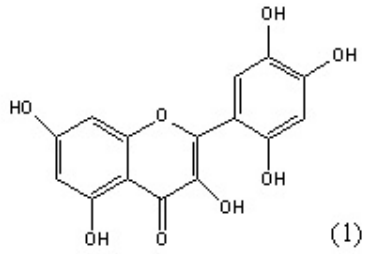
(1)

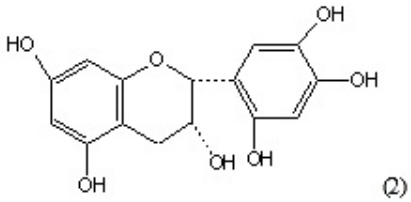
(2)

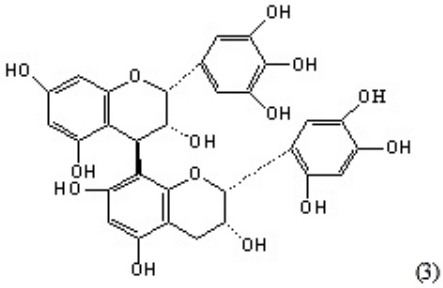
(3)

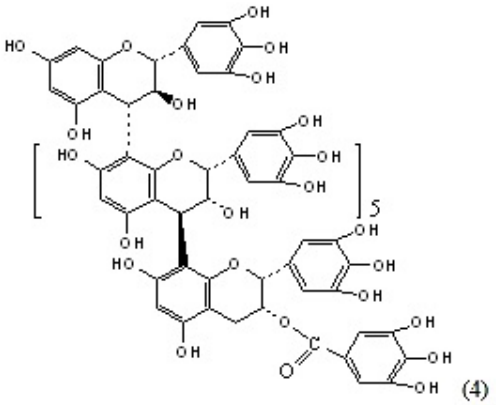
(4)

Previously unknown for this species amino and fatty acid, carbohydrate and microelement contents, vitamins and xantofills were identified. From sterols along with the known 3-O-β-D-glucopyranoside campesterol was described for the first time. Vitamins E and C, along with polyphenols are powerful antioxidants that are used to treat and prevent many diseases, pathogenesis of which is connected with increase of lipid peroxidation associated with changes in functional activity of membranes.

The amount of heavy metals does not exceed the permissible norms for herbal substance and the vital macro- and microelements are contained in required quantities, which appears as a result of synergies with other important components and causes a wide range of physiological actions of resulting preparation – substance "Limonidin".

Active antiinflammatory effect of *Cistus incanus* plant extracts, used against skin diseases, is caused by the presence of condensed tannins and proanthocyanidins [22]. *Cuscuta campestris* Juncker has characteristics, which can be used against various human pathologies, what has previously been demonstrated by the data of traditional medicine for other types of dodder, in particular, *Cuscuta chinensis* Lam. and *Cuscuta europaea* L. [23].

Materials and methods

In the experiment with CCl_4 Silibor was used as reference for Limonidin. Introduction of certain doses of aqueous Limonidin and Silibor solutions was conducted once by intragastric gavage 1 hour prior to use of hepatotoxin – carbon tetrachloride (CCl_4) for 14 days. Animal euthanasia was conducted under Nembutal anesthesia between 9 and 10 am. The content of malondialdehyde (MDA) and lipid hydroperoxide (LPO) and enzyme activity was measured in rat liver homogenate. Preclinical tests were conducted on white outbred male rats weighing 220-250 g, divided into 4 groups (of 10 animals each):

I – intact animals (control),

II – animals received 5 mg/kg of CCl_4 (50% solution in olive oil), single, intragastric;

III – animals received 100 mg/kg of Limonidin and 5 mg/kg CCl_4 once, intragastric;

IV – animals received 200 mg/kg of Silibor and 5 mg/kg CCl_4 under the same conditions.

Dried samples of field dodder were grounded to the final size of 1-3 mm. Under extraction with 50% ethanol and dimethyl sulfoxide (DMSO) two substances were obtained in the form of liquid extracts. Lipid peroxidation was induced for 60 minutes by Fe^{2+}/ascorbate system. The obtained field dodder substances were preincubated with LPA for 15 minutes at 37°C.

Results and their discussion

Animal intoxication with CCl_4 induces activation of lipid peroxidation processes, i.e., increase of MDA and LPO and inhibition of antioxidant processes by reducing the activity of enzymes – superoxide dismutase (SOD) and catalase. Table 1 shows the results of biochemical studies of rat control and experimental groups at their intoxication with CCl_4 and the combined use of CCl_4 and herbal preparations.

According to the results shown in Table 1 hepatotoxin CCl_4 when administered to animals activates LPO, content of MDA and LPO increases by 2.2 and 1.6 times and suppression of antioxidant processes by reduction of SOD and catalase enzymes by 7.0 and 1.8 times, respectively. The processes of lipid peroxidation, induced by CCl_4, are largely reduced when receiving Limonidin (IIIrd group). This is evidenced by a decrease in the content of primary and secondary products of lipid peroxidation (LPO and MDA content decrease by 1.4-1.7 and 1.3-1.4 times), as well as increased activity of antioxidant enzymes in these animals (SOD and catalase activities increase by 5.5-5.7 and 1.2 times, respectively, compared with rats fed only with CCl_4).

Table 1 – Content of LPO and MDA, SOD and catalase activities in rat liver

Group	Experimental conditions	LPO (conv.un./g)	MDA (мM/g)	SOD (conv.un./g)	Catalase (conv.un./g)
I	Control	23.9±0.6	1.9±0.1	147.2±3.2	302.2±8.4
II	CCl_4	37.9±0.3	4.2±0.1	21.5±4.6	162.7±4.2
III	CCl_4+Limonidin (100 mg/kg)	29.2±4.1	2.5±0.2	119.2±2.8	175.4±1.5
IV	CCl_4+Silibor (200 mg/kg)	28.6±2.8	2.7±0.1	122.3±2.2	172.5±3.0

Despite the fact that indicators of lipid peroxidation in poisoned rats under Limonidin have completely returned to normal, the severity of structural damage in the liver of these animals was significantly smaller. Thus, the results of morphological studies have shown that a single intragastric administration of CCl_4 in rats led to the development of acute toxic hepatitis, considerable destruction centrilobular hepatocytes. Combination of CCl_4 with phytopreparation significantly reduces the degree of destructive processes caused by CCl_4. A similar trend is to reduce the content of lipid peroxidation products, and increase the activity of antioxidant enzymes was observed in group IV, where, along with CCl_4 hepatoprotector Silibor was used. It is shown that Limonidin 100 mg/kg possesses a strong antioxidant and hepatoprotective effect comparable to that of Silibor (dose – 200 mg/kg) used in medicinal practice. In addition, experiments were carried out on animals under their poisoning with heavy metals, propellants and other xenobiotics. Comprehensive studies using various techniques (histological, morphometric, quantitative cytochemical and biochemical) showed that substance "Limonidin" increases the resistance of the liver pathological effects, strengthens its neutralizing function by increasing the activity of enzymatic monooxygenase system, and helps to restore its structure under various injuries.

To isolate the microsomal fraction rat liver tissue was weighed (0.5-1.0 g) after washing with cooled saline and being placed in 10 ml of medium containing 0.85% NaCl and 50 mM KH_2PO_4 (pH 7.4 at 4°C) and homogenized in Polytron type homogenizer within 90 seconds. The homogenate was centrifuged at 10 000 g for 20 min. Microsomal fraction was obtained by centrifuging the supernatant at 30 000 g for 60 min. The supernatant was carefully decanted and the pellet, which is a fraction of heavy microsomes suspended in medium containing 25% glycerol, 0.1 mM EDTA, 0.2 mM $CaCl_2$, 10 mM histidine (pH 7.2 at 4°C) and stored at -4°C [24].

Content of malondialdehyde (MDA) and products of lipid peroxidation is determined by reaction with 2-thiobarbituric acid according to the intensity of the developing color. Content of the products reacting with thiobarbituric acid is calculated taking into account the coefficient of MDA molar extinction equal to $1.56x10^5$ $M^{-1} \cdot cm^{-1}$ [25].

Erythrocytes were obtained by centrifuging blood for 10 minutes at 1 000 g. Plasma and white blood cells are removed and erythrocytes are washed twice with medium containing 150 mM NaCl, 5 mM Na_2NPO_4 (pH 7.4). Osmotic resistance of erythrocytes is determined by the degree of hemolysis in hypotonic solutions of NaCl (0.35-0.5 g/100ml).

Studied substances of field dodder do not affect the accumulation of thiobarbituric acid reactive substances (TBARS) without induction of lipid peroxidation. Significant reduction is observed in the presence of TBARS substance isolated using DMSO as extragent versus ethanol extract at a concentration of 20 μg substance/mg of protein (3.3 and 6.3 mmol of DMSO and ethanol extracts, respectively), which is probably due to a more thorough extraction of polyphenolic compounds from the raw material with dimethyl sulfoxide.

Results of study of dodder alcoholic extract effect on the level of lipid peroxidation in rat liver microsomes revealed that the extract reduces the formation of peroxide products, depending on the dose. Extract concentration of 40 μg/mg protein or above almost completely inhibits the formation of peroxide products in rat liver microsomes.

Conclusion

The choice of research area is based on search of Kazakhstani plants, containing a complex of synergistic biologically active substances of plant origin affecting life expectancy and health by improvement of human and animal physiological features. This refers to preservation of reserve forces and adaptive mechanisms, as well as stimulation of physiological ability of organism in adaption to changing life conditions.

References

1 Droge W. Free Radicals in the Physiological Control of Cell Function // Physiol. Rev. – 2002. – Vol. 82. – No. 1. – P. 47-95.

2 Kehrer J.P., Robertson J.D. and Smith C.V. Free Radicals and Reactive Oxygen Species // Comprehensive Toxicology. – 2010. – Vol. 1. – P. 277-307.

3 Halliwel B. Reactive Species and Antioxidants. redox biology is a fundamental theme of aerobic life // Plant. Physiology. – 2006. – Vol. 141. – P. 312-322.

4 Halliwel B. Antioxidants in human health and disease // Ann.Rev.Nutr. – 1996. – Vol. 16. – P. 33-50.

5 Valko M., Leibfritz D., Moncola J., Cronin M.T.D., Mazur M., Telser J. Free radicals and antioxidants in normal physiological functions and human disease // The International Journal of Biochemistry & Cell Biology. – 2007. – Vol. 39. – P. 44-84.

6 Storz P. Reactive oxygen species in tumor progression // Front. Biosci. – 2005. – Vol. 10. – P. 1881-1896.

7 Rice-Evans C.A., Diplock A.T. Current status of antioxidant therapy // Free Radic.Biol.Med. – 1993. – Vol. 15. – No. 1. – P.77-96.

8 Sies H. Oxidative stress: Oxidants and antioxidants // Exp.Physiol. – 1997. – Vol. 82. – No. 2. – P. 291-295.

9 Cuzzorcrea S., Thiemermann C., Salvemini D. Potential therapeutic effect of antioxidant therapy in shock and inflammation // Curr.Med.Chem. – 2004. – Vol. 11. – P. 1147-1162.

10 Manach C., Scalbert A., Morand C., Rémésy C. and Jiménez L. Polyphenols: food sources and bioavailability // Am. J. Clin.Nutrition. – 2004. – Vol. 79. – No. 5. – P. 727-747.

11 Boudet A.M. Evolution and current status of research in phenolic compounds // Phytochemistry. – 2007. – Vol. 68. – No. 22-24. – P. 2722-2735.

12 Manach C., Mazur A., Scalbert A. Polyphenols and prevention of cardiovascular diseases // Curr. Opin. Lipidol. – 2005. – Vol. 16. – No. 1. – P.77-84.

13 Arts I.C., Hollman P.Ch. Polyphenols and disease risk in epidemiologic studies // Am. J. Clin. Nutr. – 2005. – Vol. 81. – No. 1. – P. 317S-325S.

14 Zhusupova G.E., Abilkaeva S.A. Dimeric prodelphinidins from Limonium gmelinii roots. III // Chemistry of Natural Compounds. – 2006. – No. 2. – P. 134-138.

15 Lin J.K., Liang Y.C. Cancer chemoprevention by tea polyphenols // Proc. Natl. Sci. Counc. – 2000. – Vol. 24. – P. 1-13.

16 Scalbert A. Antimicrobial properties of tannins // Phytochem. – 1991. – Vol. 30. – No. 12. – P. 3875-3883.

17 Verstraeten S.V., Keen C.L., Schmitz H.H., Fraga C.G. and Oteiza P.I. Flavan-3-ols and procianidins protect liposomes against lipid oxidation and disruption of the bilayer structure // Free Radic. Biol. Med. – 2003. – Vol. 34. – No. 1. – P. 84-92.

18 Nagai T., Miyachi Y., Tomimori T., Yamada H. Inhibition of influenza virus sialidase and anti-influenza virus activity by plant flavonoids // Chem. Pharm. Bull. – 1990. – Vol. 5. – 38. – P. 1329-1332.

19 Vengerovskyi A.I., Saratikov A.S. Mechanism of action of hepatoprotectors under toxic liver damage // Pharmacology and Toxicology. – 1988. – No. 1. – P. 89.

20 Zhusupova G.E., Abilkaeva S.A. Dimeric prodelphinidins from *Limonium gmelinii* roots. III // Chemistry of Natural Compounds. – 2006. – No. 2. – P. 134-138. http://dx.doi.org/10.1007/s10600-006-0068-8.

21 Zhanar A. Kozhamkulova, Galiya E. Zhusupova, Zharilkasin A. Abilov, Mohamed M. Radwan, Samir A. Ross. A new flavonol glycoside from *Limonium gmelinii* // Planta medica. – 2010. – P. 534-535.

22 Petereit F., Kolodziej H., Nahrsted A. Flavan-3-ols and proanthocyanidins from *Cistus incanus* // Phytochem. – 1991. – Vol. 30. – No. 3. – P. 981-985.

23 Kala C.P., Farooquee N.A., Dhar U. Prioritization of medicinal plants on the basis of available knowledge, existing practices and use value status in Uttaranchal, India // Biodiver. Conserv. – 2004. – Vol. 13. – No. 2. – P. 453-469.

24 Gorgoshidze L.Sh., Kon' I.Ya., Kulakov S.N., Shevyakov A.N. Lipid peroxidation in the rats liver under light forms of vitamin A deficiency // Nutrition . – 1986. – Vol. 5. – P. 45-51

25 Ohkawa H.O., Ohishi N., Yagi K. Assay for lipid peroxides in animal tissues by thiobarbituric acid reaction // Anal.Biochem. – 1979. – Vol. 95. – No. 2. – P. 351-358.

UDC 614:623.454

Musa K.Sh., *Abdrazak P.Kh.

Al-Farabi Kazakh National University, Almaty, Kazakhstan
*E-mail: Ms.abdrazak@mail.ru

The impact of the cosmodrome «Baikonur» on the environment and human health

In article environmental problems connected with start of rockets – Proton-M carriers are considered.
Key words: pollution, environment, health.

Introduction

An assessment of the health status of ecosystems exposed to anthropogenic pollution is a vital issue for many countries. Particularly it concerns the consequences of contamination caused by the activity of the space industry. Each rocket launch is accompanied by the introduction of parts of the rocket propellant into the environment. This study aims to scrutinize the effect of the components of rocket fuel on the induction of lipid peroxidation and chromosomal aberrations on rodents inhabiting the area exposed to pollution from Baikonur cosmodrome. The results showed the increase of the level of lipid hydroperoxide and malondialdehyde in the livers of *Citellus pygmaeus* Pallas and *Mus musculus* L., which indicates an augmentation of free radical activity and DNA damage. The cytogenetic analysis of bone marrow cells revealed that the frequency of chromosomal aberrations was a few times higher in the rodents from contaminated territory. The signs of oxidative stress and high level of chromosomal aberrations indicate the environmental impact of the cosmodrome, and its possible toxic and mutagenic effects on ecosystems [1].

Main body

In 2006 from the Baikonur spaceport 16 starts of launch vehicles «M Proton» were made. The first step of the launch vehicle, separating from the ship, usually falls on the territory of the Ulytausky area. In a zone of its falling there are sites automobile and the railroads, power lines, the field camps of Kumkolsky of an oil field. The most dangerous sites where the remains of a step of the M Proton launch vehicle can fall, are in Ulytauskomi Shetsk regions of the Karaganda region: these are sites of highways Kyzylorda – Pavlodar and Yekaterinburg – Almaty, a site of the railroad Petropavlovsk – Almaty, sites of oil pipelines Pavlodar – Shymkent and Atasu – Alashankou , sites of hunting grounds and power lines. In this zone there live people, there are settlements. Sukhoputnaya Route of the Proton-M launch vehicle takes not only the territory of Kazakhstan, but also Altaiskyi Krai, the Republics of Altai, Khakassia, Tuva, Sakha of the Russian Federation, China, Mongolia, North and South Korea, Japan [2].

Population density on the route of flight at first progressively increases from 0.5-1 persons/km, and reaches a maximum – 5-7 persons/km in the territory of the Pavlodar region of RK and the Mountain Altai republic of the Russian Federation and then gradually goes down [3].

The carrier rocket of the Proton series belongs to the heavy class. It is made by the State space research and production center of M.V. Khrunichev (Russia). Since 1965 more than 320 starts of the carrier took place. Modernized «Proton-M» has three steps. Starting weight – 700 tons, length – 61.75 meters, diameter – 7.4 meters. It is equipped with the new accelerating Briz-M block and a modern digital control system. «Proton» can put to geostationary

 Printed in Kazakhstan

orbits at the same time some satellites with a total weight up to 4.2 tons [4].

Even in the regular mode the risk for health of the population in areas of the space-rocket activity (SRA) exists from a point of start of ballistic missiles and carrier rockets on all route of flight. On the district at distances from a start point to 800 km at two-level removal and to 2500 km at the three-stage the «spots» of 1500-5000 km^2 covered with fragments of the ballistic missiles (BM) and rockets – carriers (RC) are formed [5].

Essential harm to natural objects is done as elements of a design of the separating parts of carrier rockets (mainby), and the remains of not developed components of fuels. The area of one pollution depending on hydrometeorological and geographical features of a place of falling very much of RN can reach some hectares, besides the LRF (liquid rocket fuel) components and products of their transformation can migrate with natural waters on distances to several hundred kilometers [6].

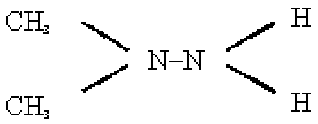

At the content in air of amount of heptyl of 0.01 mg/l in a few minutes there is a serious poisoning. Maximum concentration limit, in this measurement makes 0.0001 mg/l or 0.001 mg/m3 of atmospheric air. During long use of heptyl in Armed Forces of the USSR the big material testifying to an adverse effect of heptyl on health of staff of VS is saved up. It is established also that heptyl in a dose of 0.1 maximum concentration limits at contact with it in the open air within two years makes an adverse effect on a human body [7]. Therefore maximum concentration limit should consider 0.00001 mg/l. For children, pregnant women of maximum concentration limit of heptyl has to be 0.000001 mg/l or 0.00001 m^3 [8].

Nonspecific violations of health have a strong likeness with symptoms of a radiation injury (a cancer, leukoses, cytosinging, an adynamy, etc.) that becomes frequent the reason of the wrong diagnosis. Symptoms of a pseudo-radiation injury happen so expressed that compels doctors to make the diagnosis to sharp radiation sickness. However lack of a source of ionizing radiation gives the chance to exclude radiation defeat [9].

There is accurately expressed professional risk. Most often defeat of an organism the space rocket fuel (SRF) found in tabunshchik, shepherds, and often die cattle breeders who practically don't live up to pension from cancer [10].

The age risk is distinctly expressed: the age is less, the specific pathology is found (spasms, damage of a liver, blood, a laringostenoza, etc.) more often. Women have a bigger risk of diseases of blood, than at men. Newborns that are connected with pre-natal defeat of a fruit have the greatest risk [11].

The risk of defeat of an organism sharply increases at those persons who adjoin to RN fragments: the walls of fuel tanks, various small splinters which are giving in to manual processing (production of knives, handles, cigarette cases, etc.). They develop the states indistinguishable from radiation sickness (in the absence of the radiating source) [12].

In scientific literature collected enough data confirming an adverse effect of rockets – the carriers flying on toxic fuel on environment and health of the population. And this influence has catastrophic character, causing transient malignant diseases an iliinvalidization in the persons who got poisoning.

When falling a tank, the remains of fuel dissipate in air, forming the poisonous smog which is besieged on the earth on a trajectory of the movement of the first and second steps of rockets. Thus, there is a gradual pollution by all components of rocket fuel of environment along routes of flight of rockets. Pollution of huge territories accrues with each new start [13, 14].

For decades of a place of spill of heptyl turn into godforsaken places, life-threatening the person. Heptyl possesses high fluidity: having got on the earth, it at once leaves to humidity (in the dry easy soil on depth to 3 meters), is dissolved in water and that is interesting when it is raining, rises up. Besides, heptyl is incredibly «steady» to the place of its appearance. The Russian scientists investigating this substance find it within 34 years on the same places [15]. Specific physical and chemical properties of heptyl do the extremely difficult, and in practice – impossible its neutralization and decontamination of the district after chemical infection.

It is necessary to consider and a small bioproductivity of desert and semidesertic ecosystems of the areas which are exposed to pollution, their low ability to self-restoration is a consequence of that. Also, for the ecosystems having a strong climatic stress the maximum assimilation of biogenes and their inclusion in trophic chains is characteristic, the expressed biological accumulation and strengthening of derivatives of heptyl in links of a food chain will be a consequence of that [16].

Accepting toxicity of heptyl in a look, command of space troops of Russia in 2006 made the decision not to order more industries of RN of the class «Cyclone-3», «Space-3M» and «Roar» fuelled toxic capable to put small objects to orbit. The Angara project on development and use of RN on eco-friendly fuel is also initiated.

However the reduced types of RN were started generally from the Plesetsk and Free spaceports (closed in 2007), on Proton and Dnieper launch vehicles, the most powerful of used, such decision it was accepted not. Tests of easy, Central and heavy «Angara» – are constantly removed. Now the first tests of this class RN it is planned to carry out only in 2011 [17, 18].

Thus, the mentioned steps towards ecological safety at the moment are solved nothing for Kazakhstan, and are only urged to calm the Russian public opinion. At preservation of present dynamics of starts, for the closest five years of one «Protons» 80–100 units will be started. At such selection and the available frequency of accidents the number of emergency start-up with their catastrophic consequences can exceed 15–20 cases of emergency situations of regional scale [19]. Though already now there is an alternative to old and very dangerous equipment, for example new modifications of RN «Union» flying on kerosene, the Russian side insists on further operation of «Protons» and «Dneprov», protecting the commercial interests [20].

The first start-up of «Proton», took place in 1965, and modernization was carried out in 2001. According to experts, frequent failures at starts show that numerous programs of modifications and conversion of outdated rockets were a little effective. Frequency of accidents was over the last ten years distributed as follows: on one in 1996 and 1997, two in 1999 and on one in 2002 and 2006, and one in 2007.

Despite these accidents, demand for commercial use of «Protons» continues to remain steady also for the reason that the customer, in case of accident, sustains the minimum losses which are covered by insurance. But who is insured from those who live directly under routes of dispersal of 700-ton rockets from which 649 tons are the share of extremely poisonous and chemically aggressive fuel mix of heptyl and amil. At the last accident on September 6, 2007 at the time of falling in the rocket there were 218 tons 978 kilograms of mixes. The largest fragment of the carrier rocket fell in 43 kilometers to South-west of Zhezkazgan (total of 200,000 habitants along with the cities – satellites), which escaped thanks to combination of circumstances. If switching off of engines happened for 5 – 10 seconds later, the rocket would fail within the city. Here it should be noted that so-called «deserted territories» of Kazakhstan any more not that in the fiftieth, population density in the region grew several times and, despite it, on – former it is operated in the ground mode. The people living there are defenseless before a technological initiative of the corporations, in a pursuit of profit which are irresponsibly ignoring their essential, vital interests and the right for quiet and healthy life [21].

Kazakhstan, following own strategy, will develop by all means the space program. Also time for creation on Baikonur of the open competitive environment came, technological break or as a minimum – refusal of outdated and dangerous technologies would be a consequence of that.

It is advisable to forbid immediately use (launch and flight over the territory of the Republic of Kazakhstan) RN of all types and types of basing working at heptyl and similar types of toxic fuel as constituting extreme health hazard and wellbeing of the population of the Republic of Kazakhstan.

References

1 Asia – Economy and life. 1998. No. 11; Kazakhstanskaya pravda. 1998. 25 June.

2 Science of Kazakhstan. 1995. No. 8; Kazakhstanskaya pravda. 1997. 4.oct, 15 nov.; Panorama. 1997. No. 29.

3 Panorama. 1997. No. 23; Kazakhstanskaya pravda. 1997. 4 Oct.; Russian newspaper. 1997. 4 Oct.; Kazakhstanskaya pravda. 1998. 28 January; Panorama. 1998. No. 40; Kazakhstanskaya pravda. 1999. 9 Fev.

4 Asia – Economy and life. 1998. No. 16; The Statistical press bulletin. 1998. No. 1. Page 34; Capital review. 1998. No. 2; Express K. 1998. 15 January.

5 Asia – Economy and life. 1998. No. 16; Kazakhstanskaya pravda. 1998. 25 Apr., on June 20.

6 Statistical press bulletin. 1998. No. 2. Pp. 5-76, 95-96.

7 Sheets of the Supreme Council of the Republic of Kazakhstan. 1992. No. 6. Page 110.

8 Environmental protection and rational use of the natural resources in the Republic of Kazakhstan: Stat. Almaty, 1996. Page 8, 9, 11; Statistical press bulletin. 1998. No. 1. Page 148; Kazakhstanskaya pravda 1998. June 20; Express K. 1998. 15 January.; Panorama. 1997. No. 23; Kazakhstanskaya pravda 1998. 28 January.

9 Panin L.E., Perova A.Yu. The medico-socialand environmental problems of use of rockets on the

old man fuel (heptyl)//the Bulletin FROM the Russian Academy of Medical Science, 2006. No.1 (119).

10 Gaykalova I. Rocket relics / New generation (newspaper) – 2006. – Aug.18.

11 News of astronautics, No. 3/2006.

12 Fedorov L.A. Liquid missile propellants in the former Soviet Union, Environmental Pollution 1999, 105. – P.157-161.

13 The Maximum Permissible Concentration (MPC) of harmful substances in air of a working zone: Hygienic standards, Russian register of potentially dangerous chemical and biological substances of the Russian Ministry of Health. – M., 1998.

14 Ananyev I.A., Smolenkov A.D., Shpigun O.A. Definition of products of oxidizing transformation of asymmetrical dimethylhydrazine in soils by method of liquid hromatomass-spectrometry. Mass spectrometry, 2009, T. 6, No. 4, P. 302-306

15 Ecologically the code of the Republic of Kazakhstan of January 9, 2007. No. 212-3. – Almaty: Lawyer, 2007. – 172 p.

16 Holmuminov Zh.T. Legal questions of public administration in the field of ecology//Problems of development and standardization of the ecological and agrarian legislation of Kazakhstan and the CIS countries in the context of integration processes (Baysalov readings-2005): materials of the international scientific and practical conference. Library of the land right / B. Zh. Abdraimov. – Astana, 2005. – P. 43-51.

17 Panin L.E. Medico-social and environmental problems of use of rockets on liquid fuel (heptyl) / P. 124-131.

18 Arshins V. Yu., Shulyakovskaya T.S., Rykova A.N., Saprin A.N. Rol butilgidroksitoluola in a metabolic inactivation of a dietilnitrozoamin. Research of denitroziruyushchy activity microsomes / Reports of Academy of Sciences of the USSR. – 1984. – 102 p.

19 Sapin M.R., Yurina N.A., Etingen L.E. Lymph node (structure and function). – Moscow: Medicine, 1978. – 266 p.

20 Ergozhin E.E., V.A. Culms., Lyapunov V.V. Chemical environmental monitoring objects of environment – one of the main directions of studying ecological aspects of influence of the Baikonur spaceport // Messenger HAG. – 2001. – No. 1 (21). – P. 93-96.

21 Lebedev G.G., Musiychuk Yu.I., Klevtsov of V.I. Klinika-diagnostik and urgent the help at sharp poisonings. KZhRT. – M.: Meditsina, 1984. – P. 122.

UDC 622.276.344

[1,2*]Nurxat N., [3,4]Gussenov I., [3,4]Tatykhanova G.
[5]Akhmedzhanov T., [3,4*]Kudaibergenov S.

[1]Department of Materials Science and Engineering, Massachusetts Institute of Technology, Cambridge, USA
[2]Department of Chemical Engineering, Texas Tech University, Lubbock, Texas, USA
[3]Laboratory of Engineering Profile, Kazakh National Technical University, Satpayev Str. 22, Almaty, Kazakhstan
[4]Institute of Polymer Materials and Technology, Satpayev Str. 22, Almaty, Kazakhstan
[5]Institute of Oil and Gas,Kazakh National Technical University, Satpayev Str. 22, Almaty, Kazakhstan
*E-mail: ipmt-kau@usa.net

Alkaline/Surfactant/Polymer (ASP) Flooding

This is a review article on the subject of combining tertiary oil recovery methods like alkaline, surfactant and polymer flooding in order to achieve the synergetic effect out of the different impacts which are caused by these chemicals, affect oil and water filtration in the reservoir and increase oil recovery. In the article the main theoretical concepts of EOR (enhanced oil recovery) are summarized, mechanism of alkaline, surfactant and polymer flooding technologies are explained referring to the research works which had strong contribution to the development of the tertiary oil recovery methods. Formulation of alkaline/surfactant/polymer (ASP) chemical formula for EOR is discussed as well. Importance of numerical simulation and core flood laboratory experiments for the successful implementation of ASP technologies explained in the paper. Finally several examples of ASP flooding applications throughout the world projects are presented.
Key words: alkaline, surfactant, polymer, flooding, enhanced oil recovery.

Introduction

Crude oil is still a major energy source for the current economics of the world [1]. To meet the requirements of crude oil supply, more and more efforts have been placed on not onlyexploringnew oil reservoirs, but also further improving of oil recovery from the mature reservoirs [2, 3]. The improvement of oil production from mature oil fields is an important strategy from both economic and technical points of view [1, 2, 4]. According to the oil recovery history [5, 6], there are three stages of oil extraction, which are primary, secondary, and tertiary technologies [7]. In primary stage, oil production depends on initial reservoir pressure and may result in recovery of less than 20% of original oil in place (OOIP). To prevent depletion of the reservoir pressure and to recover more oil water injection is applied. This is a secondary oil recovery stage or water flooding. Due to the rock heterogeneity and high oil viscosity approximately two thirds of the OOIP remainsunswept by injected water. Tertiary oil recovery techniques, such as thermal, gas, chemical, and microbial approaches, have been developed and show promising results on lab scale and field scale tests [7]. Tertiary recovery technique is an important enhanced oil recovery technique based on injecting a substance that is not present in the reservoir. Chemical based enhanced oil recovery approaches cover surfactant, polymer, alkali, and combination of these chemicals called ASP and have been explored extensively because of low cost, technical simplicity, and scalability in oil field tests. The design principle of chemical methods is to consider certain properties of crude oils in the reservoir and provide one or several effects: interfacial tension (IFT) reduction, wet ability alteration, emulsification, and mobility control.

In both surfactant and alkali systems, injection of surfactants and alkaline solutions aims to convert naturally occurring naphthenic acids in crude oils to soaps what results in the improvement of oil production through obtaining ultralow interfacial tensions and forming microemulsions. In the polymer

 Printed in Kazakhstan

flooding system, addition of polymer [8] is applied to reduce mobility ratio. However, ASP flooding approach is considered to be the most promising approach since it can provide advantages over controlling the above parameters for obtaining high oil recovery rate. However, the mechanism of ASP is still not completely understood that causes difficulty in designing the ASP formula. In this review, we try to discuss the ASP system from theory to its practical application aspects [9]. Both the mechanism of ASP flooding and the performance of tertiary ASP projects are discussed. It will be a useful tutorial fora new learner and contains updated materials for experts in EOR.

Theoretical discussion for EOR

The mobility ratio [7] (M_R) (equation 1) is defined as the ratio of the mobility of displacing phase ($\lambda_{displacing\ phase}$) to the mobility of displaced phase ($\lambda_{displaced\ phase}$). The mobility of a fluid λ, is a quantitative measure of its ability to flow through channels and is equal to the permeability(k) divided by the fluid viscosity(η):

$$M_R = \lambda_{displacing\ phase}/\lambda_{displaced\ phase}=(k_w\eta_o/k_o\eta_w) \quad (1)$$

where k_w – permeability of water, η_o – viscosity of oil, k_o – permeability of oil, η_w – viscosity of water.

Theoretically, while the mobility ratio is higher than one, the displacing process is unfavorable for displacing oil. While the ratio is less than one, the process is favorable for oil to be displaced.

In the calculation of oil recovery, the overall efficiency of oil recovery [7] (E_{tot}) is the main parameter for comparison of oil production efficiency. It is defined as the ratio of the recovered amount of oil (N_{ex}) to the original amount of oil in place (N_{ooip}) (equation 2) and includes the two separate efficiencies, which are the volumetric sweep efficiency (E_{vol}) and the displacement efficiency *(E_{dis}),* as shown in the equation 3.

$$E_{tot} = N_{ex}/N_{ooip} \quad (2)$$

$$E_{tot}=E_{vol}E_{di\ s} \quad (3)$$

The volumetric sweep efficiency E_{vol} is the fraction of the volume swept by the displacing agent to the total volume of the flooded reservoir. This value characterizesa macroscopic displacement effect and is a function of the mobility ratio. Therefore, mobility control methods, including polymers, foams and alternate water and gas injection (WAG process) are applied to improve sweep efficiency. Therefore, the addition of a polymer can be applied to reduce the mobility ratio through increasing the viscosity of water and reducing permeability to water in ASP floods, which allows greater volumetric sweep efficiency. The commonly used polymers are water-soluble polymers, which include partially hydrolyzed polyacrylamide (HPAM) and xanthan gum (a biopolymer).

The displacement efficiency, E_{dis}, is the ratio of the recovered amount of oil to the amount of oil initially present in the swept volume and is a result of the microscopic effects. It is expressed as follows:

$$E_{dis}= (S_{oi}- S_{or})/ S_{oi} \quad (4)$$

where S_{oi} – initial oil saturation and S_{or} – residual oil saturation after oil recovery process.

The residual saturation of a displacement phase is related with viscous forces, surface forces (interfacial tension) and capillary number [10]. The capillary number [7], N_{cn}, is defined as a dimensionless ratio of viscous to local capillary forces (equation 5). During water flooding, some oil still remains in the reservoir, which is the residual saturation [11]. The viscous force helps to mobilize the oil, while the capillary forces cause trapping of the oil droplets due to the high IFT between water and oil.

$$N_{cn}=\text{Viscous forces/Surface forces} = \nu\eta/\delta \quad (5)$$

where ν – velocity; η – viscosity; and δ – interfacial tension.

A typical water flood capillary number is 10^{-7}. A capillary number between 10^{-4} and 10^{-3} is required to enhance oil recovery. Therefore, in order to reach the above capillary number for enhancing oil recovery, it is necessary to reduce interfacial tension from 1,000 to 10,000 folds [10].

Figure 1 shows that increasing capillary number reduces the residual oil saturation. Low residual oil saturations indicate high efficiency of oil extraction, thus large capillary number is beneficial for high displacement efficiency. Capillary number is usually in the range of 10^{-3} when the residual oil saturation is close tozero. The most efficient way to increase the capillary number is to reduce the IFT.

Therefore, the principal objective of the ASP process is to lower the interfacial tension so that the displacement efficiency will be improved.

Presence of residual oil saturation in fractured, oil-wet formations is mainly due to the capillary forces and phenomenon of wet ability. Therefore, the height of the capillary retained oil column is greater for the narrower pores as shown by the equation (6).

$$\Delta\rho gh = -2\delta\cos\theta/R \quad (6)$$

By altering the wet ability to the water-wet condition and reducing the interfacial tension to ultra-low values [4], it is possible to enhance oil recovery and provide a solution to oil retention problem. An injected fluid is required to be injected into the matrix of a fractured formation for EOR rather than into the fractures. The injected fluid must be spontaneously imbibes from fracture system into the matrix. Although spontaneous capillary imbibitions is an important mechanism for enhanced oil recovery, buoyancy will tend to allow oil to flow upward and out of the matrix into the fracture system in the ultra-low interfacial tension system. Imbibitionis a fluid flow process of increasing wetting phase saturation in a porous media. Spontaneous imbibition drives the wetting phase into the rock with no external pressure. Furthermore, in a water-wet reservoir, water will spontaneously imbibe into smaller pores to displace oil, but in an oil-wet reservoir, capillary forces inhibit spontaneous imbibition of water. The injected fluid will replace the displaced oil in the matrix and thus the spontaneous imbibition will continue as long as oil flows out of the matrix. The primary driving force for imbibition in strongly water-wet conditions is the capillary pressure. Reduction of interfacial tension reduces the contribution of capillary imbibition. Application of a surfactant alters wet ability and enhances spontaneous imbibitions (Fig. 1).

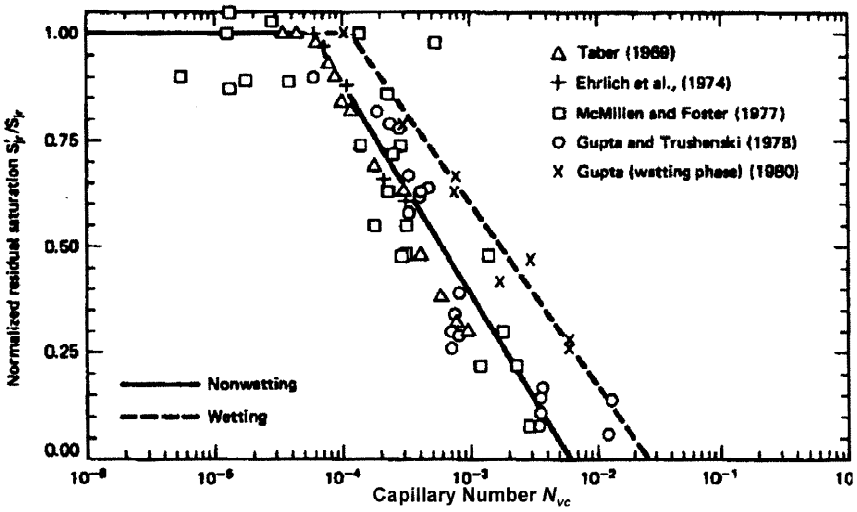

Figure 1 – Capillary desaturation curves [11]

The function of alkali, surfactant, and polymer during ASP

In EOR, flooding is based on the injection of water or another liquid, such as an alkaline solution, a surfactant solution etc., into the formation and driving the oil under the driving force of a pressure gradient.

ASP flooding [12] uses the benefits of the three flooding methods simultaneously (alkali-, surfactant-, and polymer-flood). Oil recovery mechanisms in alkali flooding are complicated. There are at least eight postulated recovery mechanisms [13, 14], which include emulsification with entrainment, emulsification with entrapment, emulsification with coalescence, wet ability reversal, wet ability gradients, oil-phase swelling, disruption of rigid films, and low interfacial tensions. The existence of different mechanisms is ascribed to the chemical property of the crude oil and the reservoir rock. Various crude oils in different reservoir rocks show widely different behavior when they are subjected to alkali under different conditions such as temperature, salinity, hardness concentration, and pH. The commonly ac-

cepted mechanism states that the acidic components in the crude oil are the most important factor for alkali flooding. Furthermore, it states that the chemicals produced by *in situ* saponification increase oil recovery. The acid number of a crude oil is one of the most important parameters in alkali flooding and illustrates the amount of natural soap that can be produced by the addition of alkali. The alkali compounds [15, 16] include sodium hydroxide, sodium carbonate, sodium silicate, sodium phosphate, ammonium hydroxide etc.

Surfactants are considered to be good enhanced oil recovery agents since they can significantly lower the interfacial tension and alter wetting properties [8, 17-19]. However, the major limiting factor is price. Therefore, it is very important to reduce the surfactant consumption for EOR process and to use it in ASP. Surfactants are classified into four groups: anionic, cationic, nonionic, and amphoteric (or zwitter ionic) surfactants. Anionic surfactants, including soap, are negatively charged, and the counter ions are usually small cations. The reason for the use of anionic surfactants in ASP is their relatively low adsorption in sandstone and clays, their stability and their relatively cheap price. Because of high adsorption of positively charged surfactants on anionic surfaces of clays and sand, cationic surfactants are not popular choice for oil recovery in sandstone. However, there are some investigations performed on cationic surfactants in recent years for carbonate reservoirs. The main mechanism of cationic surfactant flooding is wet ability alteration and the formation of ion-pairs between the positively charged surfactant monomers and negatively charged adsorbed material, which consists of mainly carboxylic groups on the surface. The resulting desorption makes the rock surface more water-wet, and water will spontaneously imbibe into the matrix due to the capillary effect. As far as nonionic surfactants are concerned, the ether groups of nonionic surfactants form hydrogen bonds with water so that nonionic surfactants exhibit surfactant properties. These chemicals derive their polarity from having an oxygen-rich portion of the molecule at one end and a large organic portion at the other end. The oxygen component is usually derived from short polymers of ethylene oxide or propylene oxide. As in water, the oxygen provides a dense electron-rich atom that gives the entire molecule a local negative charge site that makes the whole molecule polar and able to participate in hydrogen bonding with water. Amphoteric surfactants [20] may contain both positive and negative charges. These surfactants have not been tested in oil recovery. To have a successful commercial application using surfactants for oil recovery, the surfactant retention should be diminished. The retention mechanism of surfactants is attributed to adsorption, precipitation, ion exchange and phase trapping since the different mineralogy, including reservoir rocks, has different charges and properties. Furthermore, silica has a different isoelectric point in comparison with calcite, dolomite and clay, which have a positive charge on their surfaces at acidic pH. The electrical interaction between the charged solid surface and surfactant ions is the main cause of ionic surfactants adsorbing onto a solid and is explained by electrical double layer theory. For example, in hard brines, the divalent cationsreadily precipitate the surfactant as follows:

$$2R^{-} + M^{2+} \rightarrow MR_2 \downarrow$$

where R is the anionic surfactant. MR_2 is the surfactant-divalent cation complex that has a low solubility in brine.

Polymer is applied to change the mobility ratio to a favorable number since the injected fluid would not bypass the displaced fluid, i. e. crude oil in reservoir. Changing the properties of the crude oil or the permeability of the reservoir is not feasible from economic and technical points. Most mobility control methods change the properties of injected fluid. Polymer can significantly increase the apparent viscosity of the injected fluid. Foam is also a good mobility control method with water, surfactant and gas. Because low surfactant concentrations are used and much of the injected material is a gas, the cost of the chemical for foam can be much less than for the polymers. The mobility ratio will be lowered by using polymers which donot affect residual oil saturation with a few exceptions. But polymers greatly increase sweep efficiency. Two types of polymers, polyacrylamide and polysaccharide, are commonly used in enhanced oil recovery.

Numerical Simulation

Many simulation models have been developed to evaluate ASP process and direct the oil field applications of EOR techniques efficiently. Simulation techniques also minimize numbers and complexity of flooding experiments and help research-

ers to understand the characteristics of the ASP process. There has been much work simulating the ASP process by different companies to predict the EOR experiments and optimize reservoir performance. These programs use the solutions of the equations that govern multiphase fluid flow in porous media using finite difference techniques.

In 1978, a 1-D numerical simulator was developed by Pope and Nelson [21] to describe surfactant enhanced oil recovery and it has been extended to other chemical processes and to 3-D as UTCHEM [22-24]. Furthermore, ECLIPSE, which is a commercial reservoir simulator, was developed by Schlumberger. Two other software programs, VIP® and Nexus®, were developed by Halliburton. There are other simulators such as CHEARS by Chevron, and Empower by ExxonMobil. However, UTCHEM is the only model which considers natural soap as an additional surfactant [25]. A simple 1-D model is one of the most applied simulators; it illustrates the characteristics of the ASP process and is applicable to understanding and optimizing the process. A one-dimensional, two phase, multicomponential simulator has been applied to calculate the profiles and oil recovery as a function of process variables.

Design of ASP formulationMicroemulsion

Micro emulsion is a very important concept to design the formula of enhanced oil recovery. It is formed because of ultra-low interfacial tension. Phase behavior screening is an important parameter to observe the formation of micro emulsion and quickly evaluate favorable surfactant formulations. In 1954, Winsor [26] first described the phase behavior of micro emulsions for surfactant, oil and brine systems with different types and concentration of surfactants, co surfactants, oil, brine, alcohol, temperature, etc. The ternary phase diagram is a convenient tool for describing the micro emulsion phase behavior [8, 27] and shows the relationship between salinity changes and the phase behavior. Micro emulsions can be classified into three classes: lower-phase micro emulsion, upper phase micro emulsion and middle phase micro emulsion.

The main mechanism for formation of micro emulsions with ionic surfactants is derived from electrostatic forces. These forces will spontaneously change the curvature of the drops and produce the different types of micro emulsion systems. Furthermore, at low salinities, the micro emulsion is formed as an oil-in-water micro emulsion with pure excess oil. Due to the difference between the density of this kind of microemulsionand the oil phase, this micro emulsion is formed below the oil phase, which is called "lower phase" microemulsion (named as Winsor type I, or type II(-). With increase of salinity, the size of the micro emulsion drop will increase and solubilization of oil will be augmented since the repulsion between the charged head groups decreases. If the salinities are very high, the electrostatic forces change the sign of the drop curvature, and water-in-oil micro emulsion forms. Since the formed micro emulsion is lighter than the water, which is pure excess phase and above the water phase, it is called an "upper phase" microemulsion (also named type II (+) or Winsor type II). However, at intermediate salinities, amicroemulsion is in equilibrium with both excess oil and brine. The micro emulsion is between the oil and brine phase, which is called "middle phase" micro emulsion (named type Ill, or Winsor type III). The micro emulsion contains almost all the surfactants in the system. Formation of this type of micro emulsion is important to design the ASP system for oil recovery because of its ultra-low interfacial tension. The phase structure of middle microemulsionis intricate and needs to be further investigated. Scriven (1976) suggested that the middle phase micro emulsion is a bicontinuous structure. Burauer S. et al developed theoretical models and some experimental observations to understand the bicontinuous micro emulsion system. Since both the oleic phase and aqueous phase are continuous, the interfacial tensions between the middle phase and either excess brine or excess oil are very low.

Phase Behavior and Interfacial Tension

Healy and Reed [27] first established an empirical correlation between the micro emulsion phase behavior and the interfacial tension (Fig. 2). They introduced solubilization ratios and described the corresponding behavior of the solubilization parameters and IFT with different salinity. In figure 2, σ_{mo} represents the IFT between the micro emulsion and the excess oil phase, and σ_{mw} represents the IFT between the micro emulsion and water phase. Figure 2 shows that σ_{mo} is high in the type I region and does not exist in the type II region. However, σ_{mw} does not exist in the type I region and σ_{mw} is high. In the type III region, both σ_{mo} and σ_{mw} arethe lowest values and are equal. The term

corresponding to this value is the optimum salinity [28]. The solubilization parameter V_o/V_s is defined as the volumetric ratio of solubilized oil to surfactant, and V_w/V_s is the water to surfactant ratio in the micro emulsion phase. Figure 2 shows that if V_o/V_s increases with salinity, V_w/V_s decreases with salinity. However, at optimum salinity, the amount of oil and brine solubilized in the surfactant phase are approximately equal. This is also another definition of optimum salinity. These two parameters are very important in designing the ASP flooding technique.

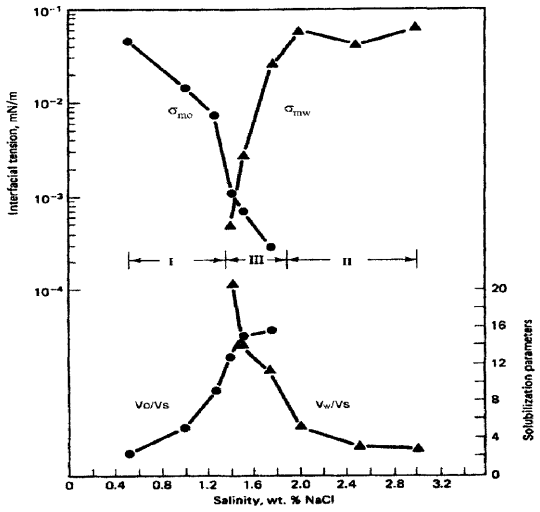

Figure 2 – Interfacial tension and solubilization parameter versus salinity [29]

As discussed in the section about the relationship between capillary number and interfacial tension, while interfacial tension is a low value, capillary number is large, and the residual oil saturation goes to zero. This is the main basis for designing the enhanced oil recovery formula. Healy and Reed [27, 30] proved that the optimum salinity was the salinity for maximum oil recovery by core flooding experiments. Clearly, one of the goals is to use the surfactant at the displacement front near optimum conditions in the ASP flooding. At this optimum salinity, the contact angles are equal. In 1979, Huh [31] developed a theoretical formula and described the relationship between solubilization ratio and IFT (equation 7). The IFT is inversely proportional to the square of the solubilization ratio, S. Based on Huh's equation [31], C=0.3 is a good approximation for most crude oils and micro emulsions.

$$\sigma = C/S^2 \qquad (7)$$

In 1979, Glinsmann [32] experimentally confirmed this relationship. Sometimes, it is difficult to measure the IFT between some crude oil and its lower phase micro emulsion. Through phase behavior observation and measurements of the solubilization ratios, the IFT of the oil / water / micro emulsion system can be estimated. It is very important to confirm a good formulation by considering both phase behavior and IFT measurement in ASP floods. Therefore, oil recovery is greatly enhanced by decreasing IFT, increasing the capillary number, enhancing the microscopic displacement efficiency, improving the mobility ratio, and increasing macroscopic sweeping efficiency. ASP flooding combines various mechanisms into a process.

Experimental evaluation approach

The results from phase behavior, IFT, adsorption and simulation helps to design ASP flooding experiments, which include a core flooding experiment. They can be used to prove those important mechanisms and provide the directions for the real field test.

IFT measurement methods [19] include capillary rise, Wilhelmy plate, Du NoUy Ring method, spinning drop, pendant/sessile drop, maximum bubble pressure method, etc. There are two methods which can be used extensively. Furthermore, pendant drop is usually applied to measure relatively high tension samples (above 1 mN/m). The pendant drop method is used to determine the interfacial tension based on geometric analysis of the interface of the drop and is performed on a drop of liquid surrounded by the other phase. But it is still very difficult to measure the tension that is less than 10^{-2}mN/m. A typical crude oil/brine interfacial tension is around 20-30 mN/m. Spinning drop [19] isa good fit for measuring the ultra- low tension system. In this method, two immiscible fluids are added in a capillary tube at the same time and rotated. Fluid A has different density from fluid B and is less dense than fluid B. Fluid A stays in the center of the capillary tube and forms an elongated drop through the centrifugal field generated by rotation forces. The geometry of the drop is related to the balance of the centrifugal force and interfacial tension force. In this force balance, the centrifugal force stretches the drop, while the IFT prevents this elongation. For a cylindrical shape drop that has a length at least four times greater than its radius, the following expression (equation 8) is often used to

calculate IFT, where σ is interfacial tension. Δρ stands for the density difference of the two fluids, whileωis a rotation rate. The radius of the less dense drop is r.

$$\sigma = \Delta\rho\omega^2 r^3/4 \quad (8)$$

Phase behavior screening is a direct and simple way to predict the low IFT flooding formula as was discussed above. Type III or middle-phase micro emulsions exhibit the lowest IFT. For anionic surfactants, increasing the salinity, among other variables, causes the characteristic transition from Type I to Type III to Type II. Healy et al. presented the concept of optimum salinity as it applies to Type III micro emulsions. They observed the volumes of oil (V_o) and water (V_w) per unit volume of pure surfactant (Vs) in middle-phase micro emulsions and defined the optimum solubilization ratio (s*) as the intersection of plots of V_o/V_s and V_w/V_s as a function of salinity or other variables that affect the phase behavior. The intersection point represented a Type III micro emulsion with an optimal solubilization ratio (s*) and optimal salinity value.

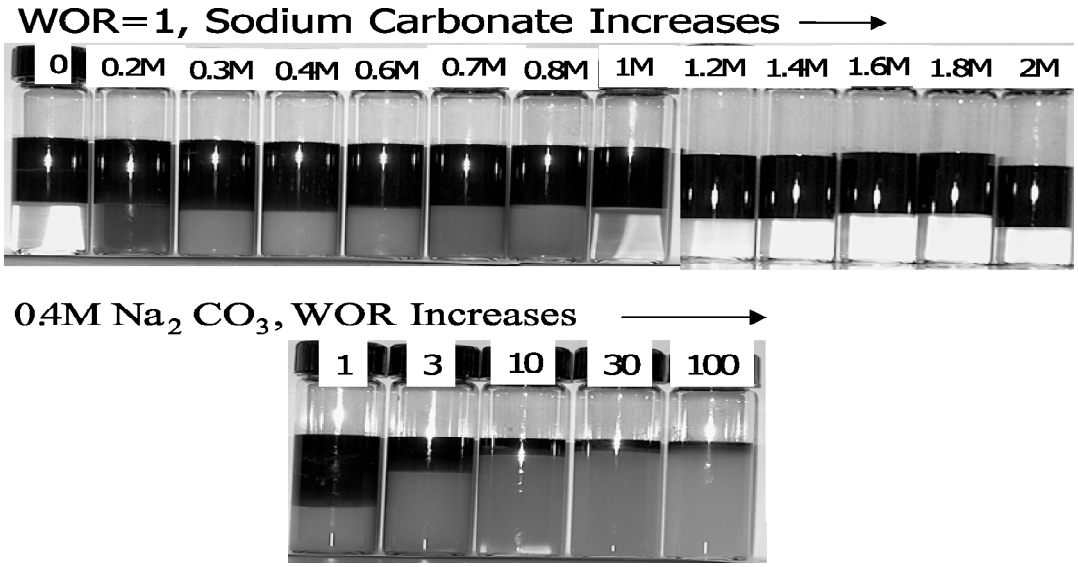

Figure 3 – Phase behavior of MY3 crude oil with 0. 2% (AM) TDA [33]

Core flood tests can be used to evaluate effects of alkali concentration, surfactant concentration, slug sizes, injection scheme, and potential use of chemical flooding for a field application. An ASP flooding system developed by Li etal [12] consists of1. 0% alkaline, 0. 5% nature mixed carboxyl ate surfactant (SDC), 1000 ppm polyacrylamide. The system that included nature mixed SDC was studied to examine phase behavior, interfacial tension and oil recovery. The ASP flooding results (Fig. 4) show high oil recovery, which is up to 26. 8%.

Survey of researches on ASP flooding

Most of researches on EOR are devoted either to one chemical component flooding such as alkali flooding, surfactant flooding, polymer flooding, or two chemical component flooding such as alkaline-surfactant (AS), alkaline-polymer (AP), surfactant-polymer flooding (SP)[34] that are effective strategy to increase oil recovery [35]. In this subchapter only ASP flooding consisting of more than two chemical components in the oil displacing formula is considered. Due to the synergetic effect and multiple functions of chemicals, the oil recovery of chemical combination flooding is higher than that of one or two component chemical flooding [36]. The contribution of alkaline (A), surfactant (S), polymer (P), and their combinations as AS, AP, SP to EOR was evaluated by authors [37]. For this a specially designed 2-D physical model was used and the dominant mechanism of enhanced heavy oil recovery was identified. Analysis of the seven 2-D sand pack flood tests shows that, for the heavy oil

tested, polymer flooding is an effective method to increase the final oil recovery, while alkalis and surfactant can help reduce the IFT, and, thus, increase the displacement efficiency. The combination of AS can reduce IFT to a much lower level, and yields a higher oil recovery than both alkaline-only and surfactant-only flooding. The combination of all three chemicals ASP yields the highest oil recovery.

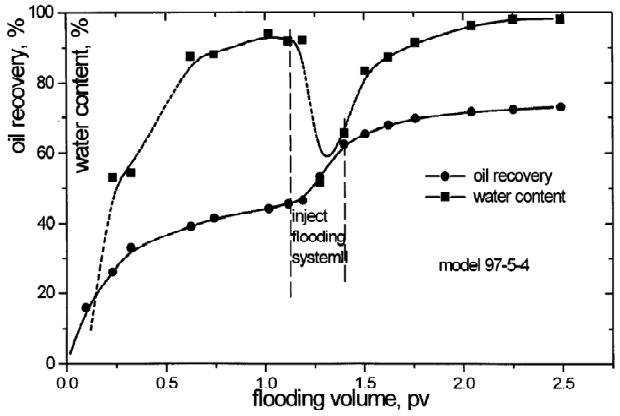

Figure 4 – Dynamic flooding process curve of system [12]

ASP flooding is complex and involves chemical reactions that depend on the oil composition, water composition, rock mineralogy, temperature, pH, etc. Authors [38] developed simplified ASP model and implemented it in a 3D chemical flooding reservoir simulator. The essence of the proposed model is that the reaction of acidic species at high pH generates soap and comprehensive phase behavior model for the mixture of soap and surfactant. Three ASP corefloods were modeled using simplified model and the proposed model can easily be implemented in any existing surfactant/polymer model. Simulation experiments were conducted to examine the effects of ASP on w/o [39] and stability o/w separation [40] in produced water from ASP flooding. The emulsion stability of water produced from ASP flooding was investigated by conducting settling experiments and measuring the oil–water interfacial properties [41]. The experimental results show that the addition of hydrolyzed polyacrylamide degrades the emulsion stability when its concentration is below 300 mg/L for the molecular weight $M_W = 1.2 \cdot 10^7$, and 800 mg/L for the $M_W = 3.0 \cdot 10^6$. But it enhances the emulsion stability when polymer concentrations are above those levels. At low polymer concentrations, flocculation induced by the polymer on oil droplets in the produced water is the dominant factor, while at high polymer concentrations the produced water viscosity plays an important role in the emulsion stability. The adsorption of surfactant on the oil–water interface increases the zeta potentials and decreases interfacial tension, and thus remarkably enhances the emulsion stability. Furthermore, the emulsion stability is enhanced gradually with the increase of NaOH concentration up to 300 mg/L due to the increase of zeta potentials and decrease of interfacial tension, and then weakened with the further increase of NaOH concentration, which is attributed to the decreased strength of the interfacial film.

Comprehensive research was devoted to determination of the impact of mineralogy and clays on the performance of ASP floods in sandstone formations [42]. Three flooding experiments (two single-phase and one two-phase flow) are carried to investigate the impact of active clays on permeability reduction and its reversibility, water chemistry changes and performance of ASP flooding.

Based on physico-chemical properties of polymer, surfactant, and alkali and their mutual interaction in solution, authors [43] recommended the following optimal composition of an ASP slug consisting of SDS: 0.1 wt. %, SDBS: 0.075 wt. %, polyacrylamide: 2000 ppm, and NaOH: 0.7 wt. %. Two sets of core-flooding experiments have been conducted using the designed ASP slug in a triaxial core holder to measure the additional recovery of oil. The average additional oil recovery over conventional water flooding was found to be more than 20% of the original oil in place (OOIP).

A dilute SP flooding system has been designed and developed for Gudong oilfield with Shengli petroleum sulfonate (SLPS) as the primary ingredient [44]. The SP flooding formulation was finalized as 0.3% (w/w) SLPS + 0.1% (w/w) 1# + 0.15% polyacrylamide (PAM), in which 1#, the secondary surfactant, is able to enhance the interfacial activity of SLPS and the flooding efficiency of the system. The pilot field trial of the system started in June 2004 and finished in 2008 exhibited outstanding performance to improve oil production that had risen by 17.8×10^4 tons, with the oil-recovery increase by 6.4%. Studies have been done to examine the applicability of natural surfactant and polymer for enhanced oil recovery.

Authors [45] investigated interfacial and rheological properties of natural polymer – guar gum

and natural surfactant obtained from extracted soap nut shell. Based on the physicochemical properties of the surfactant and polymer solutions, optimum compositions were designed for flooding experiments. Three sets of experiments were performed to study enhanced oil recovery by injecting the same pore volume of polymer, SP, and ASP slug after brine flooding. Significantly higher additional recovery (~24% OOIP) was obtained by alkaline–surfactant–polymer flooding compared to the other two methods over water flooding (~50% OOIP).

The synergistic effects of NaOH, alkylbenzylsulfonate, and partially HPAM on the emulsification and destabilization of O/W crude oil emulsion produced by ASP flooding were studied [46]. The experimental results showed that the major factors governing the stability against phase separation of O/W ASP flooding produced fluid include the enhanced emulsification of produced fluid by alkaline, surfactant and HPAM, in which smaller oil droplets are generated, and the hindrance of alkaline and surfactant to oil droplet flocculation and coalescence.

The alkali consumption regularities for five kinds of minerals (kaolinite, grundite, chlorite, feldspar and quartz) in ASP and single component NaOH solution were studied [47]. It was found that alkali consumption is mainly caused by clay minerals and is 18.3% larger in average than matrix minerals. It was concluded that the main alkali consumption style in ASP system is the physical absorption; but for matrix minerals, the main alkali consumption style is the chemical reaction.

Alternative to conventional ASP flooding the chemical formulation using a new polymeric surfactant was suggested [48]. The polymeric surfactant used was poly(sodium methyl ester sulfonate) (PMES). Using 0.6 and 1 wt. % surfactant concentration, 16.2 and 20.7 % OOIP were recovered (Fig. 5). Such high oil recovery was due to the synergistic effect between polymeric surfactant and alkali to emulsify and mobilize the crude oil.

ASP methods to improve recovery of viscous oils were developed by authors [49].

The effectiveness of ASP system on EOR was tested with the help of sand-pack systems [50]. Recovery efficiencies vary 23–33 % of OOIP over the conventional water flooding. As seen from Table 1 additional recovery increases only marginally as concentration of PHPAM is changed from 1500 to 2500 ppm. Injection of polymer increases the sweep efficiency, and hence, oil recovery. After a certain concentration of polymer, the sweep efficiency approaches to its limiting value and thus only marginal additional recovery is observed.

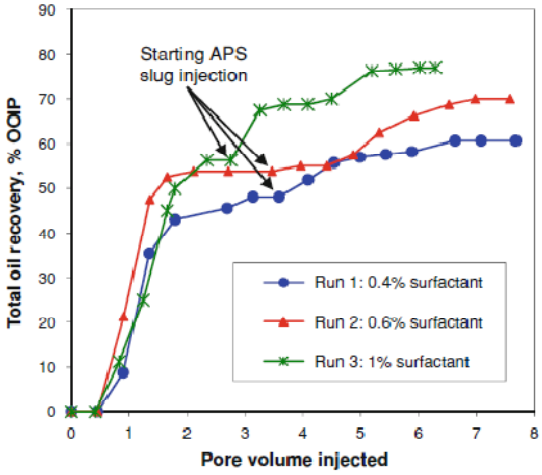

Figure 5 – Effect of various surfactant concentrations on oil recovery (Alkali 0.8 %)

Several mechanism viz., reduction IFT, emulsification of oil and water, solubilization of interfacial films, wet ability reversal, viscosity improvement, etc. are responsible for the EOR. Based on the experimental data and relative cost of different chemicals, concentration range of alkali (0.7–1.0 wt. %), polymer (1500–2500 ppm) and surfactant (0.2 wt. %) have been recommended for successful ASP flooding.

In EOR simulation model, two methods, polymer and SP floods, were compared [51]. The recovery factory for each case can be seen in Table 2. The incremental value displays the incremental recovery based on the adjusted water flood. The optimum polymer flood has a recovery contribution of 8.80%. The optimum surfactant-polymer process has another 2. 49% incremental recovery based on polymer flood.

Table 1 – Recovery of oil by ASP flooding with varying concentration of polymer

Expt. No.	Porosity (%)	Permeability, *k* (darcy)		Design of chemical slug for flooding	Recovery of oil after water flooding at 95% water cut (%OOIP)	Additional recovery (%OOIP)
		k_w (S_w=1)	k_0 (S_{wi})			
S6	37.265	1.144	0.217	0.3 PV (0.5% NaOH+0.1% SDS+1500 ppm PHPAM) + 0. 2 PV 1.5 ppm buffer + chase water	50.2	23.69
S7	36.805	1.145	0.218	0.3 PV (0.5% NaOH+0. 1% SDS + 2000 ppm PHPAM) + 0.2 PV 2.0 ppm buffer + chase water	52.8	23.5
S8	37.265	1.143	0.217	0.3 PV (0.5% NaOH + 0.1% SDS + 2500 ppm PHPAM) + 0.2 PV 2. 5 ppm buffer + chase water	52.9	24.2

Table 2 -Recovery Summary of different EOR Methods

Method	Polymer			Surfactant -polymer	
Simulation case	4 million	6 million	9 million	Process 1	Process 2
Ultimate recovery (%)	58.21	60.78	59.13	63.27	62.84
Incremental value of OOIP (%)	6.23	8.80	7.15	11.29	10.86

The main technological problems occurred in the application of chemical combination flooding are: 1) to develop high-performance, low-cost surfactants for chemical combination flooding; 2) to develop new salt-tolerance, temperature-resistance polymers and surfactants; 3) to improve chemical combination flooding supporting technology in field tests and application; 4) to develop monitoring, tracking adjustment and optimizing technology in chemical combination flooding field tests.

ASP project performance

Two process units, which are water treatment and ASP preparation, are involved in using facilities for an ASP project. The ASP unit includes three subunits of alkali, surfactant, and polymer. Water is required in treatment for fullcompatibilty with the ASP chemicals. Ion exchange resin for water treatment is applied to meet the need of water softening, which isless than about 30000 ppm of total dissolved solid (TDS) content.

The West Kiehl ASP project [53] was considered as the first ASP project. This first alkaline-surfactant-polymer project was initiated in September 1987 in Minnelusa, Wyoming. The oil recovery was up to 23% OOIP. There have been performed many ASP technologies in the Daqing Field [54-57], Peoples Republic of China. Daqing is the largest oilfield in China. The results from all ASP projectsreported incremental recoveries of 20% OOIP or greater. In 1994, the first tertiary ASP project was performed in China. This test covered four injection wells, nine production wells, and a 5.5-acre pilot in the Saertu Sand. The ASP formula includes 1.25 wt. % Na_2CO_3 (alkali) plus 0.3 wt. % active Petro step B-100 (surfactant) plus 1200 mg/L Alco flood 1275 (polymer). Oil cuts reached a peak value of 48%. Oil rate and incremental oil respectively, are 61 m^3/day and 33,000 m^3or 31% OOIP. The ASP pilot test in Karamay EZ district, China [58] was performed starting on August 21st, 1995 and showed 24% OOIP incremental recovery in the whole test area. More ASP flooding tests have been applied in other oilfields of China. ASP field projects have been conducted in Canada and India. Table 3 summarizes the performance of some of the ASP projects worldwide.

Table 3 – ASP field tests

Project	Start Date	Area(Acre)	%OOIP	Reference
West Kiehl, Wyoming	1987	106	34. 4	53
Cambridge, Wyoming	1993	72	26. 8	59
David, Alberta	1986	252	21	59
Daqing, China	1994	8. 4	31	54, 60
Gudong, China	1992	766	29. 4	61
Karamay, China	1996	766	24	54,58
Viraj, India	2002	68	24	62
Tanner Field, WY	2000	44	44	63
La Salina Field, Venezuela	2001	1,445	24. 6	64

Conclusion

ASP technology has advantages including surfactants, alkali, and polymers with mobility control chemical (polymer). An alkaline-surfactant-polymer flooding technique has proved from oil field tests more than 20 % OOIP and has been successful in three completed projects in North America as well as several projects in China. ASP flooding technique has shown to be an economically viable technology in comparison with water floods. The above described significant performance of ASP technology is the results of the combined factors: reservoir engineering and geologic studies, laboratory chemical system design, numerical simulation, facilities design, and ongoing monitoring.

Acknowledgement

This work was performed in the frame of Technology Commercialization Project (Grant No. 161 for Senior Scientific Group). Financial support from the Ministry of Education and Science of the Republic of Kazakhstan and World Bank is greatly acknowledged. N. N acknowledges the financial support from Texas Tech University.

References

1 E.J. Manrique, C.P. Thomas, R. Ravikiran, M.I. Kamouei, M. Lantz, J.L. Romero and V. Alvarado in SPE Improved Oil Recovery Symposium, Society of Petroleum Engineers, Tulsa, Oklahoma, USA, 2010.

2 A. Gurgel, M.C. P.A. Moura, T.N.C. Dantas, E.L. Barros Neto and A.A. Dantas Neto //Brazilian Journal of Petroleum and Gas. 2008, 2, 83-95.

3 J.P. Brashear and V.A. Kuuskraa //Journal of Petroleum Technology, 1978, 30, 1231-1239.

4 N. Arihara, T. Yoneyama, Y. Akita and L. XiangGuo, in SPE Asia Pacific Oil and Gas Conference and Exhibition, Society of Petroleum Engineers, Jakarta, Indonesia, 1999.

5 A.K. Flaaten, University of Texas, 2007.

6 V.O. Eme, King Fahd University of Petroleum & Minerals, 1994.

7 L.W. Lake, Enhanced Oil Recovery, Prentice-Hall, Englewood Cliffs, NJ, 1989.

8 R.C. Nelson, J.B. Lawson, D.R. Thigpen and G.L. Stegemeier, in SPE Enhanced Oil Recovery Symposium, Copyright, Society of Petroleum Engineers of AIME, Tulsa, Oklahoma, 1984.

9 T. Babadagli //Journal of Colloid and Interface Science, 2002, 246, 203-213.

10 J.J. Taber, Pure & Appi. Chem., 1979, 52, 1323–1347.

11 M. Delshad, D. Bhuyan, G.A. Pope and L.W. Lake, in SPE Enhanced Oil Recovery Symposium, Society of Petroleum Engineers, Tulsa, Oklahoma, 1986.

12 L. G-Z., M. J-H., L. Y., Y. S-L., //Colloids Surf. A., 2000, 173, 219-229.

13 E.F. deZabala, J.M. Vislocky, E. Rubin, C.J. Radke. // SPE Journal, 1982, 22, 245-258.

14 T.S. Ramakrishnan, Wasan, D.T., SPE Journal, 1983, 23, 602-612.

15 H. Rivas, Gutierrez, X., Zirrit, J.L., Anto´n, R.E., Salager, Microemulsion and optimum formulation occurrence in pH dependent systems as found in alkaline enhanced oil recovery, M. Dekker, New York, 1997.

16 A. J. Jackson // University of Texas, 2006.

17 K.O. Ajay Mandal, in the Asia Pacific Oil and Gas Conference and Exhibition, Perth, Australia, 2008.

18 D. Leslie Zhang, S. Liu, M. Puerto, C.A. Miller and G.J. Hirasaki, Journal of Petroleum Science and Engineering, 2006, 52, 213-226.

19 C.A. Miller, Neogi, P., Interfacial Phenomena, Marcel Dekker, Inc., New York, 1985.

20 X. Zhou, M. Han, A.B. Fuseni and A.A. Yousef, in SPE Improved Oil Recovery Symposium, Society of Petroleum Engineers, Tulsa, Oklahoma, USA, 2012.

21 G.A. Pope, Nelson, R.C., SPE Journal, 1978, 18, 339-354.

22 M. Delshad, K. Asakawa, G.A. Pope, K. Sepehrnoori, in SPE/DOE Improved Oil Recovery Symposium, Copyright 2002, Society of Petroleum Engineers Inc., Tulsa, Oklahoma, 2002.

23 L.E. Zerpa, N.V. Queipo, S. Pintos, J.-L. Salager, in SPE/DOE Symposium on Improved Oil Recovery, Society of Petroleum Engineers, Tulsa, Oklahoma, 2004.

24 G.A. Anderson, M. Delshad, C.L.B. King, H. Mohammadi and G.A. Pope, in SPE/DOE Symposium on Improved Oil Recovery, Society of Petroleum Engineers, Tulsa, Oklahoma, USA, 2006.

25 M. Delshad, W. Han, G.A. Pope, K. Sepehrnoori, W.Wu, R. Yang and L. Zhao, in SPE/DOE Improved Oil Recovery Symposium, Society of Petroleum Engineers, Inc., Tulsa, Oklahoma, 1998.

26 P.A. Winsor, Solvent Properties of Amphiphilic Compounds, Butterworth's Scientific Publications, London, 1954.

27 R.N. Healy, Reed, R.L., Stenmark, D.K., SPE J, 1976, 16, 147–160.

28 R.N. Healy and R. L. Reed, Contact angles for equilibrated microemulsion systems, 1979.

29 R.L. Reed and R. N. Healy, SPE Journal, 1984, 24, 342-350.

30 R.N. Healy, R.L. Reed. //SPE Journal, 1977, 17, 129-139.

31 C. Huh. // J. of Colloid and Interface Science, 1979, 71, 408–426.

32 G.R. Glinsmann, in SPE Annual Technical Conference and Exhibition, 1979, Las Vegas, Nevada, 1979.

33 G. Hirasaki, D.L. Zhang, in International Symposium on Oilfield Chemistry, Society of Petroleum Engineers, Houston, Texas, 2003.

34 Z. Youyi, Z.Yi, N. Jialing, L. Weidong, H. Qingfeng. // PETROL. EXPLOR. DEVELOP., 2012, 39(3), 371–376.

35 Z. Youyi, H. Qingfeng, J. Guoqing, M. Desheng, W. Zhe. // PETROL. EXPLOR. DEVELOP., 2013, 40(1), 96–103.

36 M. Kazempour, E.J. Manrique, V. Alvarado a, J. Zhang, M. Lantz. //Fuel,2013,104,593–606.

37 Xiaodong Zhou, Mingzhe Dong, BrijMaini. // Fuel. 2013,108, 261–268.

38 M. Delshad, Ch. Han, F.K. Veedu, G.A. Pope. // Journal of Petroleum Science and Engineering, 2013

39 K. Wanli, L. Yi, Q. Baoyan, L. Guangzhi, Y. Zhenyu, H. Jichun. // Colloids and Surfaces A: Physicochemical and Engineering Aspects. 2000, 175, 243–247.

40 S. Deng, R. Bai, J.P. Chen, G. Yu, Zh. Jiang, F Zhou. //Colloids and Surfaces A: Physicochem. Eng. Aspects2002,211, 275-284.

41 B. Wang, T. Wu, Y. Li, D. Sun, M. Yang, Y. Gao, F. Lu, X. Li. //Colloids and Surfaces A: Physicochem. Eng. Aspects. 2011,379, 121–126.

42 M. Kazempour, E.J. Manrique, V. Alvarado a, J. Zhang, M. Lantz. // Fuel 104, 2013, 593–606.

43 M.Y. Khan, A. Samanta, K. Ojha, A. Mandal. //Petroleum Science and Technology,2009, 27,17, 1926-1942.

44 W. Hongyan, C. Xulong, Z. Jichao, Z. Aimei. // Journal of Petroleum Science and Engineering. 2009, 65, 1–2, 45–50.

45 A. Samanta, K. Ojha, A. Mandal. // Petroleum Science and Technology. 2011, 29, 7, 765-777.

46 J.X.Li, Y. Liu, D. Wu, X.C. Meng, F.L. Zhao. // Petroleum Science and Technology. 2013,31, 4, 399-407.

47 J. Zhenhai, Z. Qingjie, W. Jianguang, G. Yunsong. //Advances in Petroleum Exploration and Development. 2012, 3, 1,38-43.

48 Kh.A. Elraies. //J Petrol Explor Prod Technol. 2012, 2, 223–227.

49 R. Kumar, K.K. Mohanty. ASP Flooding of Viscous Oils. SPE 135265.

50 A. Samanta, A. Bera, KekaOjha, A. Mandal. // J. Petrol Explor Prod Technol. 2012, 2, 67–74.

51 P. Gao, B. Towler. //J. Petrol Explor Prod Technol , 2011, 1, 23–31.

52 M. Nedjhiouia, N. Moulai-Mostefaa, A. Morslia, A. Bensmaili. // Desalination,2005, 185, 543–550.

53 J.J. Meyers, Pitts, M.J., Wyatt, in the SPE/DOE Enhanced Oil Recovery Symposium, Tulsa, Oklahoma, 1992.

54 H.L. Chang, Z.Q. Zhang, Q.M. Wang, Z.S. Xu, Z.D. Guo, H.Q. Sun, X.L. Cao and Q. Qiao //Journal of Petroleum Technology, 2006, 58, 84-89.

55 S. Jun, Yang, C., Yang, Z., Lio, G., Yuan, H., Dai, Z., Li, Y., and Ye, and Z., in the SPE Asia Pacific Oil and Gas Conference and Exhibition, Brisbane, Australia, 2000.

56 D. Wang, Cheng, J., Wu, J., Yang, Z., Yao, Y., Li, H., in the SPE Asia Pacific Improved Oil Recovery Conference, Kuala Lumpur, Malaysia, 1999.

57 H.L. Chang, Z.Q. Zhang, Q.M. Wang, Z.S. Xu, Z.D. Guo, H.Q. Sun, X.L. Cao. // Journal of Petroleum Technology, 2006, 2, 84-89.

58 Q. Qi, G. Hongjun, L. Dongwen, D. Ling, in International Oil and Gas Conference and Exhibition in China, Society of Petroleum Engineers Inc., Beijing, China, 2000.

59 S. Majidaie, M.T. Isa, B.M.R. Demiral, in 2010 International Conference on Integrated Petroleum Engineering and Geosciences, Kuala Lumpur, Malaysia, 2010.

60 W. Demin, Z. Zhenhua, C. Jiecheng, Y. Jingchun, G. Shutang, L. Lin, SPE Reservoir Engineering, 1997, 12, 229-233.

61 S. Gao,Q. Gao, in SPE EOR Conference at Oil & Gas West Asia, Society of Petroleum Engineers Muscat, Oman, 2010.

62 M. Pratap, M. S. Gauma, in SPE Asia Pacific Oil and Gas Conference and Exhibition, Society of Petroleum Engineers, Perth, Australia, 2004.

63 M.J. Pitts, P. Dowling, K. Wyatt, M.J. Pitts, H. Surkalo, in SPE/DOE Symposium on Improved Oil Recovery, Tulsa, Oklahoma, USA, 2006.

64 C. Hernandez, L.J. Chacon, L. Anselmi, A. Baldonedo, J. Qi, P.C. Dowling, M. J. Pitts, in SPE Latin American and Caribbean Petroleum Engineering Conference, Society of Petroleum Engineers Inc., Buenos Aires, Argentina, 2001.

UDC 541.64.02/04;678

Bazarova A.Zh., Kairalapova G.Zh., Zhumagalieva Sh.N., *Beisebekov M.K.

Al-Farabi Kazakh National University, Almaty, Kazakhstan
*E-mail: Marat.Beisebekov@kaznu.kz

Synthesis and investigation of properties of cryogel based on polyacrylic acid

This work is focused on synthesis of different ratios of cryogel based on polyacrylic acid in order to obtain the best results of cryogel in the most right moment. Studying of physico-chemical properties of obtained cryogel includes determination of equilibrium swelling, density, obtaining photographs by atomic force microscope, scanning electron and optical microscopes.
Key words: synthesis, properties, cryogel.

Introduction

Nowadays one of the main aims of scientists is an easy synthesis – processing of cryogels by available synthesis methods. The basic subject to be considered on obtaining polymeric materials is economically available, effective, ecologically harmless polymer synthesis methods. Gel materials belong to polymeric cryogels, which polymeric and monomeric bases are formed in not deeply frozen solutions. Set point of superficial processing is about ten degrees lower than set point of solvent. The systems obtained on the basis of this processing show two-phase systems which in a solid phase of crystals play role of porogen. And the other remained volume of liquid in a microphase, that is forms a cryogelic matrix for a concentrated solution of the dissolved substance [1].

Cryotrop gel formation of polymeric system happens at not deep freezing, at remaining in the frozen state and late disolution of colloid – dispers solutions or solutions containing monomeric and polymeric representatives which can give potential gel. The formed polymeric materials under these conditions got the name of cryogel (from Greek «cryos» – a frost and ice) and has specific features in comparison with sample of gels formed at temperatures above than a solvent crystallization point [2; 3].

Experimental part

Cryogel was synthesized on base of 10% polyacrylic acid (PAA) obtained by gelatin reaction (Fig. 1). As crosslinking agent was used N,N'-methylene–bis-acryl amide and as initiator was used ammonium persulphate, sodium metabisulphite, sodium hydroxide, and water. Radical polymerization was carried out at -30°C temperature for 24 hours. Cryogelic solvents have some specific features in comparison with sample gels formed at higher temperature than their crystallization point [4; 5].

Morphological structure of cryogel was studied by pictures of optical microscope, atomic force microscope and scanning electron microscope. The equilibrium swelling kinetics were researched, and the influence of external factors such as pH and temperature on it was found.

Sorption property of 10% PAA cryogels was studied. 10 μg/ml concentration of lead nitrate salt solution was used as sorbate. Metal entered into cryogel by sorption immobilization method, and between some period of time took aliquots and determined numerical values on atomic-absorption spectrometer AAS Shimadzu 6200 (Japan).

Results and their discussion

On a basis of PAA chemically crosslinked cryogel was synthesized. Obtained cryogel had density 1,4674 g/cm^3 and yield 90%. In order to see more exact picture of morphology and structure the 10% PAA cryogel was studied by using scanning electron microscope (SEM) equipment in different sizes (μm, nm). As a result, information obtained allows us to notice that cryogel consists of homogeneous microstructure unit (Fig. 2). From Figure 2 we can see that formed cryogel was porous.

 Printed in Kazakhstan

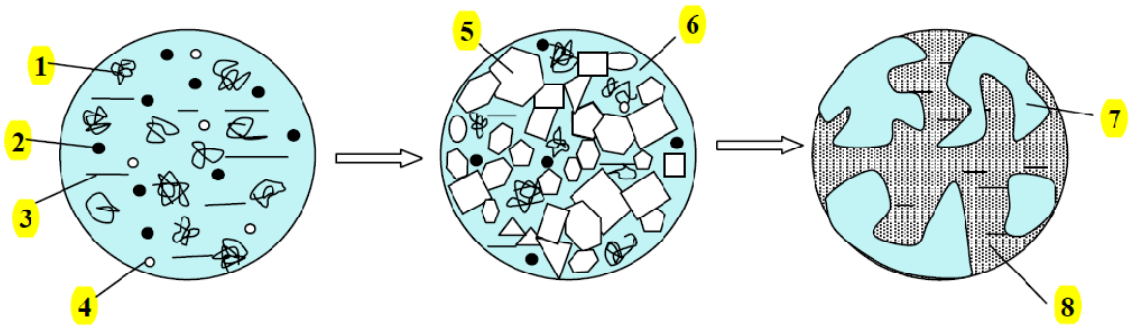

Figure 1 – Schematic diagram of cryotracks gellification
1 – polymeric gelling agent (PAA); 2 – low-molecular substances (NaOH); 3 – solvent (water);
4 – initiator (ammonium persulphate and sodium metabisulphite); 5 – polycrystals of the frozen solvent;
6 – unfrozen liquid microphase; 7 – polymeric grid of a gel phase of heterophase cryogel; 8 –macropore.

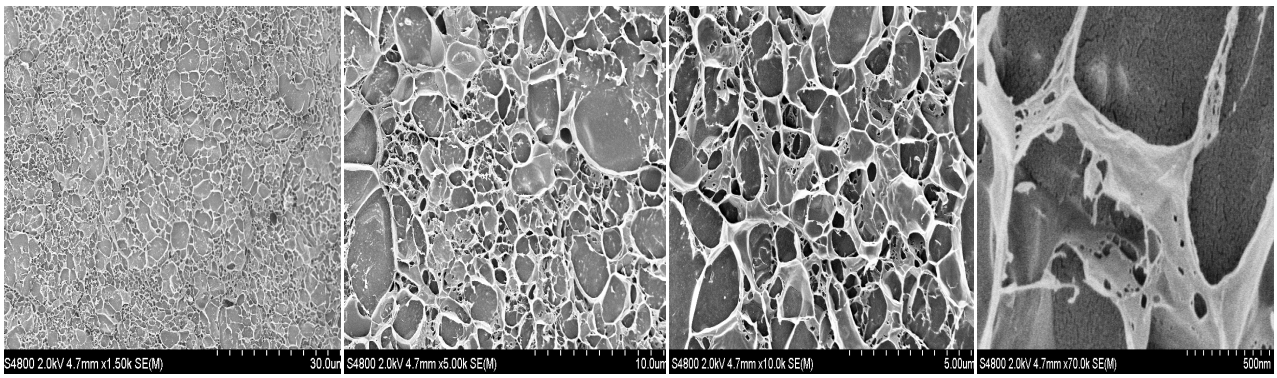

(a) (b) (c) (d)

30 μm (a); 10 μm (b); 5 μm (c); 500 nm (d) the reduced figures

Figure 2 – Photographs obtained by the scanning electronic microscope

One of the important properties of cryogel – equilibrium swelling degree was investigated (Fig. 3.) [6]. Equilibrium swelling kinetic of cryogel based on PAA was determined approximately in one day (Fig. 3 (a)).

We checked influence of external factors on swelling of 10% PAA cryogel [7]. Swelling dependence on pH and temperature during 30 minutes is shown (Fig.3.). We can notice sharp increasing of swelling when turning from acid to alkaline environment and it also increases with increasing of temperature. On dependence of pH shows good dissociation at turning from acid to alkaline environment and ionic strength increase. Such regulations can be easily explained by interaction nature of polymeric components. PAA is polyanionic polymer. Due to what at pH increasing by mutual repulsion of the same charged particles it is proceed the volume increasing of polymer grid. And in the case of temperature increasing it is necessary to notice big investment of hydrogen bonds into polymer interaction in gels. As it is known, extension of temperature allows hydrogen bonds breaking and leads to weakening of polymeric framework. That is why for PAA cryogels it is observed some increasing of volume of polymeric grid at temperature 60^0C.

One of the most important properties of composition gels is sorption [8; 10]. Recently, the researches of cryogels in direction of polymer composition materials (PCM) have shown the importance of using cryogels to purify production sewage. Heavy metals that are in deep waters have a technological action; it describes basic geochemical action of water of area. Sorption is an important method at sewage purification. Due to it, at the last time, the PCM with more involved sorption, physico-chemical, mechanical properties of compliance of organic and inorganic polymers are highly developed.

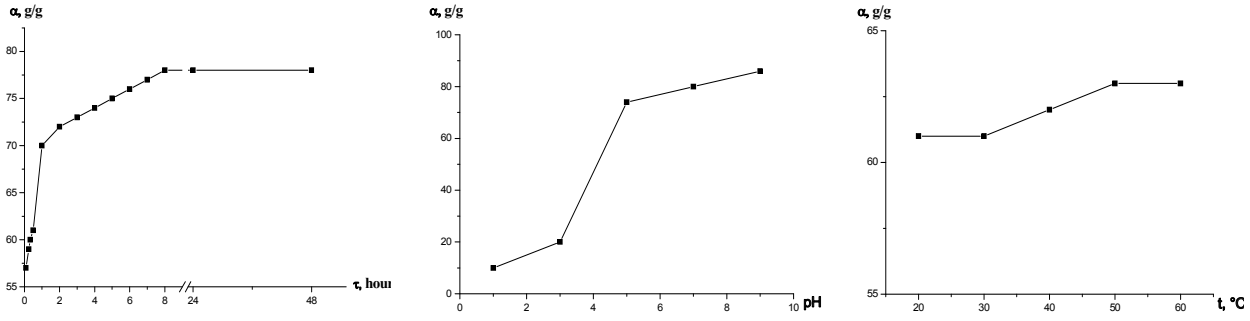

(a) dependence of extent of swelling on time

(b) dependence of extent of swelling on pH

(c) dependence of extent of swelling on temperature

Figure 3 – Dependence of swelling of cryogel 10 % PAA

In order to prove binding of cryogel with ions of metal we observed sorptioned sample in lead nitrate solution by optical and atomic force microscopes (Fig. 4). By optical microscopy, it was noticed that heavy metal – lead ions sit on cryogel surface. Atomic force microscope shows that metal ions go to porous internal structure and sorptioned.

It is important to know numerical values of sorption at entering of metal ions into composite materials. Figure 5 shows percentage value of metal ions sorption into cryogel based on PAA. Also here is shown swelling kinetics of cryogel on the basis of PAA in water and Pb^{2+} solutions, swelling in lead salt solution is lower due to negative charge of PAA, it is electrostatically linked with metal solution. It is good index of sorption ability. Thus, due to research of lead nitrate sorption results, at room temperature during 6 hours sorption value reached 90%. As seen, swelling and sorption are closely connected with each other. If swelling increases by time, the sorption increases too.

Figures by an optical microscopy

Figures by atomic-force microscopy

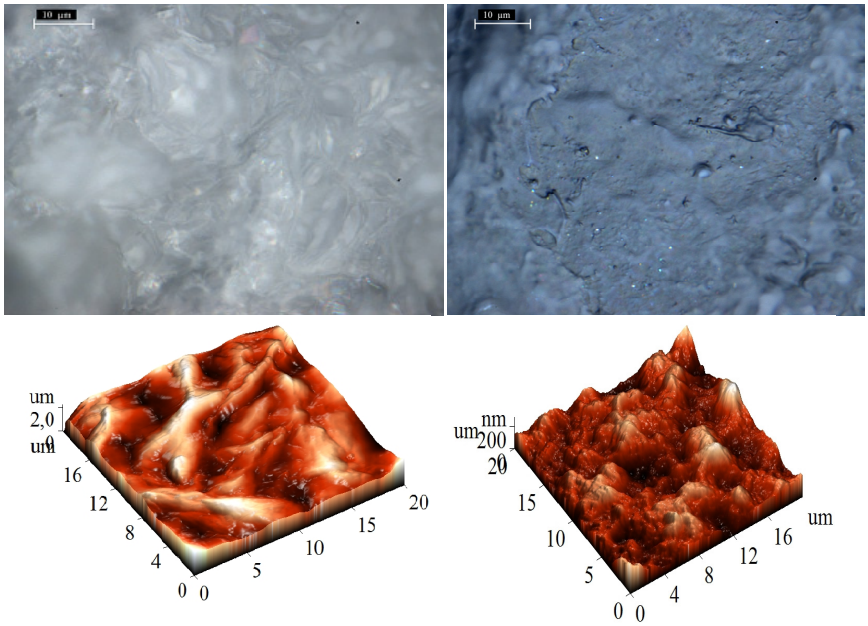

Figure 4 – Sorption figures in polyacrylic acid and in solution Pb^{2+}

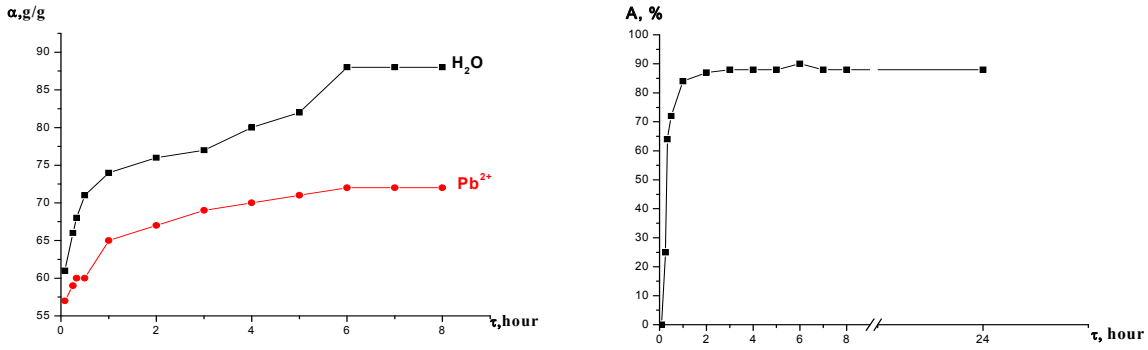

(а) swelling of PAA cryogel in solution Pb^{2+}

(б) sorption of PAA cryogel in solution Pb^{2+}

Figure 5 – Sorption and swelling of PAA cryogel in solution Pb^{2+}

Conclusion

In conclusion, cryogel based on polyacrylic acid was obtained. Equilibrium swelling degrees and density were determined, pictures on atomic–force microscope, scanning electron and optical microscopes were obtained. Structure of PAA based cryogel is porous, that is why its swelling degree is high. Also we studied sorption ability of PAA 10% cryogel, and proved its high value – 90%. According to conducted research, cryogel based on PAA can be used to purify sewage from heavy ions.

References

1 I.U. Filippova, Ye.N. Lysogorskaia, A.V. Bacheva, V.I. Lozincki, «Cryogels on the basis of natural and synthetic polymers: obtaining, properties and scopes» // Thesis report. XVIII Mendeleevsky congress in the general and applied chemistry. – Moscow, 2007. – No4. – 490 p.

2 T. Yamauchi, E. Kokufuta, Y. Osada, «Offers an in-depth look at the properties, thermodynamic formation, structure, latest trends, and scientific application of bio and synthetic polymer gels» // Polymer Gels Networks. – 1993. – No1. – 247 p.

3 S.M. Gautier, P.E. Phillippe, «Use of Poly Vinyl Alcohol (PVA) Cryogelation for Tissue Engineering: compositis, scaffold formation and cell Encapsulation» // J. Blum, Anal. Lett. – 1994. – No27. – 2055 p.

4 A.V. Belyaeva, A.V. Bacheva, Ye.S. Ocsenoit, Ye.N. Lysogorskaia, V.Y. Lozinski, I.U. Filippova «Studying of cryostructuring polymeric systems. Influence of speed of cooling of water solutions of polyvinyl alcohol at their freezing on physical and chemical properties and porous morphology of the cryogels which are turning out after thawing» // Inorg.chemistry – 2005. – No 31. – 586 p.

5 G.B. Sergeev, V.A. Batuk, Cryochemistry. – M.: Chemistry, 1978. – 295 p.

6 O.G. Nikitina, V.N. Maximova, N.G. Bulgakova, N.Ye. Nikitin, «Bioestimation – a new control method of process of clarification of water and its comparison with bioindication» // Water resourses. – 2009. –T.36. – No 4. – P. 475-480.

7 R.N. Nurdillaeva, A.B. Baeshov, A.N. Zhylysbaeva, «Sewage treatment and the fulfilled solutions from ions of heavy metals», Th. Intern. conf., «Actual environmental problems». – Karaganda, 2003. – P. 167-169.

8 R.N. Nurdillaeva, L.A. Sunatullaeva, A.N. Zhylysbaeva, K.A. Baeshova «Electrochemical method of purification of wire waters»// Innovative development and demand of science in modern Kazakhstan.– Coll. of article International research conf. – Almaty, 2010. – P. 199-203.

9 B.K. Kaliyeva, Ye.Ye. Yergozhin, N.A. Bektenov, A.Y. Nikitina,» Studying of selectivity of sorption of ions of Hg^{2+}, Pb^{2+} phosphorus-containing cationite on the basis of wheat straw and a glycidyl metacrylate», News NAN RK, No 5. – 2008. – P. 31-33.

10 K.K. Hamitova, M.K. Nauryzbayev, V.V. Mogilnyi, Sorption extraction of ions of heavy metals the modified nanocarbon sorbents // Theses of reports of the International conference «Colloids and Nanotechnologies in the Industry» of Almaty: KazNTU, 2010. – 25 p.

UDC 544:615.322

*Ikhsanov Y.S., Vizuete Castro P., Litvinenko Y.A., Burasheva G. Sh., Abilov J.A.

al-Farabi Kazakh national university, Kazakhstan, Almaty, al-Farabi ave 71
*E-mail: erbol.ih@gmail.com

Phytochemical study of conditional phytopreparation and liposoluble contents of *Halostachys caspica* with immunostimulatory activity

The study presents the results of a biologically active complex (BAC) study obtained from the aerial part of Halostachys caspica from the *Chenopodiaceae* family. Studies using gas chromatography-mass spectrometry revealed a significant amount of biologically active substances (BAS) in the BAC obtained by hydroalcoholic extraction, followed by lyophilization of the extract obtained, compared to the raw material. By passing this, the result of this study is the detection of such esters of higher saturated and unsaturated carboxylic acids and fatty acids as ethyl esters of oleic, hexadecanoic and octadecanoic acids.

Key words: *Halostachys caspica, Chenopodiaceae,* phytochemical composition of biologically active substances (BAS), biologically active complex (BAC), herbal, gas chromatography-mass spectrometry.

Introduction

To date, with all the certainty we can say that one of the most promising areas of development of drugs, is the search of physiologically active compounds through research phytochemical composition of plant facilities. However, determining the precise phytochemical composition as vegetable and herbal remedies obtained therefrom is still a difficult and time consuming task. However, technological progress and the associated development of physico-chemical methods of analysis, as exemplified by the widespread use of hybrid methods of analysis, the most important in the chemistry of natural compounds, as most of the analyzed samples are mixtures. Even with the use of effective methods of sample preparation for the isolation of interesting compounds still have to analyze the mixture. The value of gas and liquid chromatography is their ability to separate multicomponent mixtures. The combination of gas chromatography and mass spectrometry provides a method by which all components of a complex mixture can be separated and identified, even if their content in a sample is extremely small [1; 3].

Thus, the relevance and appropriateness of discharge from the aerial part of the *Halostachys caspica* polyphenol complex as well as a study of its phytochemical composition, based on the meager assortment inmunostimulatory herbal drugs in the global pharmaceutical practice, high immunostimulatory, antidiabetic and antioxidant actively and there is sufficient commercial reserves in Kazakhstan [4; 5].

GC-MS is a hybrid method of analysis for this reason should be viewed as a combination of chromatography (gas or liquid) and mass spectrometry. The processes of separation and analysis here occur entirely independently of each other [6].

Materials and methods

At the initial stage of raw material was dried, shredded and standardized in accordance with the procedures described in the USSR and GF RK [7; 9].

In the next stage, 500 g of the vegetable raw material was obtained BAC by the following procedure:

500-1000 g of plant (from the aerial part *Halostachys caspica*) were poured in 2500-5000 ml of 50% ethanol-water at a ratio of raw materials – 1:5 extractant, and infused for 24 hours protected from light at a temperature of 24-28 °C. The flask contents were cooled, thoroughly stirred, and filtered through filter paper into a dry flask. The extraction process was repeated three more times as described above. Then extracts were combined, filtered through the same filter to the same flask and concentrated to dryness under water pump vacuum at a temperature of 35-40 °C to a volume of 100-120 ml. At last, the extraction was poured into special molds and placed in

 Printed in Kazakhstan

a freezer at -20°C for 12 hours. Then frozen extract was sublimated in the freeze-drying Rime-4.

At the end of the process we obtained 150g of BAC, and the phytochemical composition of the plant and BAC were studied.

Also the standardized BAC was investigated by gas chromatography-mass spectrometry according to the following procedure in order to determinate the liposoluble contents in the conditional phytopreparation [10].

The operating mode chromatography-mass spectrometer was:

Type column: DB35ms
Detector: mass spectrum Agilent 5975s
Chromatograph: Agilent 7890A
Pressure: 12,051psi
Flow rate: 18 mL / min
Time: 38min

5g BAC were poured in 50ml of chloroform and were stirred for 1 hour and filtered through filter paper. The resulting filtrate was concentrated on a rotary evaporator and dewatered. Then prepared samples are sent to the center of physical and chemical methods of research and analysis for studying the phytochemical composition by gas chromatography-mass spectrometry.

Results and their discussion

Object of study is the aerial part of the *Halostachys caspica* from the *Chenopodiaceae* family, collected in the flowering phase in Ili district of Almaty region in 2013 and the BAC obtained form this plant.

These study results of the high quantitative indicators of raw materials were shown in Table 1.

Table 1 – High quantitative indicators from the aerial part of the *Halostachys caspica* and BAC of the plant

Parameter	Content %	
	Plant raw material	BAC
Humidity	4.14	8.48
Total ash	30.24	43.19
Ash insoluble in 10% hydrochloric acid	30.34	38.90
Sulphated ash	35.41	50.58
Extractives (water)	53.76	-
Extractives (50% propyl alcohol)	31.51	-
Extractives (50% ethanol)	41.98	40.05

As can be seen from the data presented in Table 1, the aerial part of the tested plant and its BAC, we can remark the high ash content, which means a significant amount of mineral components in the medicinal plant of raw materials and a high content of extractives on the ground, which may suggest a high content of biologically active substances. Based on the data obtained as the optimal solvents we selected 50% aqueous ethyl alcohol and water, as they are more than 40% recovered from vegetable material.

Also study of the mineral composition of the phytopreparation revealed high content of calcium and sodium compounds and other metals, which explains how the properties of medicinal plants belonging to class *Salicornia* and close proximity to the place of gathering Balkhash metallurgical combine. However, it should be noted that the metal content of the plant material does not exceed the maximum allowable concentrations.

According to generally accepted methods of GF USSR and the State Pharmacopoeia of Kazakhstan was quantified the amount of the main BAS groups. The results are presented in Table 2.

Table 2 shows that in the quantitative content from the aerial part of the *H. caspica* the highest percent of BAS are amino acids, riboflavin, saponins, flavonoids and carotenoids, and in the BAC from this plant, free organic acids, amino acids, carotenoids, alkaloids and flavanoids have the higher index. And we see that the amount of the main groups of biologically active substances increases in more than two times in most of the groups.

Table 2 – The contents of the main biological active substances groups from the aerial part of *Halostachys caspica* and BAC of the plant

Main BAS groups	Content %	
	Plant raw material	BAC
Free organic acids	4.95	13.09
Amino acids	10.56	12.29
Coumarins	0.31	0.60
Carbohydrates	0.21	0.36
Polysaccharides	0.25	0.37
Riboflavin	4.49	5.83
Carotenoids	4.21	9.52
Alkaloids	1.30	14.16
Flavonoids	2.63	18.03
Tannins	2.40	6.10
Saponins	4.23	7.03

In order to extend the study of the BAC we used gas chromatography-mass spectrometry method to determinate the substances in the liposoluble contents. The results are given in Figure 1 and Table 3.

Table 3 – Determined compounds of liposoluble contents of a 50% aqueous ethanol extract from *Halostachys caspica* by using the method of gas chromatography-mass spectrometry

N	RT	Area	Substance
1	9.067	0.13	2-butenal, 3-methyl- 2h pyran
2	9.214	0.25	1-pentene, 3,3-dimethyl- 4-trifluoroacetoxyoctane 1-pentyn-3-ol
3	9.750	0.39	1-butene, 4-methoxy
4	9.980	0.18	2-pentene
5	24.182	0.02	n-heptadecane
6	25.201	0.11	ethyl ester of tetradecanoic acid
7	25.289	0.12	Octadecane
8	25.761	0.16	2-pentadecanone, 6,10,14-trimethyl
9	26.049	0.1	phthalic acid, isobutyl 4-methylpent-2-yl ester
10	26.338	0.11	Nonadecane
11	26.592	0.12	1-pentadecene
12	26.980	0.08	methyl 9,12-heptadecadienoate
13	27.028	0.32	1,2-benzenedicarboxylic acid, buty
14	27.081	0.19	ethyl 9-hexadecenoate
15	27.193	0.01	isohexyl trans-hex-3-enyl ester
16	27.263	6.27	hexadecanoic acid,ethyl ester
17	27.340	0.14	Eicosane
18	27.434	0.13	5-ethyl-8-(trimethylsilylmethyl)dimethylsilyloxydecane
19	27.705	0.05	nonane, 2,5-dimethyl-
20	27.959	0.05	heptadecanoic acid, ethyl ester

Continuation of table 3

N	RT	Area	Substance
21	28.029	0.17	n-heneicosane
22	28.171	0.23	bicyclo(3.3.1)nonane-2,6-dione
23	28.224	0.08	heptadecanoic acid, ethyl ester
24	28.295	0.07	Heneicosane
25	28.336	0.16	9-octadecenoic acid, methyl ester,(e)-
26	28.943	6.33	ethyl oleate
27	29.008	75.67	ethyl oleate
28	29.208	6.62	octadecanoic acid, ethyl ester
29	30.333	0.27	Nonadecane
30	31.152	1.60	.alpha.-(p-chlorobenzoyl)-p-chloroacetophenone
31	31.424	0.65	heptadecanoic acid ethyl ester
32	32.166	0.01	(3.beta.,24r)-(24r)-5-ergosten-3.beta.-ol (24r)-5-ergoste n-3beta-ol
33	32.655	1.51	9-octadecenal, (z)-
34	33.480	0.27	bis(2-ethylhexyl) phthalate
35	34.358	0.13	docosanoic acid, ethyl ester
36	36.415	0.32	Heptacosane

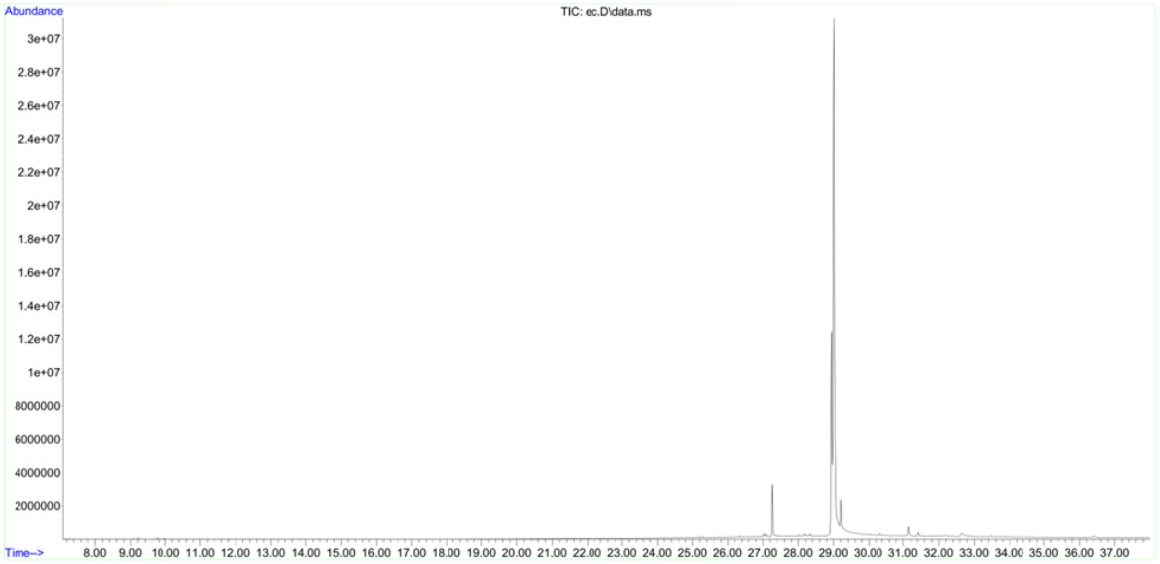

Figure 1 – Gas chromatography-mass spectrum of liposoluble contents of a 50% aqueous ethanol extract from *Halostachys caspica*

These data of the gas chromatography-mass spectrum adduces that most of the compounds in the liposoluble contents in the BAC are esters of higher carboxylic acids (oleic acid ethyl ester, hexadecanoic acid ethyl ester, octadecanoic acid ethyl ester).

Conclusion

We identified the high quantitative indicators and the phytochemical composition of the aerial part of the *Halostachys caspica* and BAC of the plant.

By using gas chromatography-mass spectrometry was done a study of the liposoluble fraction from the hydroalcoholic extract of *Halostachys caspica* by for the first time.

We still go on our studies of the chemical composition and the biological activity of *Halostachys caspica* and phytopreparations obatained from the aerial parts of the plant.

References

1 Zadorozhnyiy A.M., Koshkin A.G., Sokolov S.Ya., Shreter A.I. Spravochnik po lekarstvennyim rasteniyam. – M.: Lesnaya promyishlennost, 1989. – S. 4-8.

2 Bender K.I., Gomenyuk G.A., Freydman S.L. Ukazatel po primeneniyu lekarstvennyih rasteniy v nauchnoy i narodnoy meditsine. – M., 1988. – 111 s.

3 Beklemishev N.D. Rukovodstvo po rabote s lekarstvennyimi rasteniyami. – Almatyi, 1999. – 231 s.

4 Ushbaev K.U., Kuramyisova I.I., Aksenova V.F. Tselebnyie travyi. – «Kaynar», Almatyi, 1976.-S.3-7 Rastitelnyie resursyi SSSR // pod red. A.A. Fedorova. – L.: Nauka, 1985. – S.232.

5 Ye. Ikhsanov, P. Vizuete Castro, Yu. Litvinenko, G. Burasheva, and Zh. Abilov, Development of New Phytodrugs of Some Plants Growing in Arid Zones of Kazakhstan, 14th Asian Symposium on Medicinal Plants, Spices and Other Natural Products «ASOMPS-XIV», Karachi, 2013. – P. 209

6 Gosudarstvennaya farmakopeya Respubliki Kazahstan.. – Almatyi: Izdatelskiy dom «Zhibek zholyi», 2008., T.1 – 592 s.

7 Gosudarstvennaya Farmakopeya SSSR. Vyip.1: metodyi analiza lekarstvennogo rastitelnogo syirya. – M.: Meditsina, 1987. – 387 s.

8 Gosudarstvennaya Farmakopeya SSSR. Vyip.2: Obschie metodyi analiza. – M.: Meditsina, 1990. – 387s.

9 Avtsyin A.P., Zhavoronkov A.A., Remi M.A. i dr. Mikroelementyi cheloveka. – M.: Meditsina, 1991. – S.446.

10 Karasek F., Klement R. Vvedenie v hromato-mass-spektrometriyu: Per. s angl. – M.: Mir, 1993. – 237 s.

UDC 541.64.02;678

[1,2*]Klivenko A.N., [2,3]Tatykhanova G.S., [1]Mun G.A., [2,3]Kudaibergenov S.E.

[1]Faculty of Chemistry and Chemical Technology, al-Farabi Kazakh National University, Kazakhstan, Almaty
[2]Institute of Polymer Materials and Technologies, Kazakhstan, Almaty,
[3]Kazakh National Technical University after K.I. Satpayev, Kazakhstan, Almaty
[*]E-mail: alexeyklivenko@gmail.com

Synthesis and physicochemical properties of macroporous cryogels

The current review reveals the analysis of recent research in the field of synthesis and characterization of cryogels. The theoretical aspects of the process of cryotropic gelation are considered. The influence of freezing temperature and concentrations of initial monomer mixture on the pore size of the material is discussed. The concept of process of cryotropic gelation is revealed. The potential need for further research in the field of cryotropic gelation is highlighted.
Key words: hydrogels, cryotropic gelation, cryogels, cryopolymerization

Introduction

Hydrogels are defined as a cross-linked three-dimensional polymeric networks, insoluble in water and hydrophilic media. Hydrogels exhibit the unique ability to absorb large amounts of water or other biological liquids [12]. Hydrogels attracted a great interest of researchers and significant progress was achieved both in their synthesis and applications biomedical, biotechnological and pharmaceutical areas. Polymeric hydrogels can be used as water supersorbent materials [7], contact lenses [7], wound dressings [14, 35], drug delivery [31, 21, 36, 37].

Stimuli-responsive nano- and microporous gels may be applied as drug delivery systems, biological sensors and materials for separation and purification of cells, organelles and proteins. Amphoteric microgels attracted a great interest due to their ability to a reversible phase transitions upon changing external conditions (e.g. pH, temperature and ionic strength of solution). Amphoteric microgels contain acidic and basic functional groups, which provide macromolecules positive and negative charges, as well as a isoelectric point. Depending on pH of the solution amphoteric gels may exhibit polyelectrolyte properties. For example, a recent study showed the possibility of polyelectrolite complex formation under cryo-conditions, which resulted in macroporous amphoteric hydrogels [14, 25]. For polyelectrolytes these interactions occur simultaneously and compete against each other. The response of amphoteric nano- and microgels to the changes in external environment typically takes place within seconds.

Most studies were so far focused on the application of amphoteric nano- and microgels as stimuli-responsive systems [22, 29, 32, 38-46]. In most cases, the properties of these amphoteric particles can be changed under an external stimuli, which finally reflects on the size, structure and nature of interactions. The volume phase transitions occur in polymer gels as a result of many factors such as competing interactions, elasticity of polymer chains, osmotic pressure, H-bonding, hydrophobic and van der Waals interactions [2, 25, 26].

Among polymer hydrogels macro- and super-porous polymeric cryogels attracted a particular interest. These hydrogels are widely used in biotechnology [18] and regenerative medicine as

- effective carriers of immobilized enzymes and live cells; [5, 13, 19, 35].
- matrices of immunosorbents and affinity sorbents for use with biological nano- and microparticles; macroporous scaffold for various metal nanoparticles [9].
- substrates for cultivation of animal cells;
- special matrices composed of mainly whole bacterial cells [1, 15].

 Printed in Kazakhstan

Macroporous structure of cryogels provides unhindered diffusion of substrates to the immobilized active principles and the withdrawal of products, when cryogels used as a carrier of immobilized biocatalysts. Supermacroporous spongy cryogel structure can be effectively used for chromatographic separation and purification of biological macromolecules and live cells [8, 10, 20, 23].

Polymeric cryogels as an object of research

Cryogel is a macroporous hydrogel in which ice crystals were used as a porogen during gelation process. The last two decades revealed a growing interest towards polymeric cryogels as an object of fundamental research and as a promising material for application in various areas (Fig. 1).

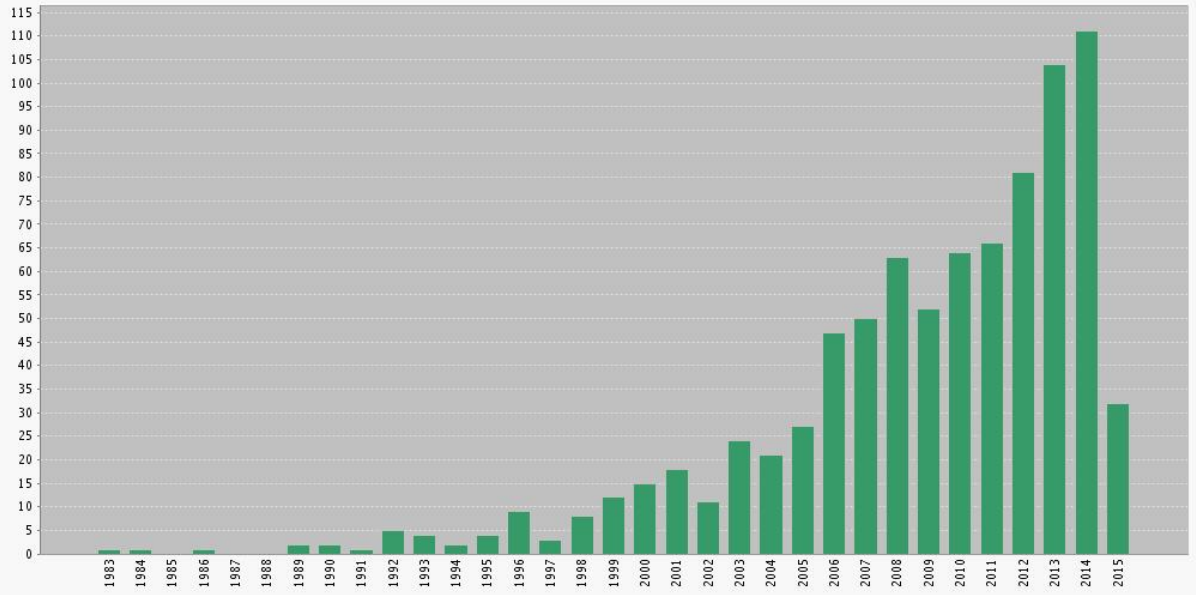

Figure 1 – The growth in the publications on «cryogels» as revealed by the analysis of ISI Web of Science

The areas of application of macro-porous materials is continuously expanding. New cryogenic technologies have been developed for food industry. Filters, sorbents [4], mechanochemical gel actuators, leather-like materials [33], catalytic systems are currently being developed [9]. Macroporous polymeric materials are commonly used in biotechnology and biomedicine [13, 24]. There are many different approaches for macroporous materials preparation such as lyophilization, cavitation, microemulsion polymerization, gas bubbling, and phase separation [11].

Polymeric cryogels are macroporous heterophase systems in which formation of pores occurs through a crystallization of a solvent. The specific feature of cryogels is their macroporous structure. The growth of each ice crystal is continuing until close contact with other growing crystals where all solutes are expelling into a non-frozen liquid microphase. Thus, the radical polymerization or cross-linking of polymers (natural, synthetic, bio molecules etc.) is taking place in a liquid microphase. After reaction occurred the thawing of the system leads to melting of ice crystals where the polymer network remains unaffected, which repeats the geometrical form of ice crystals, therefore the material has interconnected pores structure [5, 16, 18, 28].

It worth to note that cryogels can also be prepared from low molecular weight compound without the use of any cross-linking agents or macromolecules and even without formation of chemical bonds.

Specific features of cryogelation process at subzero temperatures

Effects which are used in the synthesis of organic materials in aqueous solutions were named cryo-structuring and cryogelation. These materials were named «cryogels» (from Greek κριοσ (cryo) – ice) [5, 16, 18, 28, 47]. Some of the first reports of using the cryo-structuring phenomena for the preparation of supermacroporous hydrogels were published by the group of Lozinsky in the 1980s [28].

Thus, cryogelation is the formation of polymers, proteins or composites at temperatures below the freezing point of a solvent [19, 23]. It starts from freezing of an initial reaction mixture, by keeping it frozen for certain period of time to allow for the pore formation with a precursor cryo-concentrated in residual liquid microlayers, influenced by microcrystallites of frozen bulk solvent, with physical or chemical cross-linking of the compounds forming macropore walls and following thawing at room temperature.

By varying the characteristics of the polymers used for cryogel synthesis (molecular weight, molecular weight distribution, polymer concentration in the system, solvent composition etc.), as well as processing conditions of cryogelation (temperature, freezing time, freezing rate, number of thawing cycles etc.) it is possible to regulate a wide range of physicochemical parameters, micro- and macrostructure of the final gels [16].

Some special effects are observed when the freezing of the reaction mixture occurs under parameters far out of balance, for instance, dependence of cooling rate of the sample on polymerization rate; reaction vessel geometry and the chemical nature of reaction vessel walls; holding time in a frozen state; the amount of water in the reaction mixture and many other factors [5, 12].

From a thermodynamical point of view, the cause of formation of liquid microphase in a multicomponent frozen solutions is that the incorporation of the solutes into a solid lattice of the solvent requires more energy than is expended to raise the chemical potential with increasing concentrations of the components in the liquid microphase [16].

Typically, when the freezing rate is high, then fine polycrystals of freezable liquid are formed. The size of ice crystals for aqueous solution of polyvinyl alcohol (PVA) (7%) frozen at -10^0C is several times lower than that for 14% solution of PVA- and last one by 1-2 orders lower than the ice crystals obtained from pure water [5, 48].

From practical point of view of characterization of cryogels there are some important characteristics such as specific surface area(S), pore volume (Vp), pore size distributions (PSD), pore wall thickness distribution (PWTD), pore connectivity and tortuosity. Typically, cryogels are micro/macroporous materials (average pore diameter in the range of $1<d<300$ μm) with pore walls of several micrometers in thickness. According to the life sciences classification, pore sizes at diameter $d_{nano}<0.1$ μm, $0.1<d_{micro}<100$ μm, and $d_{macro}>100$ μm correspond to nano-, micro-, and macropores, respectively [12]. The formation of cryogels with internal nanoporosity is a complicated task. Recently, the possibility of cryogel formation with additional internal nanoporosity in the pore walls was shown [14]. Ozmen et. all showed the dependence of microporosity of polyacrylamide cryogel from temperature and composition of solvent mixture [17].

There are some difficulties in quantitative characterization of the native texture of cryogels because of their softness and highly hydrated structure. Therefore, in most published studies the structural and textural characteristics of cryogels were carried out only on a qualitative or semi-quantitative level [14, 17, 25, 49]. Representative examples of these characteristics are the microscopic images of dried or freeze-dried cryogels without determination of the above mentioned parameters (Vp, S, PSD, and PWTD) or with an estimation of average pore size and porosity [3]. However, in some studies, PSD and other textural characteristics were determined in detail by using mercury porosimetry and image analysis [4, 27, 50]. Currently our group is working under development and investigation of amphoteric cryogels composed of various compositions of dimethylaminoetylmethacrylate (DMAEMA) and methacrylic acid. As shown in Figure 2 the pore size of the cryogel can be roughly estimated by the use of Image J program. Cryogels DMAEMA-MAA characterized by well distributed microporosity with mean diameter of pores 75 μm (with 2.5% MBAA as a crosslinking agent) and 44.7 μm (with 2.5% MBAA as a crosslinking agent).

Using high magnification SEM image of the cryogel one can graphically estimate average thickness of walls.

The variation of the freezing temperature during cryopolymerization process allows to regulate the morphology of macroporous materials. This approach was used to obtain cryogels based on the so-called «stimuli-responsive» or «sensitive» polymers macroporous hydrogels [23]. These cryogels have the ability of a reversible collapse at change of parameters of the environment, are considered as promising materials for biomedical and biotechnological applications.

Thermosensitive cryogels, where a chain conformation of an appropriate linear polymer is reversibly changing when passing through the upper or lower critical solution temperature (LCST or UCST), capable of significant thermo-induced reversible changes in the degree of swelling. These systems include cryogels based on pNIPAAm or poly-N-vinylcaprolactam [5].

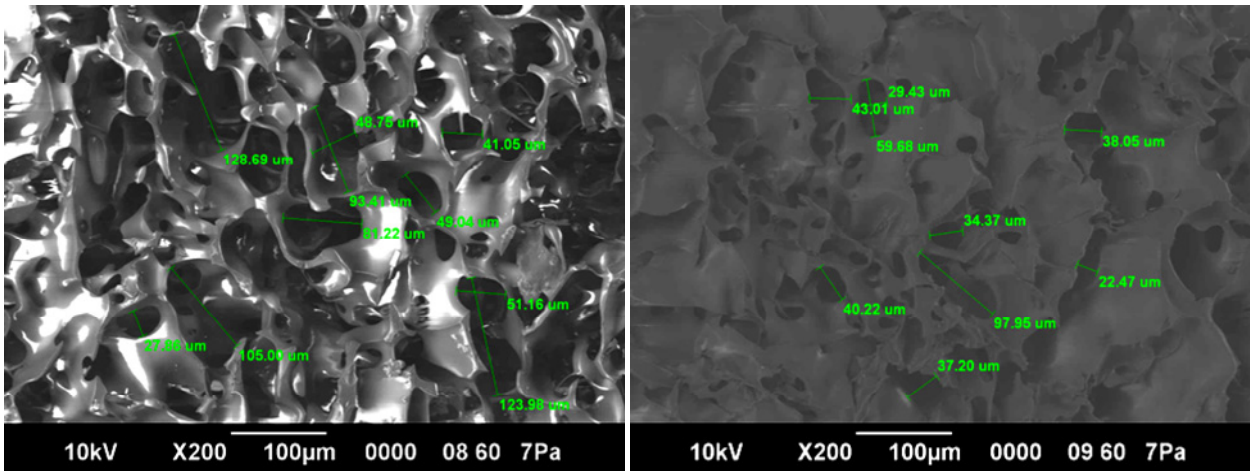

Figure 2 – SEM images of DMAEMA-MAA 1:1 with 2,5% MBAA (left), with 10% MBAA (right)

Thus, pNIPAAm cryogels rapidly and reversibly react to minor changes in the environment can be called «smart» cryogels [30, 34]. It is known that under heat treatment of aqueous solution of pNIPAAm the hydrophobic aggregation is taking place at 32^0C, which leads to phase separation in the system [26]. The degree of swelling of pNIPAAm cryogel determined at sub-zero temperatures was much smaller than that for the pNIPAAm hydrogel synthesized at 22^0C [5].

This phenomenon can be explained by the swelling of pNIPAAm cryogel depending on concentration of monomers in the initial monomer mixture and the degree of cross-linking. The study of cryogel containing pNIPAAm at temperature range from 4 to 40^0C revealed a sharp rapid phase transition at 30^0C. As shown in Figure 3, the thermosensitivity of pNIPAAm cryogel is a reversible process, where a rapid response of the gel to change of temperature takes place in oscillatory regime at 19^0C and 37^0C. The lower the concentration of monomers and the degree of crosslinking in pNIPAAm cryogel, the greater the changes in swelling and the greater the amplitude of the mechanical deformation occurring at temperature change from 19^0C to 37^0C [5].

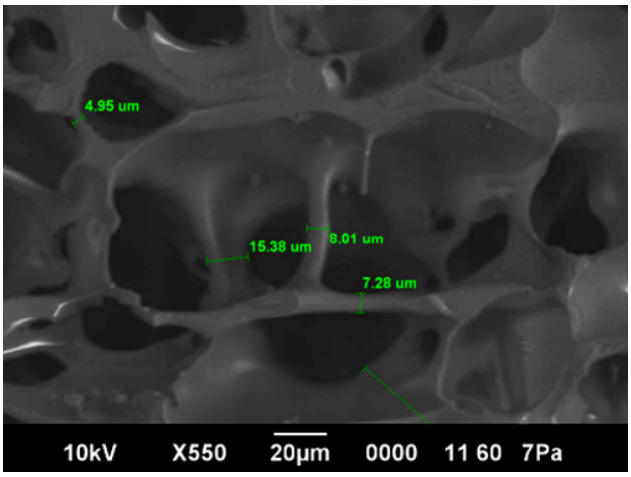

Figure 3 – SEM image of DMAEMA-MAA 1:1 with 5% MBAA as a crosslinking agent

The temperature and the rate of freezing

One of the most important parameters which controls the cryogelation process is the rate of freezing [28]. The pore size of cryogels depended on the rate of freezing in the following way: a low rate of freezing (or a higher temperature) the larger crystals of ice and therefore the larger pores in cryogels [28]. In order to avoid the surfusion the freezing temperature of reaction mixture should be sufficiently low, but not lower than the temperature of transition to glass state. The surfusion (or supercooling) is the process where the temperature passes the freezing point without formation of crystals of ice. This is the metastable state of water. The temperature of the formation of ice (or other solution) crystals related to the rate of freezing, volume of sample, nuclei forming agents. Variation of temperature during the freezing process allows to discern phase and structural changes in the system. Figure 5 shows the freezing curves of monomer mixture (acrylamide (AAm), methylene-bis-acrylamide (BisAAm), allylglycidyl ether) at temperatures -12, -20, -30^0C, respectively, where a phase states of the systems are well discerned. It is known that during the freezing of the reaction mixture at -12 °C the system exists in supercooled state, the following crys-

tallization process brings about the simultaneous abrupt rise of the temperature up to -11°C, indicating the crystallization of the solvent. After the reaction the mixture was transferred into cryostat with lower temperature the critical mass of nuclei of crystals formation reaches the limit within 2.6 minutes. The formation of nuclei of the crystals begins at -2.5°C. Cryoconcentration of solutes was reached through the freezing-out process of water from the solution. The increase in the viscosity of the unfrozen liquid phase slowed further crystallization, which completes in 8 minutes. The freezing of solutions at -20^{0}C or -30^{0}C in most cases completes with crystallization of solvent without the supercooling state. On the thermogram recorded at -30^{0}C a small peak appeared at 3.3 minutes related to the temperature -20^{0}C which is lower than the eutectic point for water/acrylamide system). This indicates the complete crystallization of liquid microphase, which exists in nonfrozen state at high temperatures [25].

Influence of concentration and composition of the initial monomer mixture

The increase in the concentration of monomers in the reaction mixture leads to an increase of polymer concentration in the non frozen phase, therefore formed pore walls have higher density and as a result the elastic modulus of the material is higher [14, 35]. However this rule is right to some extent. Thus, the freezing of too concentrated monomer mixture brings about the formation of small ice crystals and as a consequence the pore sizes is small and mutual connection of macropores is low. This phenomenon is related to the smaller amount of the frozen solvent. As a result small ice crystallytes formed have poor connection with each other. For example, previously we had observed this phenomenon for amphoteric cryogel [4]. Amphoteric cryogel composed of equimolar composition of allylamine (AA) and methacrylic acid (MAA) (50/50 mol %) obtained from 10% initial monomeric mixture possessed a very low water permeability Figure 4 compare to the cryogel containing less ionic monomers in the initial monomer mixture. Thus, for cryogels composed of AAm-AA-MAA (80/10/10 mol %) and AA-MAA 50-50 mol% the difference in water permeability was about 60 times [4].

By adjusting the concentration and type of crosslinking agent cryogels with different pore sizes and pore wall thickness can be obtained.

Polyacrylamide cryogels (cryoPAAm) were synthesized by radical copolymerization of acrylamide (AAm) with N, N'-methylene bisacrylamide (BisAAm) in an aqueous solution. For initiation of radical copolymerization a redox system ammonium persulfate/ tetramethylethylenediamine (APS/ TEMED) was used, which generates radical ions even at low temperatures.

The critical concentration of gelation (CCG) is a concentration of monomer mixture, leading to formation of hydrogel. For instance, for preparation of polyacrylamide hydrogel at 20°C it is necessary to use 2% monomer solution composed of AAm and BisAAm. However, when the reaction mixture is frozen at -10 ºC immediately after initiating of radical polymerization it is possible to obtain a cryoPAAm using 1% of the same comonomers. The reduction of CCG in this case is an apparent decline, which is related to cryoconcentration effect. In fact the concentration of monomer in a non-frozen microphase where the polymerization is taking place is greater than that at room temperature. It is worth noting that this apparent decline of CCG is typical for all types of cryotropic gelation [5].

Cryogels based on acrylamide have a spongy morphology, which is mainly determined by temperature regimes of cryotropic gelation. Previously, the influence of freezing temperature on the morphology of the material has been shown. Thus, the structure of cryogels from solutions with constant concentration of the monomers prepared at -10 and -20°C and frozen in different ways. The monomer mixture solution placed in a cryostat with a predetermined temperature, where the freezing front was moving from above); an initial rapid freezing of mixture in liquid nitrogen to -196°C and the following transfer of samples to the cryostat at a predetermined moderate sub zero temperature. This technique minimizes the effect of the duration of cooling and freezing process on the kinetics of chemical reactions in so-called low-temperature hardening [5].

The formation of cryogel under this freezing regime results in decreasing of temperature from -10 to -20°C which leads to increase of the amount of porogen particles – ice crystals that significantly affects the diameter of the macropores in cryoPAAm [5]. Furthermore, the lower the temperature the more solvent is frozen, i.e. ULM volume becomes smaller, and the concentration of solutes therein becomes higher. Thus, the obtained pore walls are thinner, and built of more concentrated gel [13]. Using the technique of low-temperature hardening cryoPAAm morphology is changed. The architecture of the cryogel formed at –10°C combines the porosity of the sample obtained by above freezing regime, and the structure

of macropore walls of the material obtained at -20°C using above freezing regime. This means that during thawing of the frozen solution within a few minutes from -196 to -10°C the primary elements of the gel phase structure are forming. This is an evidence of rapid polymerization under cryoconditions. Additionally, the microporosity of cryogels can be regulated by introduction of special «molecular» porogen (e.g. oligoethyleneglycol with MW 1000 [6]), which after cryopolymerization can be washed out with excess of water. This leads to the formation of additional porosity of a certain size in the porewalls of cryogel. Another way to form an additional porosity inside of macroporous material is the use of foaming agents, which often leads to the formation of a certain amount of closed pores [27].

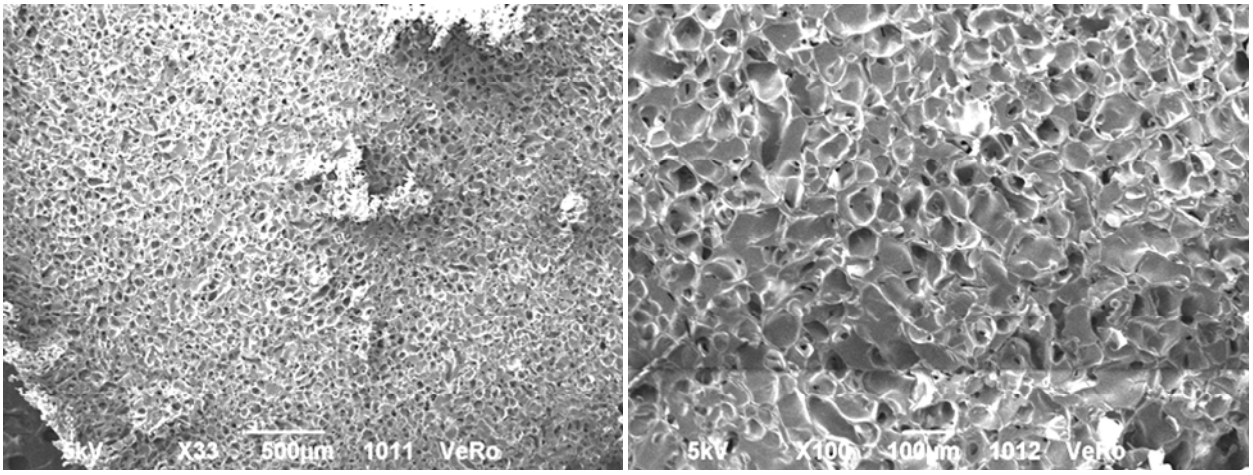

Figure 4 – SEM image of amphoteric cryogel AA-MAA 50-50 mol% at low x 33 (right) and high x 100 (left) magnifications.

Porous structure of various cryogels is a complex system composed of a 3D labyrinth, which is often observed in aqueous systems due to branched forms of polycrystalline ice, creating a complex configuration macropores in the bulk of a sample. The pore size and their shape can be changed though the directed crystallization of the solution, which allows to obtain cryogels with regularly oriented macropores. For example, the directional cooling of formamide solution brings about the crystallization of the solvent with formation of elongated crystals [2]. Using formamide and directed cooling process it is possible to prepare cryoPAAm regularly oriented macropores. In this case in the obtained cryogel contains a long capillary channels oriented in the direction of the temperature gradient [2]. Thus, it is possible within certain limits, to «manage» polymer cryogel macroporosity by adjusting the solvent and mode of its crystallization.

Osmotic characteristics (swelling in different media) of cryogel cryoPAAm mainly determined by factors such as the initial concentration of precursors [4], the nature of solvent [17] and the conditions of cryogenic treatment [5]. The total volume of liquid that absorbs cryogels consists of two components: solvate associated solvent and capillary solvent. From one side the solvate associated solvent is firmly connected with the polymer network, from the other side the capillary solvent fills the space in the macropores and can be simply removed through the gentle squeezing of cryogel structure [2].

The freezing and melting (thawing) process of frozen solutions of complex substances is a complicated process, which affected by various factors.

The process of freezing or thawing of the system solvent-polymer-low molecular weight additive is strongly influenced by the polydispersity of polymers. This leads to non-equivalence of phase diagrams of liquid-solid for the same pair of solvent – polymer with different molecular weights (MW) and molecular weight distribution (MWD) of high molecular weight component. Furthermore, a slow relaxation process in viscous non-frozen liquid phase in the frozen sample is strongly dependent on their thermal prehistory during freezing process.

Another problem, which makes the investigation of gelation process using a phase diagram more complicated, is self-association of polymers [9, 14, 28]. It is known that concentrated aqueous solution of polymers at low temperature have the ability to

spontaneous association. Therefore, in this case the obtained the phase diagram for the same system with the same sub zero temperature can be different. In each particular case the phase diagram is dependent on the dynamics of cooling of a sample and the rate of crystallization of a solvent [12].

Developing new simple and inexpensive methods of investigation of cryogelation process is a promissing direction for further research.

Thus, the physical and chemical properties of products of radical cryopolymerization can be widely changed through the variation of concentration and nature of monomer precursors. These scaffolds can be used as carriers for immobilization of enzymes, antibodies, protein-free biopolymers and different types of cells.

Conclusion

The cryotropic treatment of the reaction mixture does not stop the radical polymerization process. The cryogelation process is taking place in nonfrozen liquid microphase. The temperature and the regime of freezing, as well as composition of the monomer mixture determines the porosity of the material as the pore diameter, the thickness of walls, the area of internal surface. Two methods of cryogelation were discussed. The first one is the gradual cooling of the reaction mixture from room temperature to freezing point of the solvent and gradual thawing to ambient temperature. The second method is a rapid freezing of the solution in liquid nitrogen and the following gradual thawing of the sample to the temperature of crystallization of the solvent. The complete description of a porosity of cryogel structure can be performed via the determination of various parameters: pore volume (Vp), specific surface area (S), pore size distributions (PSD), pore wall thickness distribution (PWTD), then using these data and a modern software one can also calculate pore connectivity and tortuosity.

Acknowledgement

Financial support from the Ministry of Education and Science of the Republic of Kazakhstan is greatly acknowledged.

References

1 Aragão Börner R., Zaushitsyna O., Berillo D., Scaccia N., Mattiasson B., Kirsebom H. Immobilization of Clostridium acetobutylicum DSM 792 as macroporous aggregates through cryogelation for butanol production // Process Biochemistry. – 2014. – 1//. – Vol. 49. – P. 10-18.

2 Berillo D., Elowsson L., Kirsebom H. Oxidized Dextran as Crosslinker for Chitosan Cryogel Scaffolds and Formation of Polyelectrolyte Complexes between Chitosan and Gelatin // Macromolecular Bioscience. – 2012. – Aug. – T. 12. – C. 1090-1099.

3 Berillo D., Mattiasson B., Galaev I. Y., Kirsebom H. Formation of macroporous self-assembled hydrogels through cryogelation of Fmoc-Phe-Phe // Journal of Colloid and Interface Science. – 2012. – 2/15/. – T. 368. – C. 226-230.

4 Berillo D., Volkova N. Preparation and physicochemical characteristics of cryogel based on gelatin and oxidised dextran // Journal of Materials Science. – 2014. – 2014/07/01. – T. 49. – C. 4855-4868.

5 Macroporous Polymers. / Bo M., Ashok K., IgorYu G.: CRC Press, 2009. – 1 c.

6 Chen J., Park K. Synthesis and characterization of superporous hydrogel composites // Journal of Controlled Release. – 2000. – Mar 1. – T. 65. – C. 73-82.

7 Cook M.T., Saratoon T., Tzortzis G., Edwards A., Charalampopoulos D., Khutoryanskiy V.V. CLSM Method for the Dynamic Observation of pH Change within Polymer Matrices for Oral Delivery // Biomacromolecules. – 2013. – 2013/02/11. – T. 14. – C. 387-393.

8 Dainiak M.B., Galaev I.Y., Mattiasson B. Macroporous monolithic hydrogels in a 96-mini-column plate format for cell surface-analysis and integrated binding/quantification of cells // Enzyme and Microbial Technology. – 2007. – 3/5/. – T. 40. – C. 688-695.

9 Dainiak M.B., Kumar A., Plieva F.M., Galaev I.Y., Mattiasson B. Integrated isolation of antibody fragments from microbial cell culture fluids using supermacroporous cryogels // Journal of Chromatography A. – 2004. – Aug. – T. 1045. – C. 93-98.

10 Dainiak M.B., Plieva F.M., Galaev I.Y., Hatti-Kaul R., Mattiasson B. Cell chromatography: Separation of different microbial cells using IMAC supermacroporous monolithic columns // Biotechnology Progress. – 2005. – Mar-Apr. – T. 21. – C. 644-649.

11 Fatima M.P., Igor Yu G., Bo M. Production and Properties of Cryogels by Radical Polymerization // Macroporous PolymersCRC Press, 2009. – C. 23-47.

12 Gun'ko V.M., Savina I.N., Mikhalovsky S.V. Cryogels: Morphological, structural and adsorption

characterisation // Advances in Colloid and Interface Science. – 2013. – 1//. – T. 187–188. – C. 1-46.

13 Hentze H.P., Antonietti M. Porous polymers and resins for biotechnological and biomedical applications // Reviews in Molecular Biotechnology. – 2002. – 3//. – T. 90. – C. 27-53.

14 Kirsebom H., Elowsson L., Berillo D., Cozzi S., Inci I., Piskin E., Galaev Igor Y., Mattiasson B. Enzyme-Catalyzed Crosslinking in a Partly Frozen State: A New Way to Produce Supermacroporous Protein Structures // Macromolecular Bioscience. – 2013. – T. 13, № 1. – C. 67-76.

15 Kudaibergenov S., Adilov Z., Berillo D., Tatykhanova G., Sadakbaeva Z., Abdullin K., Galaev I. Novel macroporous amphoteric gels: Preparation and characterization // Express Polymer Letters. – 2012. – May. – T. 6, № 5. – C. 346-353.

16 Lozinsky V.I. Cryogels on the basis of natural and synthetic polymers: preparation, properties and application // Russian Chemical Reviews. – 2002. – T. 71, № 6. – C. 489.

17 Lozinsky V.I. Polymeric cryogels as a new family of macroporous and supermacroporous materials for biotechnological purposes // Russian Chemical Bulletin. – 2008. – May. – T. 57, № 5. – C. 1015-1032.

18 Lozinsky V.I., Galaev I.Y., Plieva F.M., Savinal I.N., Jungvid H., Mattiasson B. Polymeric cryogels as promising materials of biotechnological interest // Trends in Biotechnology. – 2003. – Oct. – T. 21, № 10. – C. 445-451.

19 Lozinsky V.I., Plieva F.M., Galaev I.Y., Mattiasson B. The potential of polymeric cryogels in bioseparation // Bioseparation. – 2001. – T. 10. – №4-5. – C. 163-188.

20 Martynenko N.N., Gracheva I.M., Sarishvili N.G., Zubov A.L., El'Registan G.I., Lozinsky V.I. Immobilization of champagne yeasts by inclusion into cryogels of polyvinyl alcohol: Means of preventing cell release from the carrier matrix // Applied Biochemistry and Microbiology. – 2004. – Mar-Apr. – T. 40, № 2. – C. 158-164.

21 Morrison P. W. J., Connon C. J., Khutoryanskiy V.V. Cyclodextrin-Mediated Enhancement of Riboflavin Solubility and Corneal Permeability // Molecular Pharmaceutics. – 2013. – Feb. – T. 10. – №2. – C. 756-762.

22 Ogawa K., Nakayama A., Kokufuta E. Preparation and characterization of thermosensitive polyampholyte nanogels // Langmuir. – 2003. – Apr. – T. 19. Ц № 8. – C. 3178-3184.

23 Ozmen M.M., Dinu M.V., Okay O. Preparation of macroporous poly(acrylamide) hydrogels in DMSO/water mixture at subzero temperatures // Polymer Bulletin. – 2008. – Mar. – T. 60. – № 2-3. – C. 169-180.

24 Peppas N.A., Huang Y., Torres-Lugo M., Ward J.H., Zhang J. Physicochemical, foundations and structural design of hydrogels in medicine and biology // Annual Review of Biomedical Engineering. – 2000. – 2000. – T. 2. – C. 9-29.

25 Piskin K., Arca E., Piskin E. Radiopolymerized mixture of acrylic-acid, methyl-methacrylate, and polyethylene-glycol as an enzyme support system // Applied Biochemistry and Biotechnology. – 1984. – T. 10. – C. 73-79.

26 Plieva F., Xiao H. T., Galaev I.Y., Bergenstahl B., Mattiasson B. Macroporous elastic polyacrylamide gels prepared at subzero temperatures: control of porous structure // Journal of Materials Chemistry. – 2006. – T. 16. – № 41. – C. 4065-4073.

27 Plieva F.M., Karlsson M., Aguilar M.R., Gomez D., Mikhalovsky S., Galaev I. Y. Pore structure in supermacroporous polyacrylamide based cryogels // Soft Matter. – 2005. – Oct 14. – T. 1. – № 4. – C. 303-309.

28 Rogozhin S.V., Lozinskii V.I., Vainerman E.S., Korshak V.V. The influence of freezing of the polymerizing monomer solutions on the molecular-weight of polymers obtained // Doklady Akademii Nauk Sssr. – 1983. – 1983. – T. 273. – № 5. – C. 1140-1143.

29 Schachschal S., Balaceanu A., Melian C., Demco D.E., Eckert T., Richtering W., Pich A. Polyampholyte Microgels with Anionic Core and Cationic Shell // Macromolecules. – 2010. – May. – T. 43. – № 9. – C. 4331-4339.

30 Schild H.G. Poly (N-isopropylacrylamide) – experiment, theory and application // Progress in Polymer Science. – 1992. – 1992. – T. 17. – №2. – C. 163-249.

31 Storha A., Mun E.A., Khutoryanskiy V.V. Synthesis of thiolated and acrylated nanoparticles using thiol-ene click chemistry: towards novel mucoadhesive materials for drug delivery // Rsc Advances. – 2013. – T. 3, № 30. – C. 12275-12279.

32 Tan B.H., Ravi P., Tam K.C. Synthesis and characterization of novel pH-responsive polyampholyte microgels // Macromolecular Rapid Communications. – 2006. – Apr. – T. 27, № 7. – C. 522-528.

33 Tatykhanova G.S., Sadakbayeva Zhansaya K., Berillo D., Galaev I., Abdullin Khabib A., Adilov Z., Kudaibergenov Sarkyt E. Metal Complexes of Amphoteric Cryogels Based on Allylamine and Methacrylic Acid // Macromolecular Symposia. – 2012. – T. 317-318, № 1. – C. 18–27.

34 Yu H., Grainger D.W. Thermosensitive swelling behavior in cross-linked n-isopropylacrylamide networks - cationic, anionic, and ampholytic hydrogels // Journal of Applied Polymer Science. – 1993. – Sep 5. – T. 49, № 9. – C. 1553-1563.

35 Zaushitsyna O., Berillo D., Kirsebom H., Mattiasson B. Cryostructured and Crosslinked Viable Cells Forming Monoliths Suitable for Bioreactor Applications // Topics in Catalysis. – 2014. – Mar. – T. 57, № 5. – C. 339-348.

36 Zhao Q., Sun J.Z., Ling Q.C., Zhou Q.Y. Synthesis of Macroporous Thermosensitive Hydrogels: A Novel Method of Controlling Pore Size // Langmuir. – 2009. – Mar. – T. 25, № 5. – C. 3249-3254.

37 Lozinsky V.I. A Brief History of Polymeric Cryogels // Polymeric Cryogels: Macroporous Gels with Remarkable Properties. – 2014. – T. 263. – C. 1-48.

38 Dogan T., Bayram E., Uzun L., Senel S., Denizli A. Trametes versicolor laccase immobilized poly(glycidyl methacrylate) based cryogels for phenol degradation from aqueous media // Journal of Applied Polymer Science. – 2015. – T. 132, № 20. – C. 9.

39 Gorgieva S., Kokol V. Processing of gelatin-based cryogels with improved thermomechanical resistance, pore size gradient, and high potential for sustainable protein drug release // Journal of Biomedical Materials Research Part A. – 2015. – T. 103, №3. – C. 1119-1130.

40 Jackson N., Verbrugghe P., Cuypers D., Adesanya K., Engel L., Glazer P., Dubruel P., Shacham-Diamand Y., Mendes E., Herijgers P., Stam F. A Cardiovascular Occlusion Method Based on the Use of a Smart Hydrogel // Ieee Transactions on Biomedical Engineering. – 2015. – T. 62, № 2. – C. 399-406.

41 Kuo C.Y., Chen C.H., Hsiao C.Y., Chen J.P. Incorporation of chitosan in biomimetic gelatin/chondroitin-6-sulfate/hyaluronan cryogel for cartilage tissue engineering // Carbohydrate Polymers. – 2015. – T. 117. – C. 722-730.

42 Papancea A., Patachia S., Dobritoiu R. Crystal violet dye sorption and transport in/through bio-based PVA cryogel membranes // Journal of Applied Polymer Science. – 2015. – T. 132, № 17. – C. 12.

43 Percin I., Khalaf R., Brand B., Morbidelli M., Gezici O. Strong cation-exchange chromatography of proteins on a sulfoalkylated monolithic cryogel // Journal of Chromatography A. – 2015. – T. 1386. – C. 13-21.

44 Sahiner N., Seven F. A facile synthesis route to improve the catalytic activity of inherently cationic and magnetic catalyst systems for hydrogen generation from sodium borohydride hydrolysis // Fuel Processing Technology. – 2015. – T. 132. – C. 1-8.

45 Sahiner N., Yildiz S., Al-Lohedan H. The resourcefulness of p(4-VP) cryogels as template for in situ nanoparticle preparation of various metals and their use in H-2 production, nitro compound reduction and dye degradation // Applied Catalysis B-Environmental. – 2015. – T. 166. – C. 145-154.

46 Sahiner N., Demirci S., Sahiner M., Yilmaz S., Al-Lohedan H. The use of superporous p(3-acrylamidopropyl)trimethyl ammonium chloride cryogels for removal of toxic arsenate anions // Journal of Environmental Management. – 2015. – T. 152. – C. 66-74.

47 Uygun M., Akduman B., Uygun D.A., Akgol S., Denizli A. Dye functionalized cryogel columns for reversible lysozyme adsorption // Journal of Biomaterials Science-Polymer Edition. – 2015. – T. 26, № 5. – C. 277-289.

48 Van Rie J., Declercq H., Van Hoorick J., Dierick M., Van Hoorebeke L., Cornelissen R., Thienpont H., Dubruel P., Van Vlierberghe S. Cryogel-PCL combination scaffolds for bone tissue repair // Journal of Materials Science-Materials in Medicine. – 2015. – T. 26, № 3. – C. 7.

49 Loo S.L., Krantz W.B., Fane A.G., Gao Y.B., Lim T.T., Hu X. Bactericidal Mechanisms Revealed for Rapid Water Disinfection by Superabsorbent Cryogels Decorated with Silver Nanoparticles // Environmental Science & Technology. – 2015. – T. 49, № 4. – C. 2310-2318.

50 Tabakli B., Topcu A.A., Doker S., Uzun L. Particle-Assisted Ion-Imprinted Cryogels for Selective Cd-II Ion Removal // Industrial & Engineering Chemistry Research. – 2015. – T. 54, № 6. – C. 1816-1823.International Journal of Biology and Chemistry 7, №1, 10 (2015)

UDC 542.941.7:547.36:547.3

[2]Nurgaziyeva E.K., [1,3]Tatykhanova G.S., [2*]Mun G.A., [4]Khutoryanskiy V.V., [1,3]Kudaibergenov S.E.

[1]Laboratory of Engineering Profile, K.I. Satpayev Kazakh National Technical University, Almaty, Kazakhstan
[2]Al-Farabi Kazakh National University, Almaty, Kazakhstan
[3]Institute of Polymer Materials and Technology, Almaty, Kazakhstan
[4]Reading School of Pharmacy, Universityof Reading, Whiteknights, Reading, UK
[*]E-mail: grigory.mun@kaznu.kz

Oxidation of Cyclohexane Mediated with Gel-Immobilized Gold Nanoparticles

This paper reports the study of hydrogen peroxide decomposition and oxidation of cyclohexane catalyzed by polymer-protected gold nanoparticles (AuNPs) immobilized within polyacrylamide hydrogel. The stabilization of AuNPs was achieved using nonionic, anionic and cationic polymers. Embedding of AuNPs stabilized with various polymers into polyacrylamide hydrogels was carried out using threeways: «in situ» polymerization, sorption and boronhydride methods. Size, shape and morphology of AuNPs were characterized by various physicochemical methods. Application aspects of polymer-protected AuNPs in catalysis are outlined.
Key words: gold nanoparticles, hydrogels, hydrophilic polymers, stabilization, catalysis.

Introduction

Hydrogels have found numerous applications due to their unique properties such as high water content, softness, flexibility, biocompatibility and ease of synthesis.Their resemblance to living tissue opens up many opportunities for applications in biomedical areas. Nowadays, hydrogels are used for manufacturing contact lenses, hygiene products, tissue engineering scaffolds, drug delivery systems and wound dressings [1, 2].

Hydrogels are three-dimensional, hydrophilic, polymeric networks capable of absorbing large amounts of water or biological fluids. Due to their high water content, porosity and soft consistency, they resemble natural living tissues, more so than any other class of synthetic biomaterials. Hydrogels may be chemically stable or they may degrade and eventually disintegrate and dissolve. There are numerous original papers, academic reviews and monographs focused on the synthesis, properties and applications of hydrogels [1-4].

New technologies rely on the development of modern materials, and these may simply be the innovative combination of known components. The structural combination of a polymerichydrogel withnanoparticles (metals, nonmetals, metal oxides, and polymers) often provides superior functionality to the composite materialswith potential applications in various fields, including catalysis, electronics, biosensing, drug delivery, nanomedicine, and environmental remediation. This mixing may result in a synergistic property enhancement of each component: for example, the mechanical strength of the hydrogel could be improved with embedded nanoparticles and concomitantly the aggregation of nanoparticles could be prevented within a polymeric network. These mutual benefits and the associated potential applications have seen a surge of interest in the past decade from multi-disciplinary research groups. Recent advances in nanoparticle–hydrogel composites are herein reviewed with a focus on their synthesis, design, potential applications, and the inherent challenges [5-13].

This paper reports the study of oxidation of cyclohexane catalyzed by polymer-protected gold nanoparticles (AuNPs) immobilized within polyacrylamide hydrogel (PAAH).

Materials and methods

Poly-N-vinylpyrrolidone (PVP, MW 40 kDa), branched polyethylenimine (PEI, MW 25 kDa) and NaOH werepurchased fromSigma – Aldrich (USA). $HAuCl_4$ was purchasedfrom Altey (Kazakhstan). $NaBH_4$ was purchased from AppliChem (Germany). All chemicals were used without further purification.

 Printed in Kazakhstan

Synthesis of AuNPs

AuNPs were synthesised bymixing 4mL 0.5M KOH with5mL4 w/v % PVP or 5 mL 4 w/v % PEI, then addition of5 mL of 100 mg/L $HAuCl_4$solution into the mixture and heating it at 100°(1) «in-situ» immobilization method: Gel-immobilized AuNPs were prepared by polymerizing the mixture of 500 mg acrylamide dissolved in 5 mL PEI- or PVP-protected AuNPsaqueous dispersionsin the presence of 10 mgmethylene bisacrylamide as a crosslinking agent and 10 mg ammonium persulfate as an initiator. The reaction mixture was purged with argonfor 5 min; then it was kept at 60^0C. The hydrogels were formed within 30 min of the reaction and then they were washed in distilled water for 3-4 days to get rid of unreacted monomers.The purified hydrogel samples were crushed and dried in air to a constant mass.

(2) Sorbtion method:

Pure polyacrylamide hydrogels were synthesized using three-dimensional polymerization of 500 mg acrylamide in 5 mL waterin the presence of 10 mg of methylene bisacrylamide and 10 mg of ammonium persulphate. This solution mixture was held at 60°C for 30 min to form hydrogels. These hydrogels were purified as described above. Then these materials were air dried and 1 g of dry sample was immersed in 10 mL AuNPs aqueous dispersion for 24 hours. After washing and grinding, the hydrogels were dried to a constant mass. The sorption of AuNPs by dry hydrogelsresulted in colouredsamples, which were subsequently dried in air.

(3) Borohydride method: The preparation of AuNPs immobilized hydrogels in this method was carried out by immersing dried hydrogel samples into 100 mg/L solution of $HAuCl_4$ for 24 hours. After sorption the hydrogel samples were placed into 5 mL 0.1 M solution of sodium borohydride for 20 min, which resulted in colored samples indicatingthe formation of AuNPs. These hydrogels were cut into smaller pieces and dried in air to a constant mass.

Dynamic Light Scattering

Particle size distributions and zeta-potential of gold nanoparticles (AuNPs) in aqueous dispersions were measured using dynamic light scattering (DLS, MalvernZetasizerNanoZS90, UK).

Transmission electron microscopy (TEM)

Transmission electron microscopyimages of gold nanoparticles in aqueous dispersions and in gels were recorded using JEM-1011 (Japan) at an accelerating voltage of 80 kV. The samples for investigation were applied as a dispersion of AuNPs dripped onto standard copper grid with subsequent drying in air. Gel samples were micronized and a drop of microgel aqueous suspension was placed on TEM grid and air dried.

Gas-liquid chromatography (GLC)

Products of oxidation the cyclohexane were identified using GLC «MasterGCGasChromatograph» (DANIMaster, Italy) using DN-5 column with the length of 30m, diameter of 0.25 mm, thickness of phase 0.45 μm, and a flow rate of 1 mL/s.

Cyclohexane oxidation using gold nanoparticles

The oxidation of cyclohexane was carried out in a closed reactor BuchiLimbo (Switzerland). 0.07 g of a dry hydrogel with AuNPs were placed into the reactor, followed by addition of 4 mL of acetonitrile, 1 mL of cyclohexane and 0.59 mL of 30% hydrogen peroxide. Cyclohexane oxidation was carried out at 70°C for 6 hours. In these experiments the oxidant was taken in an equimolar amount relative to the substrate (cyclohexane). In this case, the theoretical amount of oxygen obtained during decomposition of hydrogen peroxide was 112 mL.

Results and their discussion

The hydrogel samples for UV-Vis analyses were prepared as following: the gel-immobilized hydrogel samples were prepared in quartz cuvettes by «in-situ» method. The AuNPs solutions were diluted for UV-Vis: 0.5 mL of AuNPs solution was added 2.5 mL water. In this diluted solution the hydrogels were synthesized: red – AuNPs/PEI, purple – AuNPs/PVP (Fig. 4).

Synthesis and characterization of AuNPs

AuNPs were synthesized by reduction of $HAuCl_4$ in aqueous solutions containing either 4 w/v % of PVP or 4 w/v % PEI under alkali conditions (achieved by addition of 4 mL 0.5M KOH to the reaction mixture). The reaction was initiated by increasing temperature up to 100°C, which resulted in the aqueous mixtures becoming colored within a few minutes. The change of solution color indicated the formation of AuNPs sols. The synthesized nanoparticles were initially

characterized using dynamic light scattering and TEM (Fig. 5).

The use of different water-soluble polymers for reduction of $HAuCl_4$ results in formation of nanoparticles substantially differing in their sizes as measured by dynamic light scattering: the hydrodynamic diameters are 46 ± 10 nm and 128 ± 20 nm for AuNPs synthesized in the presence of PVP and PEI, respectively. It is interesting to note that the comparison of DLS data with TEM images of the nanoparticles reveals a significant difference in sizes. The analysis of TEM results using ImageJ software indicates that the nanoparticles formed in PEI have diameters of 8.170 nm. This dramatic discrepancy between DLS and TEM results is explained by different physical principles used by these two sizing techniques. DLS is a technique that measures light scattered by the objects present in solutions and will be able to detect individual macromolecules. AuNPs formed in the presence of water-soluble polymers have a core-shell structure with the core made of gold and a hydrophilic shell made of macromolecules of a water-soluble polymer. DLS measurements in this case will provide the size distribution for the nanoparticles together with a hydrated shell. TEM, on the contrary, is based on transmission of accelerated electrons through the sample and, in the absence of specific staining agents, this technique will be able to detect only dense objects such as gold-based core. The comparison of both DLS and TEM data allows establishing the structural features of AuNPs prepared in the presence of PVP and PEI.

Hydrogel immobilized gold nanoparticles were prepared using three approaches: (1) «in-situ» immobilization method; (2) sorption method; and (3) borohydride method. Figure 6 shows the images of selected hydrogel samples with immobilized AuNPs prepared using «in-situ» and sorption methods.

Table 1 presents the comparison of the dimensions and other physicochemical properties of AuNPs in aqueous dispersions and immobilized within hydrogels. Analysis of TEM images of AuNPs immobilized within a hydrogel indicates that the size of gold core has a diameter very similar to the sizes of the nanoparticles before their incorporation into the hydrogels. Zeta-potential measurements indicate that of AuNPs formed in the presence of PVP and PEI in aqueous dispersions have slightly negative values (-10.52 mV and -9.31 mV, respectively).

Considering that these nanoparticles are very stable in dispersion, it could be concluded that their stabilization is related to the sterical effects caused by highly hydrated macromolecules forming their shell rather than their charge interactions.

Figure 1 – PVP (purple)- and PEI (red)-protected gold nanoparticles

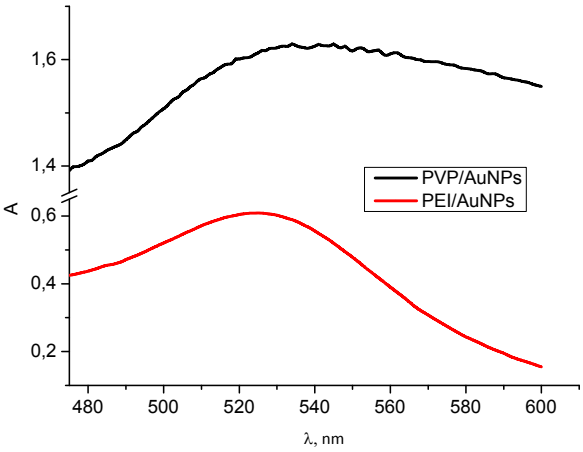

Figure 2 – UV-Vis spectra of AuNPs solutions

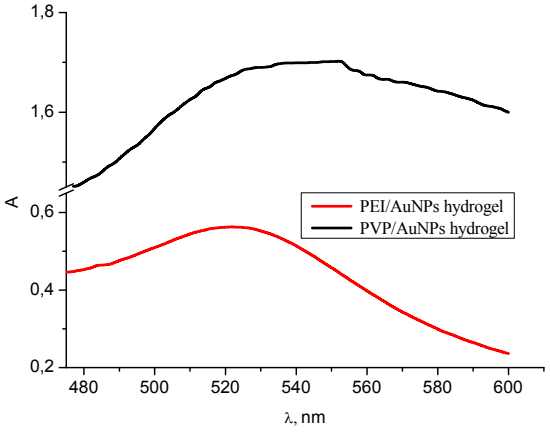

Figure 3 – UV-Vis spectra of AuNPs hydrogels

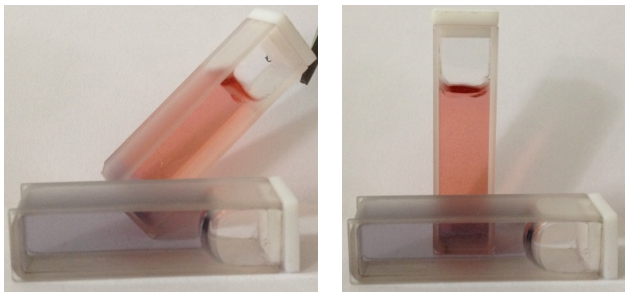

Figure 4 – Gel-immobilized AuNPs

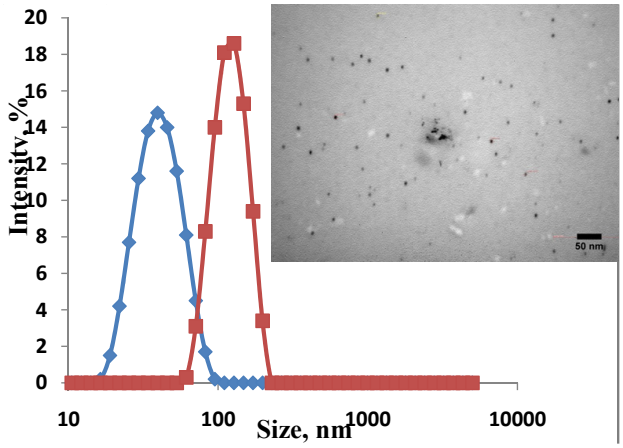

Figure 5 – Size distributions of gold nanoparticles as measured by dynamic light scattering. AuNPs were synthesized in the presence of PVP (1) and PEI (2). Insert: Exemplary TEM image of AuNPs synthesized in the presence of PEI.

Oxidation of cyclohexane by AuNPs immobilized within PAAH

Catalytic conversion of saturated hydrocarbons to oxygenated compounds has been studied intensively in the last decade due to the important industrial synthesis of a plurality of organic compounds. Among oxygenation process the alkane oxidation is of greatest interest, because reaction products of cyclohexane – cyclohexanol and cyclohexanone are the basis for the production of adipic acid using in the further for polyamide materials and plastics, foams, and the acid itself is used in the food industry and as lubricant materials.

In this case, the process proceeds in acetonitrile having weakly basic character, which basifiesthe solution that prevents the complete decomposition of hydrogen peroxide.

When using the gel-immobilized catalyst expected to show «catalase» (enzyme catalase promotes the decomposition of hydrogen peroxide to water and oxygen), and the «oxidase» (group peroxidase enzymes allows oxygenation alkanes with hydrogen peroxide) activity.

After the reaction mixture was filtered and the reaction products were analyzed by gas chromatography Dani Master GS (Italy). Figure 2 (supplementary materials) shows the chromatogram of the oxidation products of cyclohexane. AuNPs immobilized in hydrogel only catalyze the oxidation of cyclohexane to cyclohexanol and cyclohexanone with minimal formation of oxygenated products. According to the results of the chromatographic investigations revealed that the yield of cyclohexanol and cyclohexanone in the presence of a catalyst Au / PEI (adsorption method) is 55.1 and 44.9% respectively (Table 1). By using this catalyst conversion of reactionis a maximum which is 37%.

In the presence of catalysts Au / PVP (adsorption method), Au / PEI (method «in-situ»), Au-$NaBH_4$ (method borohydride), conversion varies between 5-7% and the yield of the cyclohexanol being within 47.6-55.4% and cyclohexanone – 44.6-52.4%.

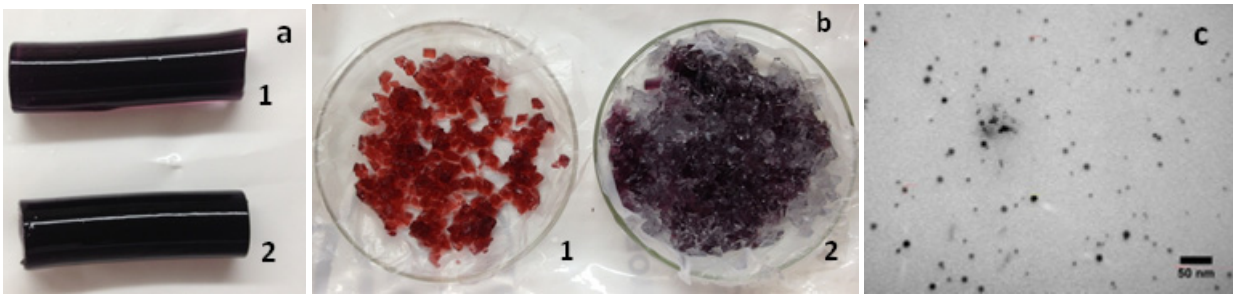

Figure 6 – Hydrogel samples with immobilized AuNPs, prepared using «in-situ» method (a) and sorption method (b). PVP (1) and PEI (2) were used for stabilization of nanoparticles. TEM image of PEI-protected AuNPs immobilized within a hydrogel using «in-situ» method (c).

Table 1 – Physicochemical properties of AuNPs in dispersions and in hydrogels

Samples	TEM, nm	DLS, nm	PDI	Zeta potential, mV
PEI-protected AuNPs (solution)	7.0±0.53	128±20	0.427	-9.31
PVP-protected AuNPs (solution)	*	46 ± 10	0.553	-10.52
PEI-protected AuNPs within a hydrogel	7.310±0.005	*	*	*

* – not measured.

Table 2 – The yield of cyclohexane oxidation according to chromatographic analyses

Catalyst	Compounds	Conversion, %	Selectivity, %
Au/PEI «in-situ» method	Cyclohexanol	7.2	55.4
	Cyclohexanon		44.6
Au/PVP sorption method	Cyclohexanol	6.37	47.6
	Cyclohexanon		52.4
Borohydride method	Cyclohexanol	5.15	53.6
	Cyclohexanon		46.4
Au/PEI Sorption method	Cyclohexanol	37	55.1
	Cyclohexanon		44.9

Thus, the best catalyst for the oxidation of cyclohexane to cyclohexanol and cyclohexanone is stabilized with polyethyleneimine (PEI), and immobilized in a polyacrylamide hydrogel matrix gold nanoparticles, obtained by sorption method. In the presence of Au / PEI matrix immobilized in a polyacrylamide hydrogel by sorption method, the yield of cyclohexanol and cyclohexanone is 55.1 and 44.9% respectively (conversion 37%).

Conclusion

Gold nanoparticles stabilized by various hydrophilic polymers incapsulated within hydrogel matrix. The catalytic properties of gel-immobilized gold nanoparticles were investigated in oxidation of cyclohexane. The physico-chemical properties of prepared gold nanoparticles were studied by TEM, UV-Vis an DLS measurements.The best catalyst for the oxidation of cyclohexane to cyclohexanol and cyclohexanone is stabilized with polyethyleneimine (PEI), and immobilized in a polyacrylamide hydrogel matrix gold nanoparticles, obtained by sorption method. In the presence of Au / PEI matrix immobilized in a polyacrylamide hydrogel by sorption method, the yield of cyclohexanol and cyclohexanone is 55.1 and 44.9% respectively (conversion 37%).

References

1 Enrica Caló, Vitaliy V. Khutoryanskiy, Biomedical applications of hydrogels: a review of patents and commercial products, European Polymer Journal.

2 K. Pal, A. K. Banthia, D. K.Majumdar, Polymeric Hydrogels: Characterization and Biomedical Applications – a mini review, Designed monomers and polymers 12 (2009). – P. 197-220.

3 Bindu Sri. M, Ashok. V and Arkendu Chatterjee. Review on Hydrogels as Drug Delivery in the Pharmaceutical Field, Vol. 1 (2) Apr – Jun 2012 Pages 642-661.

4 Enas M. Ahmed. Hydrogel: Preparation, characterization, and applications: a review. Journal of Advanced Research, Volume 6, Issue 2, March 2015, Pages 105–121.

5 Praveen Thoniyot, Mein Jin Tan, Anis Abdul Karim, David James Young, Xian Jun Loh. Nanopar-

ticle–Hydrogel Composites: Concept, Design, and Applications of These Promising, Multi-Functional Materials, Adv. Sci. 2015.

6 V. Pardo-Yissar, R. Gabai, A.N. Shipway, T. Bourenko, I. Willner, Adv. Mater. 2001, 13, 1320.

7 C. Wang, N.T. Flynn, R. Langer, Adv. Mater. 2004, 16, 1074.

8 N.S. Satarkar, D. Biswal, J.Z. Hilt, Soft Matter 2010, 6, 2364.

9 S. R. Sershen, S. L. Westcott, N. J. Halas, J. L. West, Appl. Phys. Lett. 2002, 80, 4609.

10 N. Ravi, H. A. Aliyar, P. D. Hamilton, Macromol. Symp. 2005, 227, 191.

11 Q.-B. Wei, F. Fu, Y.-Q. Zhang, L. Tang, J. Polym. Res. 2014, 21, 1.

12 K.A. Juby, C. Dwivedi, M. Kumar, S. Kota, H.S. Misra, P. N. Bajaj, Carbohydr. Polym. 2012, 89, 906.

13 R.-C. Luo, Z.H. Lim, W. Li, P. Shi, C.-H. Chen, Chem. Commun. 2014, 50, 7052.

UDC 542.941.7

Buribayeva M.S., Kunakbayeva A., Abebova L., *Irmukhametova G.S.,
Muldagulova K.B., Mun G.A.

Al-Farabi Kazakh National University, Almaty, Kazakhstan
*E-mail: i_galiya@mail.ru

Transdermal study of hydrogel ointments and bandages with antituberculosis activity

Transdermal study for hydrogel ointments and bandages based on polyvinylpirrolidone was conducted for application as transdermal therapeutic drug delivery systems for skin tuberculosis treatment. The ointments and bandages based on polyvinylpyrrolidone (PVP) and carbomer with drugs isoniazid and ethambutol were obtained. The transdermal characteristics were investigated using cellulose membrane and pig skin. The experiment was carried out by the device Franz cell and diffusion coefficient (D), permeability (P) and permeation rates (F) of the drugs were calculated. It was established that the rate of isoniazid penetration through the skin faster than that for ethambutol which is related to the structure peculiarities of drugs. The higher transdermal activity of hydrogel ointments was shown in comparison with hydrogel dressings. Also the prolongation effect of developed transdermal drug delivery systems based on PVP and carbomer was observed.

Key words: transdermal therapeutic system, drug delivery, polyvinylpyrrolidone, isoniazid, ethambutol, carbomer

Introduction

In recent years there has been an extreme rise in tuberculosis worldwide. In modern medicine as one of the basic issues is the creation of new forms of drugs with high therapeutic activity, for controlled release of drugs and their exact delivery to the site of the pathological process. Due to this, drugs (DS) based polymers are promising, because they provide prolonged action. Such important drugs include DS used against tuberculosis, because treatment of tuberculosis takes a very long time. The reason is excessively accumulation of DS that's why minor allergic reactions are manifested. In connection with this the creation of hydrogel ointments based on biopolymers as transdermal systems are important in medicine application. Almost all medications which are used to treat tuberculosis can cause toxic side effects. Therefore, there is an obvious need for new biopolymers such as hydrogel based on polyvinylpyrrolidone (PVP). At the same time, by research of their transdermal systems through the skin, their use in medicine could be predicted [1].

Skin of an average adult body covers a surface of approximately 2 m^2 and receives about one-third of the blood circulating through the body. Skin contains an uppermost layer, epidermis which has morphologically distinct regions; basal layer, spiny layer, stratum granulosum and upper most stratum corneum, it consists of highly cornified (dead) cells embedded in a continuous matrix of lipid membranous sheets. These extracellular membranes are unique in their compositions and are composed of ceramides, cholesterol and free fatty acids.

The human skin surface is known to contain, on an average, 10-70 hair follicles and 200-250 sweat ducts on every square centimeters of the skin area. It is one of the most readily accessible organs of the human body. The potential of using the intact skin as the port of drug administration to the human body has been recognized for several decades, but skin is a very difficult barrier to the ingress of materials allowing only small quantities of a drug to penetrate over a period of time. Transdermal drug delivery – the delivery of drugs across the skin and into systemic circulation – is distinct from topical drug penetration,

 Printed in Kazakhstan

which targets local areas. Transdermal drug delivery takes advantage of the relative accessibility of the skin [3].

The drug has to go through these structural layers, encountering several lipophilic and hydrophilic barriers in the dermis, where absorption into the systemic circulation is rapid because of the large capillary bed. Dermis is the thickest of the skin layer (5.3 mm) and include hair follicles, sweat glands, nerve endings and blood and lymph vessels. The dermis acts as a systemic absorption of drugs.

The more common pathway through the skin is via the intercellular route. Drugs crossing the skin by this route must pass through the small spaces between the cells of the skin, making the route more tortuous. Although the thickness of the stratum corneum is only about 20 μm, the actual diffusional path of most molecules crossing the skin is on the order of 400 μm. The 20-fold increase in the actual path of permeating molecules greatly reduces the rate of drug penetration (Fig. 2).

A less important pathway of drug penetration is the follicular route. Hair follicles penetrate through the stratum cornea, allowing more direct access to the dermal microcirculation. However, hair follicles occupy only 1/1,000 of the entire skin surface area. Consequently, very little drug actually crosses the skin via the follicular route [6].

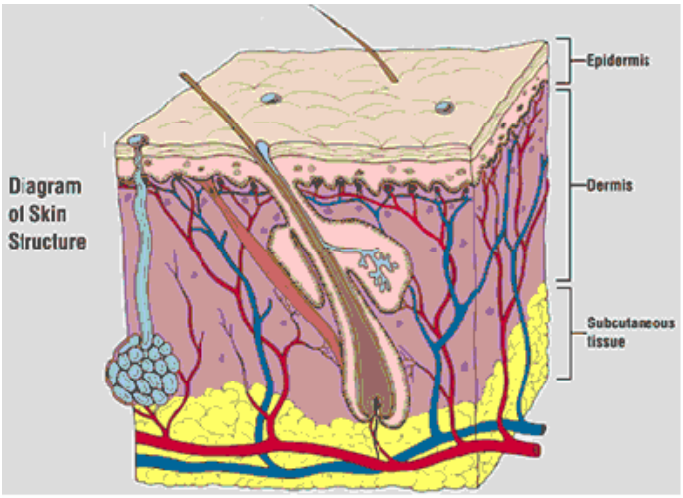

Figure 1 – Diagram of skin structure [4]

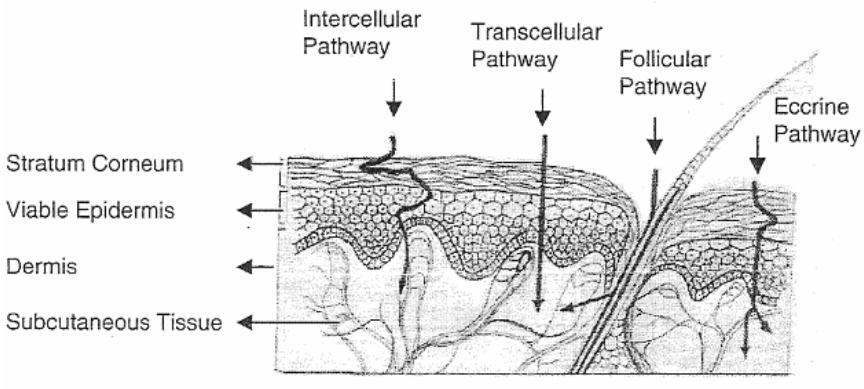

Figure 2 – Various routes of drug absorption [5]

Materials and methods

Polyvinylpirrolidone (M_n=1000000), polyethylene glycole (M_n=2000) were purchased from Merck Chemie and used as received, agar-agar micribiologycal and gellan were purchased from Sigma Aldrich and was used without purification. Carbomer was purchased from Aromamaslo and was used as received.

Hydrogel ointment preparation. The carbopol was placed into distilled water for swelling during the 2-3 minutes. Then the mixture was thoroughly stirred on magnetic stirrer then gradually added to the aqueouse solutions of drugs isoniazid (0.06 g/ml) and ethambutol (0.1 g/ml) and stirred until getting homogeneous consistency. Then, the solution of 50% NaOH was dropwise added to the mixture in order to increase the pH from 3 to 7 and thicken the hydrogel ointment.

Hydrogel dressings preparation. PVP was completely dissolved in distilled water at 40-50^{0}C during the 30-40 minutes. Agar-agar was dissolved in distilled water at 70-80^{0}C. In case of using gellan as a thickener no temperature was used for gellan dissolving process. Then, the dissolved agar-agar (or gellan) was mixed with PVP and PEG was added under discontinuous mixing. After, the solution of drugs isoniazid (0.06 g/ml) and ethambutol (0.1 g/ml) were added to prepared mixtures and stirred at 40-50^{0}C until getting to homogeneous mixture. Prepared mixtures were poured onto the plastic substrate, cooled to room temperature, sealed and sent to radiation crosslinking and sterilization. The composition of the hydrogel dressing is presented in Table 8.

Transdermal study. The penetration ability of drugs was studied using cellulose membrane and pig ears skin. Dialysis tubing MWCO 12-14 kDa (Medicell Int. Ltd, UK) was used for this purpose. Pig ears thickness about 500-600 microns were purchased from Almaty (individuals age 3-4 months; weight 25-30 kg). Pig ears were stored at 20 °C until use. Before each experiment, they were warmed to room temperature. The full-thickness of pig ear skin samples was measured before diffusion assay. The mean thickness of intact and excoriated skin samples was respectively 1.07 ± 0.10 mm and 0.92 ± 0.05.

The Franz diffusion cells system used for determined penetration of drug. Franz cell receptor compartment was filled with 35 ml of 0.2 M phosphate pH 6,86 buffer solution (Sigma–Aldrich) homogenized by magnetic stirring (400 rpm) and maintained at 37°C. Skin biopsies were placed between the donor and the receptor compartment ensuring that the dermal face was in contact with the receptor medium, whereas the epidermal face was turned to the donor compartment. The whole device was then fixed with a clamp.

Diffusion of drugs into the receptor compartment of Franz cell was measured spectroscopically by UV spectrometer Philips 8715 Model PU, at a wavelength of isoniazid λ = 270 nm and ethambutol λ = 275 nm, spectra were recorded in the wavelength range 190-500 nm.

Results and their discussion

The modern pharmaceutical technology as one of the basic tasks considers the establishment of new hydrogel ointments and dressings with drugs based on biocompatible polymers such as polyvinyl pyrrolidone, polyvinyl alcohol. These drug delivery systems can have high therapeutic activity and used for controlled drug release and its specific delivery directly to the pathological process. This is important as there are groups of serious diseases, which could be overcome, not because of drug effect itself, but also depend on the method of drug delivery into the body. In this research the transdermal properties of hydrogel ointments and dressings with DS through porcine skin was studied.

In this paper the hydrogel ointment and bandages based in biocompatible polymers for application as a transdermal therapeutic delivery systems with antituberculosis drugs isoniazid and ethambutol were developed and its transdermal activity was studied. As we can see from the figures 3 and 4, the amount of DS permeated through the skin in both cases increases by increasing of its concentration in the ointment. In this case, the permeability of isoniazid through the skin is much better than ethambutol, which is related to the chemical structure of drugs. It should be noted that isoniazid has less branched structure, and it belongs to the most effective drugs of the first class. Ointment with isoniazid DS are characterized by significant physiological indifference, the ability to be absorbed by intact skin and a relatively easiness of release of the incorporated drug substances. The reason is that they are more hydrophobic than ethambutol.

Drug dialysis through a cellulose membrane was investigated and based on obtained results the diffusion coefficients (D), the degree of penetration of drug (P) and the flow rate of drug (F) were calculated. These calculations are presented in Table 1. Calculated results from table confirm the results shown in Figures 3-4.

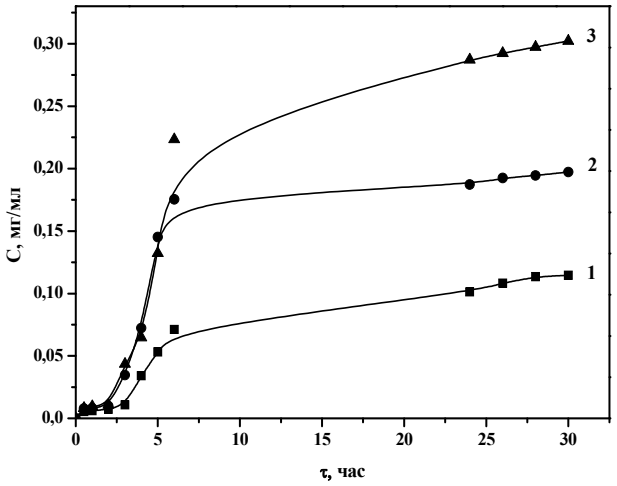

C_{Drug}= (1)-0,03mg/ml; (2)-0,06 mg/ml; (3)-0,09 mg/ml

Figure 3 – Kinetics of isoniazid penetration from ointment through the pig skin

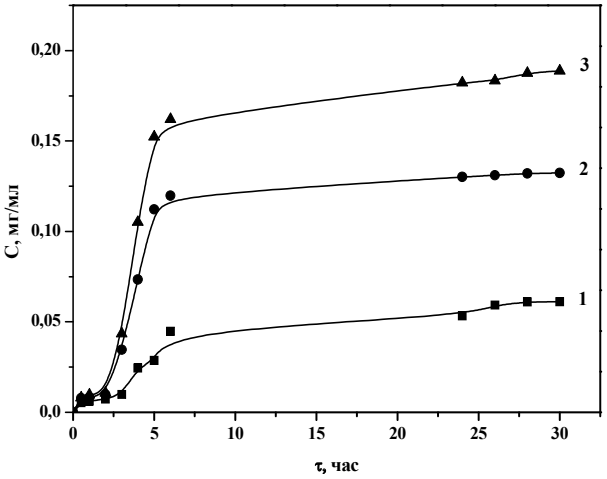

C_{Drug}= (1)-0,05mg/ml; (2)-0,1 mg/ml; (3)-0,15 mg/ml

Figure 4 – Kinetics of ethambutol penetration ointment through the pig skin

Table 1 – Penetration parameters of drugs from cellulose membrane and skin

Drug	Concentration, g/ml	Through membrane		Through pig skin		
		P, $sm^2 \times sec^{-1}$	F, mg×min	D, $sec^1 \times cm^2 \times mm$	F, mg×min	P, $sm^2 \times sec^{-1}$
isoniazid	0.03	12.52×10^{-2}	$2{,}19 \times 10^{-2}$	3.6958	1.94×10^{-2}	4.52×10^{-2}
	0.06	15.28×10^{-2}	$2{,}98 \times 10^{-3}$	5.0567	4.34×10^{-4}	9.81×10^{-2}
	0.09	20.52×10^{-2}	3.77×10^{-3}	8.9861	5.03×10^{-3}	16.04×10^{-3}
ethambutol	0.05	14.09×10^{-2}	$3{,}84 \times 10^{-3}$	1.1646	2.79×10^{-2}	6.31×10^{-1}
	0.1	14.72×10^{-2}	$3{,}94 \times 10^{-3}$	1.1838	5.33×10^{-2}	9.83×10^{-1}
	0.15	22.56×10^{-2}	$5{,}62 \times 10^{-3}$	3.6487	8.44×10^{-2}	10.18×10^{-1}

For investigation the transdermal activity of hydrogel dressings the bandages (adhesive area of 2 cm^2) based on PVP and PVA with a therapeutic concentration of DS isoniazid and ethambutol (therapeutic doses of isoniazid 1.2 g/day; ethambutol 2 g/day) were prepared.

Investigation of DS concentration impact on transdermal activity of hydrogel bandages is shown in figures 5-6. It is seen that the amount of drug isoniazid and ethambutol, permeated through the skin is equal to zero in the interval of 0-30 minutes from the start of the experiment. This segment of the curve is called the «lag time», its describes the time needed for DS penetrate through the layers of skin. It can be seen that with increasing DS concentration in the hydrogel bandages the number of penetrated DS increases. The maximum amount of penetrated DS from PVP agar-agar based dressings is 0.165 mg/mL for isoniazid and 0.12 mg/mL for ethambutol during 23-24 hours. And from PVP-gellan based dressings 0.13 mg/mL for isoniazid and 0.08 mg/mL for ethambutol during 23-24 hours.

It can be seen from obtained results, the penetration ability of isoniazid through the skin much better that that is for ethambutol. It can be related to chemicak structure of drugs. The isoniazid has branched structure and it's more effective first class DS.

Comparison study of transdermal activity of hydrogel ointment and dressings showed that the drug release rate from ointment higher than that is for hydrogel dressing (Fig. 7) but prolongation effect of dressings is better. Also it can be seen from the picture 7 that the transdermal activity of PVP and agar-agar based dressing is higher the PVP and gellan based formulation. It can be related to higher swelling degree of PVP and agar-agar hydrogel dressing.

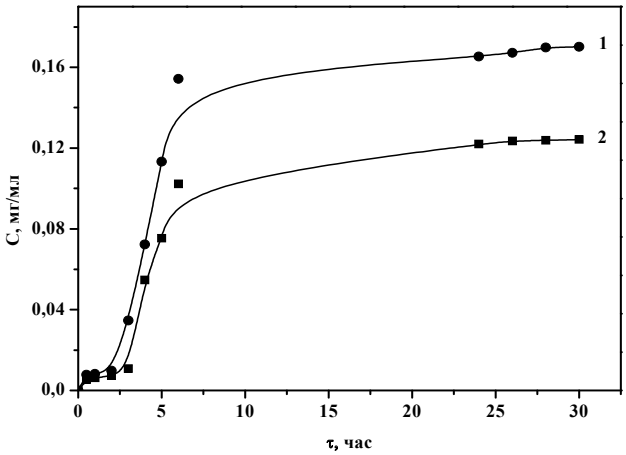

$C_{isoniazid}$= (1)-0,06 mg/ml;
$C_{ethambutol}$= (2)-0,1 mg/ml

Figure 5 – Kinetics of drugs penetration from PVP and agar-agar based hydrogel dressing through the pig skin

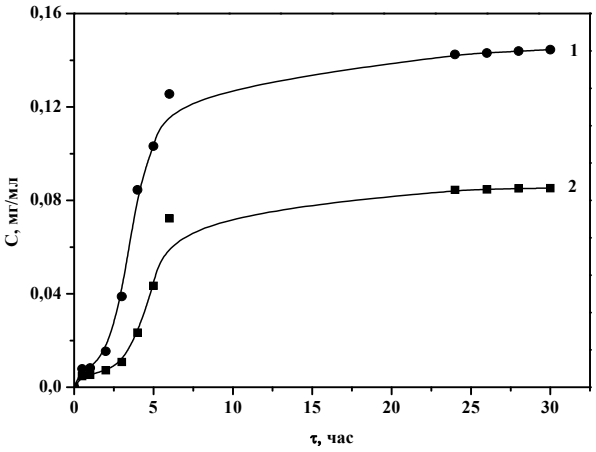

$C_{isoniazid}$= (1)-0,06 mg/ml;
$C_{ethambutol}$= (2)-0,1 mg/ml

Figure 6 – Kinetics of drugs penetration from PVP and gellan based hydrogel dressing through the pig skin

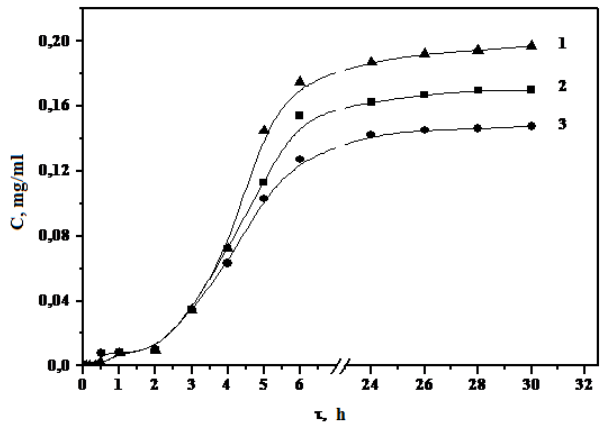

$C_{isoniazid}$= 0,06 g/ml

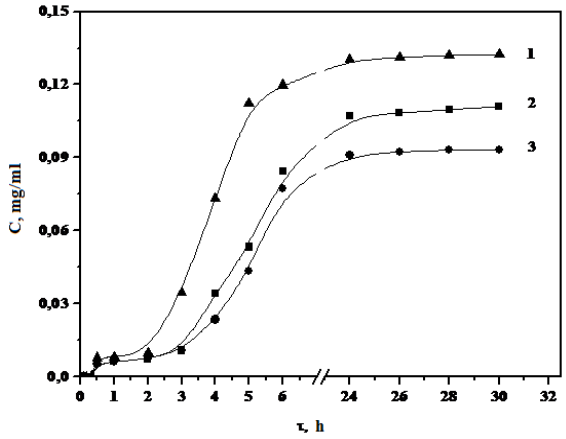

$C_{ethambutol}$= 0,1 g/ml

1 – hydrogel ointment, 2 – hydrogel dressing based on PVP and agar-agar, 3 – hydrogel dressing based on PVP and gellan

Figure 7 – Penetration kinetics of DS from hydrogel dressings and ointment.

Conclusion

Thus in present study the transdermal activity of hydrogel ointments and bandages based on PVP with antituberculosis drugs isoniazid and ethambutol of different concentrations was investigated. It is shown that both drugs penetrate the skin at a rate sufficient to achieve the daily therapeutic dose. Moreover the rate of penetration of isoniazid higher than the rate of penetration of ethambutol, which is related to chemical structure of DS. Investigation of transdermal activity of two types of hydrogel dressings showed that PVP and agar-agar based formulations shows higher rate of drug penetration through the skin. The comparison of hydrogel ointments and dressings resulted in better prolongation effect of dressings but the smaller rate of DS penetration and as a result its lower transdermal activity.

References

1 Jasti BR, Abraham W, Ghosh TK. Transdermal and Topical drug delivery systems. In: Ghosh TK, Jasti BR, editors. Theory and Practice of Contemporary Pharmaceutics. 1st ed. Florida: CRC Press; 2005. p. 423-53.

2 Baker H. The skin as barrier. In: Rook A, Wilkinson DS, Ebling FJG, Champion RH, Burton JL, eds. Text Book of Dermatology. Vol. I, 4th ed. Oxford: Blackwell Scientific Publications, 1986:355-66.

3 Barr M. Percutaneous absorption, J Pharm Sci 1962; (61):395-409.

4 Chein YW. Advances in transdermal systemic drug delivery. Drugs of Future 1988; (13):343-62.

5 N. Blanchin, S. Desloires, L. Grappin, A.M. Guillermin, P. Lafon, A. Miele, Protocols in an occupational medical facility for the management of internal plutonium exposure incidents in a nuclear plant: development–application–analysis–validation from 1996 to 2002, Radioprotection 39 (2004) 59–75.

6 B.M. De Rey, H.E. Lanfranchi, R.L. Cabrini, Percutaneous absorption of uranium compounds, Environ. Res. 30 (1983) 480–491.